Plane Deformations Generated by Prescribed Finite Rotation Fields: Issues and Applicatons

By

Gregory James Rizza

B.S., Mechanical Engineering, University of California Santa Barbara, 2008

Sc.M., Engineering, Brown University, 2010

A dissertation submitted in partial fulfillment of the

requirements for the Degree of Doctor of Philosophy

in the School of Engineering at Brown University

Providence, Rhode Island

May 2013

This dissertation by Gregory James Rizza is accepted in its present form by

the School of Engineering as satisfying the dissertation requirement for

the degree of Doctor of Philosophy

Date________________ ____

Professor Janet Blume, Advisor

Recommended to the Graduate Council

Date________________ ____

Professor Pradeep Guduru

Date________________ ____

Professor Justin Holmer

Approved by the Graduate Council

Date________________ ____

Peter Weber

Dean of the Graduate School

VITA

Gregory James Rizza is originally from Westminster, California, and was born in Southern California on March 27, 1986. He completed his B.S. in Mechanical Engineering at the University of California, Santa Barbara in June, 2008. Following, he attended Brown University as a member of the Solid Mechanics Research Group, where he completed his Sc.M. in Engineering in May 2010. Upon entering Brown, he received the Paul S. Symonds Fellowship for the 2008-2009 academic year. During his tenure at Brown, he was awarded a National Science Foundation GK-12 Fellowship for the 2010-2012 academic years, as well as became a member of the honorary societies Tau Beta Pi and Sigma Xi.

ACKNOWLEDGEMENTS

I would first like to thank and acknowledge collectively Brown University and specifically the Engineering Solids Group in granting me the opportunity to study and extend my education with them. Achieving this degree has been a long and maturing road, and I truly feel privileged that I was able to complete my academic journey at such an amazing place with such a dedicated faculty and staff. I want to acknowledge the works and dedication of my absolutely amazing advisor Janet Blume, and her constant guidance, mentoring, and unlimited patience without which this accomplishment would not have been possible. I would also like to thank various faculty, whose works were monumental towards the completion of my degrees at both Brown and UCSB during my college tenure in engineering: Karen Haberstroh, Huajian Gao, Anthony Evans, Theodore Shugar, Bob McMeeking, Pradeep Guduru, Allan Bower, and Igor Mezic.

I would like to give a sincere and loving thank you to Elizabeth (Lizzy) Doyel, who has always been by my side during this tumultuous process defined by: moving across the country together, settling into new lives away from our homes, and both of us completing rigorous degree programs, in which none of it would have been remotely possible without her constant love and support. I love her dearly, and I am so appreciative that I have had

the opportunity to spend this portion of my life with her. I cannot wait to see what the future holds for the both of us, since I know I can handle anything with her by my side.

I would like to also thank the friends I have met throughout the years, who have been so influential in keeping my sanity during this program. First, all the little homies from the Carden days: Ian, Mark, Albert, and company. The very successful Mater Dei alum: Peter, Brooke, Erica, and Kris. The main reason why UCSB was an amazing experience: Goran, Miko, Jonesy, Emir, GC, Jon, Stephanie, Nicole, Alyse, Maegan, Ana, Tomio, Nick, Kelii, Kekoa, Gordon and DeMarco. And finally all the people who I have had the greatest of privileges in knowing during these past years in Providence, in which there are too many names to do them all justice, however, I would like to give a special thank you to my partner in crime during this program and forever shots buddy Jennet Toyota.

Finally, and with my deepest emotion, I would like to thank with all my love and affection my family: my dad James, my mom Rose, and my sister Sabrina, whom which I dedicate my thesis. I love them all so much, and I am truly blessed to be able to share this accomplishment with them. I also would like to thank the family I have gotten to know during my time on the East Coast, from my drives to Connecticut, to the flights to Sicilia. Their company and food has always been a warm reminder of family. One last thank you I would like to give is to the family of Elizabeth Doyel, who have always been supportive throughout my program and have always been so great to spend time with during their numerous visits.

To My Family.

CONTENTS

LIST OF TABLES

LIST OF FIGURES

rotations $\theta^{+}(x_1, x_2) = 2x_1$ and $\theta^{-}(x_1, x_2) = x_1^2 + x_2^2$, with the rectangle mapped to its image, and the twin boundary mapped to a sine wave $C*$.

3.5 **(A)** Contour plot of the Jacobian determinants J^{+} and J^{-} for the deformation (3.3.73) and (3.3.74), which are continuous across the twin boundary $C:\{x_2=0,\ (-1 \le x_1 \le 1)\}$. In the unshaded regions $J^{+} > 0$ or $J^{-} > 0$ depending on which side of the twin boundary is being examined, and in the shaded region $J^{+} < 0$ or $J^{-} < 0$. Also, a rectangle with side lengths 0.2 and 0.4 centered at the origin. **(B)** The deformation generated from rotations $\theta^{+}(x_1, x_2) = 2x_1$ and $\theta^{-}(x_1, x_2) = 2x_2$, with the rectangle mapped to its image, and the twin boundary mapped to a parabola $C*$.

3.6 **(A)** Contour plot of the Jacobian determinants J^{+} and J^{-} for the deformation (3.3.83) and (3.3.84), and twin boundary $C:\{x_1=0,\ (-1 \le x_2 \le 1)\}$. In the unshaded regions $J^{+} > 0$ or $J^{-} > 0$ depending on which side of the twin boundary is being examined, and in the shaded region $J^{+} < 0$ or $J^{-} < 0$. Also, a rectangle of side lengths 1.0 and 0.2 centered at the origin. **(B)** The deformation generated from rotations $\theta^{+}(x_1, x_2) = 2x_1$ and $\theta^{-}(x_1, x_2) = 2x_2$, with the rectangle mapped to its image, and the twin boundary mapped to the unit circle $C*$.

3.7 Schematic of the twin boundary C and its image $C*$ separated by an angle ϕ, measured from $\dot{\boldsymbol{x}}$ to $\dot{\boldsymbol{y}}$.

3.8 **(A)** Contour plot of the Jacobian determinants J^{+} and J^{-} for the deformation (3.4.27) and (3.4.28), and the twin boundary $C:\{x_1=0,\ (-0.5 \le x_2 \le 0.5)\}$. In the unshaded regions $J^{+} > 0$ or $J^{-} > 0$ depending on which side of the twin boundary is being examined, and in the shaded region $J^{+} < 0$ or $J^{-} < 0$. Also, a rectangle of side lengths 0.6 and 0.1 centered at the origin. **(B)** The deformation generated from rotations $\theta^{+}(x_1, x_2) = 2(x_1 + x_2)$ and $\theta^{-}(x_1, x_2) = 2x_2$, with the rectangle mapped to its image, and the twin boundary mapped to itself.

3.9 **(A)** Contour plot of the Jacobian determinants J^+ and J^- for the deformation (3.4.33) and (3.4.34), and the twin boundary $C:\{x_1=0,\ (-1\le x_2\le 1)\}$. In the unshaded regions $J^+>0$ or $J^->0$ depending on which side of the twin boundary is being examined, and in the shaded region $J^+<0$ or $J^-<0$. Also, a rectangle of side lengths 0.6 and 0.15 centered at the origin. **(B)** The deformation generated from rotations $\theta^+(x_1,x_2)=2(x_1+x_2)$ and $\theta^-(x_1,x_2)=2x_2$, with the rectangle mapped to its image, and the twin boundary mapped to the unit circle C^*.

3.10 **(A)** Contour plot of the Jacobian determinants J^+ and J^- for the deformation (3.4.44) and (3.4.45), and the twin boundary $C:\{x_2=0,\ (-1.5\le x_1\le 1.5)\}$. In the unshaded regions $J^+>0$ or $J^->0$ depending on which side of the twin boundary is being examined, and in the shaded region $J^+<0$ or $J^-<0$. Also, a rectangle of side lengths 0.6 and 1.0 centered at the origin. **(B)** The deformation generated from the rotation fields fully determined by (3.4.40) and (3.4.41), with the rectangle mapped to its image, and the twin boundary mapped to a slanted line C^* with slope 1 corresponding to an angle $\phi=\pi/4$.

3.11 **(A)** Contour plot of the Jacobian determinants J^+ and J^- for the deformation (3.4.56) and (3.4.57), and the twin boundary $C:\{x_2=0,\ (-1\le x_1\le 1)\}$. In the unshaded regions $J^+>0$ or $J^->0$ depending on which side of the twin boundary is being examined, and in the shaded region $J^+<0$ or $J^-<0$. Also, a rectangle of side lengths 0.6 and 1.5 centered at the origin. **(B)** The deformation generated from rotations fields fully determined by (3.4.52) and (3.4.53), with the rectangle mapped to its image, and the twin boundary mapped to a parabola C^* approximated by (3.4.50).

4.1 (A) An undeformed square of side length 2 located in the first quadrant of the x_1, x_2 axes. (B) Square after deformation which corresponds to the prescribed θ in (4.3.1).

4.2 (A) An undeformed unit square located in the first quadrant of the x_1, x_2 axes, and the curve C defined as a horizontal line along the x_1-axis. (B) A close up view of the undeformed unit square. (C) Square after deformation which corresponds to the prescribed θ in (4.4.20), and the curve C mapped to a parabola, C^*. (D) A close up view of the deformed unit square.

4.3 (A) An undeformed square of side length 0.4 located in the first quadrant of the x_1, x_2 axes, and the curve C defined as a horizontal line along the x_1-axis. (B) A close up view of the undeformed square. (C) Square after deformation which corresponds to the prescribed θ in (4.4.20), and the curve C mapped to a parabola, C^*. (D) A close up view of the deformed unit square.

CHAPTER 1

INTRODUCTION

Compatibility conditions for various strain measures are well known in both small and finite strain kinematics. For many plane problems in solid mechanics, such conditions enable boundary value problems to be formulated using the strains, stresses, or a generating potential function, as the fundamental dependent variable(s). These methods are effective, as most strain fields fully determine the generating deformations up to an arbitrary rigid deformation. This thesis is concerned with the compatibility issue for the rotation field. Although it is not a direct measure of the distortion in a deformation, the rotation associated with a deformation and its variation from point to point within a body turns out to carry quite a bit of information about the actual deformation.

In **Chapter 2**, it is shown that any suitably smooth proper orthogonal tensor field may serve as a finite rotation tensor for generating a deformation field. A basic means is provided for finding the generated deformation. A method is also explained and introduced for constructing a deformation from a prescribed rotation field that takes on specific values on a given curve. Some examples are presented for both methods. The work in this chapter was first presented at the 2011 American Physics Society, March

Meeting, and has since been published as a paper in the Journal of Elasticity under the same chapter title.

In **Chapter 3**, I build on the analysis done in the previous chapter, and show that given a defined smooth curve which separates two arbitrarily prescribed rotation fields, a twin deformation field can be generated in a neighborhood surrounding such curve. Some examples are presented for cases where the Jacobian determinant of the finite deformation field is discontinuous or continuous across the prescribed twin boundary. Also, twinning in an elastic region is analyzed in some detail. The work in this chapter was first presented at the 2011 Society of Engineering Science, Fall Meeting, and has since been submitted as a paper for publication in the Journal of Elasticity under the same chapter title.

In **Chapter 4**, I conclude my study of plane deformations generated by prescribed rotation fields, by generating deformations that are locally area preserving in which the deformation takes on specific values on a given curve. Also, deformation fields in which the Jacobian determinant is prescribed are analyzed in some detail.

CHAPTER 2

PLANE DEFORMATIONS GENERATED BY A PRESCRIBED ROTATION FIELD

2.1 Introduction

In this chapter, we will show that any planar proper orthogonal tensor can serve as a rotation field for a finite planar deformation, and present a means of constructing the generating deformations.

In **Section 2.2**, the analogous issue for infinitesimal plane deformation is reviewed, in which case any skew-symmetric two-dimensional tensor field can serve as a plane rotation field.

In **Section 2.3**, some background for finite plane deformations is reviewed, including the relation between the deformation components and the rotation field.

In **Section 2.4**, it is shown that given any prescribed rotation field, a generating deformation may be constructed. A method is presented for generating a finite deformation. Several examples are given.

In **Section 2.5**, it is shown that a deformation can be constructed from a prescribed rotation field in which the deformation takes on certain prescribed values on a given curve. This is demonstrated in several types of example problems.

2.2 Infinitesimal plane deformation

Let $\boldsymbol{u}$ be an infinitesimal plane displacement field defined on a planar region B. The infinitesimal strain and rotation fields $\boldsymbol{E}$ and $\boldsymbol{W}$ are respectively given by

$$\boldsymbol{E} = \frac{1}{2}\left(\nabla\boldsymbol{u} + \nabla\boldsymbol{u}^T\right), \ \boldsymbol{W} = \frac{1}{2}\left(\nabla\boldsymbol{u} - \nabla\boldsymbol{u}^T\right). \tag{2.2.1}$$

The tensor field $\boldsymbol{W}$, being skew-symmetric, is determined by the single scalar field

$$\theta = W_{12} = -W_{21} = \frac{1}{2}\left(\frac{\partial u_1}{\partial x_2} - \frac{\partial u_2}{\partial x_1}\right) \ , \ (W_{11} = W_{22} = 0)\,, \tag{2.2.2}$$

which corresponds to the angle of right-hand rotation about an out-of-plane axis. Given a plane deformation, the associated rotation field is easily calculated. Conversely, suppose that one considers the function $\theta = \theta(x_1, x_2)$ to be prescribed. To construct a deformation $\boldsymbol{u}$ that generates $\boldsymbol{W}$ in the sense described above, one can set

$$u_1(x_1, x_2) = 2\int_{x_2^0}^{x_2} \theta(x_1, \xi_2)\, d\xi_2 + \frac{\partial}{\partial x_1} v\left(x_1, x_2\right) \ , \ u_2(x_1, x_2) = \frac{\partial}{\partial x_2} v\left(x_1, x_2\right), \tag{2.2.3}$$

in which x_2^0 is the x_2-coordinate of a point in B, while $v(x_1, x_2)$ is a scalar field (Buck, 1978). One can easily confirm that all plane infinitesimal deformations with the rotation field $\boldsymbol{W}$ admit this representation. Note that two deformations with the same rotation field differ by an additive irrotational displacement field.

2.3 Some kinematics of plane finite deformations

Let $\boldsymbol{y} = \boldsymbol{y}(\boldsymbol{x})$ be a deformation on a plane region B. The mapping $\boldsymbol{y} = \boldsymbol{y}(\boldsymbol{x})$ is one-to-one, continuously differentiable, and has a positive Jacobian determinant, J. The deformation gradient tensor field $\boldsymbol{F}$ is defined as $\boldsymbol{F} = \nabla \boldsymbol{y}$, and the left and right polar decompositions fields for $\boldsymbol{F}$ are

$$\boldsymbol{F} = \boldsymbol{RU} = \boldsymbol{VR}, \quad \boldsymbol{U} = \sqrt{\boldsymbol{F}^T \boldsymbol{F}}, \quad \boldsymbol{V} = \sqrt{\boldsymbol{F}\boldsymbol{F}^T}, \quad \boldsymbol{R} = \boldsymbol{F}\boldsymbol{U}^{-1}. \tag{2.3.1}$$

The left and right stretch tensors $\boldsymbol{U}$ and $\boldsymbol{V}$ are both symmetric and positive definite, and the rotation tensor field $\boldsymbol{R}$ is proper orthogonal. As in the small-strain case, the rotation field is fully determined by a single scalar field θ, corresponding to an angle of rotation through an out-of-plane axis. In terms of θ, the components of the matrix of a plane rotation tensor admit the following basis-independent representation:

$$\boldsymbol{R} = \begin{bmatrix} \cos\theta & -\sin\theta \\ \sin\theta & \cos\theta \end{bmatrix}, \tag{2.3.2}$$

The rotation field admits this simple representation in terms of the components of $\boldsymbol{F}$ (Hoger and Carlson, 1984):

$$\boldsymbol{R} = \frac{1}{2\rho} \begin{bmatrix} F_{11} + F_{22} & F_{12} - F_{21} \\ F_{21} - F_{12} & F_{11} + F_{22} \end{bmatrix}, \tag{2.3.3}$$

where ρ is defined as,

$$\rho = \frac{1}{2}\sqrt{(F_{11}+F_{22})^2+(F_{12}-F_{21})^2}. \tag{2.3.4}$$

In terms of the invariants I and J, ρ is expressible as

$$\rho = \frac{1}{2}\sqrt{I+2J}, \tag{2.3.5}$$

where invariants I and J are defined as follows:

$$I = F_{11}^2+F_{12}^2+F_{21}^2+F_{22}^2, \quad J = Det\{\boldsymbol{F}\} = F_{11}F_{22}-F_{12}F_{21}. \tag{2.3.6}$$

Upon comparing equation (2.3.2) with (2.3.3), one finds that

$$\cos\theta = \frac{F_{11}+F_{22}}{2\rho} \quad , \quad \sin\theta = \frac{F_{21}-F_{12}}{2\rho}. \tag{2.3.7}$$

The relationship between θ and its generating deformation $\boldsymbol{y}$ is neatly expressible using the complex-valued function $\hat{y}$ defined as

$$\hat{y}(z,\overline{z}) = y_1(x_1,x_2)+iy_2(x_1,x_2) \ , \ \ y_1 = \mathrm{Re}\{\hat{y}\} \ , y_2 = \mathrm{Im}\{\hat{y}\}, \tag{2.3.8}$$

in which,

$$z = x_1+ix_2, \quad \overline{z} = x_1-ix_2. \tag{2.3.9}$$

Differentiating (2.3.8) with respect to z gives

$$\begin{aligned}\frac{\partial}{\partial z}\hat{y}(z,\overline{z}) \equiv \hat{y}_z(z,\overline{z}) &= \frac{1}{2}\left[y_{1,1}+y_{2,2}+i(y_{2,1}-y_{1,2})\right] \\ &= \frac{1}{2}\left[F_{11}+F_{22}+i(F_{21}-F_{12})\right] \\ &= \hat{\rho}(z,\overline{z})e^{i\hat{\theta}(z,\overline{z})} \quad ,\end{aligned} \tag{2.3.10}$$

with $\hat{\theta}(z,\overline{z}) = \theta(x_1, x_2)$, $\hat{\rho}(z,\overline{z}) = \rho(x_1, x_2)$. Thus, the rotation field for a plane deformation is determined by the argument of the complex derivative $\hat{y}_z$. The derivative of $\hat{y}$ with respect to $\overline{z}$ is

$$\frac{\partial}{\partial \overline{z}} \hat{y}(z,\overline{z}) \equiv \hat{y}_{\overline{z}}(z,\overline{z}) = \frac{1}{2}\left[y_{1,1} - y_{2,2} + i(y_{2,1} + y_{1,2}) \right]. \tag{2.3.11}$$

For simplicity purposes, we define a scalar function $\hat{\lambda}(z,\overline{z})$ such that,

$$|\, \hat{y}_{\overline{z}} \,| = \hat{\lambda} = \frac{1}{2}\sqrt{I - 2J} \,. \tag{2.3.12}$$

As an aside we note that the derivations done thus far are similar to those done by Fosdick and Schuler (1969), (1971), in their analysis of strain-deformation relations for the Ericksen's problem (Ericksen, 1954).

According to (2.3.5), (2.3.10) and (2.3.12), the Jacobian determinant of the deformation field may be expressed as

$$J = |\, \hat{y}_z \,|^2 - |\, \hat{y}_{\overline{z}} \,|^2 = \hat{\rho}^2 - \hat{\lambda}^2, \tag{2.3.13}$$

such that a positive Jacobian demands that

$$\hat{\rho} > \hat{\lambda} \,. \tag{2.3.14}$$

2.4 Building a finite deformation from a prescribed rotation field

Suppose now a rotation field is determined by an arbitrary, but continuous function $\theta(x_1, x_2)$ on a plane region B. A generating mapping $\boldsymbol{y}$ can be constructed in terms of the complex-valued function $\hat{y}$ by defining a real-valued, positive scalar function $\rho(x_1, x_2) = \hat{\rho}(z, \overline{z})$ and a function $\tilde{h}$ that is analytic in $\overline{z}$, and setting

$$\hat{y}(z, \overline{z}) = y_1(x_1, x_2) + i y_2(x_1, x_2) = \int_{z_0}^{z} \hat{\rho}(\zeta, \overline{z}) e^{i\hat{\theta}(\zeta, \overline{z})} d\zeta + \tilde{h}(\overline{z}), \qquad (2.4.1)$$

where $\hat{\theta}(z, \overline{z}) = \theta(x_1, x_2)$, $z_0 = x_1^0 + i x_2^0$ is a point in region B, and $\zeta = \zeta_1 + i\zeta_2$. One can easily confirm by direct differentiation and a comparison with equations (2.3.10), that $\hat{y}$ as defined in (2.4.1) generates the prescribed rotation field in (2.3.2).

In order to ensure that (2.4.1) is one-to-one and invertible locally in a neighborhood N bounded by a radius δ surrounding the point z_0, the Jacobian determinant J of the deformation field must be positive in N. To meet this criterion, the functions $\hat{\rho}$ and $\tilde{h}$ must be chosen such that the inequality in (2.3.14) holds. In what follows, it is shown that it is always possible to assign functions $\hat{\rho}$ and $\tilde{h}$ that will lead to a deformation with a positive Jacobian in a neighborhood N surrounding a prescribed point z_0. The deformation so-defined will be locally one-to-one and invertible in N.

Take $\hat{\rho} = \rho_0$ to be a positive constant. The derivative of equation (3.1) with respect to $\overline{z}$ is then

$$\hat{y}_{\bar{z}}(z,\bar{z}) = i\rho_0\int_{z_0}^{z}\hat{\theta}_{\bar{z}}(\zeta,\bar{z})e^{i\hat{\theta}(\zeta,\bar{z})}d\zeta + \tilde{h}'(\bar{z}), \tag{2.4.2}$$

where $\tilde{h}'(\bar{z}) \equiv \dfrac{d\tilde{h}(\bar{z})}{d\bar{z}}$. The modulus $\hat{\lambda}$ of $\hat{y}_{\bar{z}}$ is bounded by

$$\hat{\lambda} \equiv |\hat{y}_{\bar{z}}| \le \rho_0\delta\,|\hat{\theta}_{\bar{z}}(\zeta,\bar{z})|_{\max}|e^{i\hat{\theta}(\zeta,\bar{z})}|_{\max} + |\tilde{h}'(\bar{z})|_{\max}, \tag{2.4.3}$$

with $|\hat{\theta}_{\bar{z}}(\zeta,\bar{z})|_{\max}$, $|e^{i\hat{\theta}(\zeta,\bar{z})}|_{\max}$, and $|\tilde{h}'(\bar{z})|_{\max}$ standing for the largest values of the associated quantities in the neighborhood *N*. Substituting (2.4.3) into (2.3.14) gives

$$\rho_0\delta\,|\hat{\theta}_{\bar{z}}(\zeta,\bar{z})|_{\max}|e^{i\hat{\theta}(\zeta,\bar{z})}|_{\max} + |\tilde{h}'(\bar{z})|_{\max} < \rho_0, \tag{2.4.4}$$

which must be true to ensure a positive Jacobian. Taking $\tilde{h} = 0$, we see that (2.4.4) holds for a neighborhood *N* as long as

$$\delta < \frac{1}{|\hat{\theta}_{\bar{z}}|_{\max}|e^{i\hat{\theta}}|_{\max}} \quad , \quad |\hat{\theta}_{\bar{z}}|_{\max} \ne 0. \qquad (2.4.5)^{1}$$

Like with $\hat{\rho}$, $\tilde{h}$ does not have to be defined this way and can be chosen to be any analytic function of $\bar{z}$, the only requirement being that the inequality in (2.3.14) and (2.4.4) hold for the chosen $\hat{\rho}$ and $\tilde{h}$. For this case, (2.4.1) simplifies to

$$\hat{y}(z,\bar{z}) = \rho_0\int_{z_0}^{z} e^{i\hat{\theta}(\zeta,\bar{z})}d\zeta\ . \tag{2.4.6}$$

---

[1] If $|\hat{\theta}_{\bar{z}}|_{max} = 0$, then $\hat{\theta}$ is constant, and equation (2.13) becomes $J = |\hat{y}_z|^2 = \rho_0{}^2 > 0$.

This construction of $\hat{y}$ shows, by taking $\hat{\rho}$ to be a positive constant and $\tilde{h}=0$, it is always possible to make a deformation that is one-to-one in a neighborhood N surrounding the point (x_1^0, x_2^0), from any smooth plane proper orthogonal tensor field. However, it will be shown later that conditions of assigning $\hat{\rho}$ be constant, or $\tilde{h}=0$ are not required to find generating deformations from prescribed rotation fields. Finally, we note that the deformation generated from a prescribed rotation field in (2.4.1) is not unique, since there are an infinite number of possibilities of $\hat{\rho}$ and $\tilde{h}$ which meet the conditions in (2.3.14) and (2.4.4) for any prescribed rotation field.

Example 2.1: Finite deformation around a point

Suppose the rotation field is defined by the scalar function

$$\theta(x_1, x_2) = 2x_1 \ \ , \ \ \hat{\theta}(z, \overline{z}) = z + \overline{z} \ . \tag{2.4.7}$$

Take $\tilde{h}=0$, and let $\hat{\rho}$ be a constant such that $\hat{\rho}=\rho_0=1$ in (2.4.6). We will construct a generating deformation that is one-to-one in a neighborhood N of the point $(x_1^o, x_2^o) = (0,0)$ with radius δ. For this choice of $\hat{\theta}$, one has

$$\hat{\theta}_{\overline{z}}(\zeta, \overline{z}) = |\hat{\theta}_{\overline{z}}|_{\max} = 1 \, , \tag{2.4.8}$$

and the inequality in (2.4.5) becomes

$$\delta < \frac{1}{|e^{i\hat{\theta}(\zeta,\overline{z})}|_{\max}} \, . \tag{2.4.9}$$

To determine the maximum magnitude of $e^{i\hat{\theta}}$ for the prescribed function $\hat{\theta}$, we note that

$$e^{i\hat{\theta}(\zeta,\bar{z})} = e^{i(\zeta+\bar{z})}, \tag{2.4.10}$$

where $\zeta = \zeta_1 + i\zeta_2$ describes the complex variable of integration in equation (2.4.6). Equation (2.4.10) can be rewritten as

$$e^{i\hat{\theta}} = e^{i(\zeta+\bar{z})} = e^{i(\zeta_1+i\zeta_2+x_1-ix_2)} = e^{(x_2-\zeta_2)}(\cos(\zeta_1+x_1)+i\sin(\zeta_1+x_1)) . \tag{2.4.11}$$

The maximum value of $|e^{i\hat{\theta}}|$ occurs when $x_2 - \zeta_2 = 2\delta$, since $x_2 - \zeta_2 \le 2\delta$ for ζ and x_2 in N. The inequality in (2.4.9) becomes

$$\delta\,|e^{i\hat{\theta}}|_{\max} = \delta e^{2\delta} < 1, \tag{2.4.12}$$

which requires the neighborhood N to be bounded by a radius $\delta < 0.425$. In this neighborhood, $\hat{y}$ as defined by (2.4.6) is one-to-one and invertible.

Integrating (2.4.6) with $\rho_0 = 1$, $\hat{\theta}$ as defined in (2.4.7) and $z_0 = 0$ gives the following deformation

$$\hat{y}(z,z) = i\left(e^{iz} - e^{i(z+\bar{z})}\right). \tag{2.4.13}$$

From (2.3.8) we find the components of $\hat{y}$ to be

$$\begin{aligned} y_1(x_1,x_2) &= \mathrm{Re}\{\hat{y}\} = \sin(2x_1) - e^{x_2}\sin(x_1)\ , \\ y_2(x_1,x_2) &= \mathrm{Im}\{\hat{y}\} = -\cos(2x_1) + e^{x_2}\cos(x_1)\ . \end{aligned} \tag{2.4.14}$$

The deformation gradient matrix $\boldsymbol{F}$ and Jacobian determinant J are given by

$$\boldsymbol{F} = \begin{bmatrix} 2\cos(2x_1)\text{-}e^{x_2}\cos(x_1) & \text{-}e^{x_2}\sin(x_1) \\ 2\sin(2x_1)\text{-}e^{x_2}\sin(x_1) & e^{x_2}\cos(x_1) \end{bmatrix}, \tag{2.4.15}$$

$$J = 2e^{x_2}\cos(x_1)\text{-}e^{2x_2}\ . \tag{2.4.16}$$

This deformation can be shown to have a positive Jacobian in a region defined by a radius of 0.69 centered at $(x_1^o, x_1^o) = (0,0)$. When we compare this region to the neighborhood N described by radius $\delta < 0.425$, we see that our calculations in (2.4.8)-(2.4.12) agree with (2.4.16) on showing a neighborhood where $J > 0$. Further, one can easily confirm that the polar decomposition for the matrix $\boldsymbol{F}$ is

$$\boldsymbol{R} = \begin{bmatrix} \cos(2x_1) & -\sin(2x_1) \\ \sin(2x_1) & \cos(2x_1) \end{bmatrix} \ , \ \boldsymbol{U} = \begin{bmatrix} \text{-}e^{x_2}\cos(x_1)+2 & e^{x_2}\sin(x_1) \\ e^{x_2}\sin(x_1) & e^{x_2}\cos(x_1) \end{bmatrix}. \tag{2.4.17}$$

Figure 2.1 illustrates this deformation.

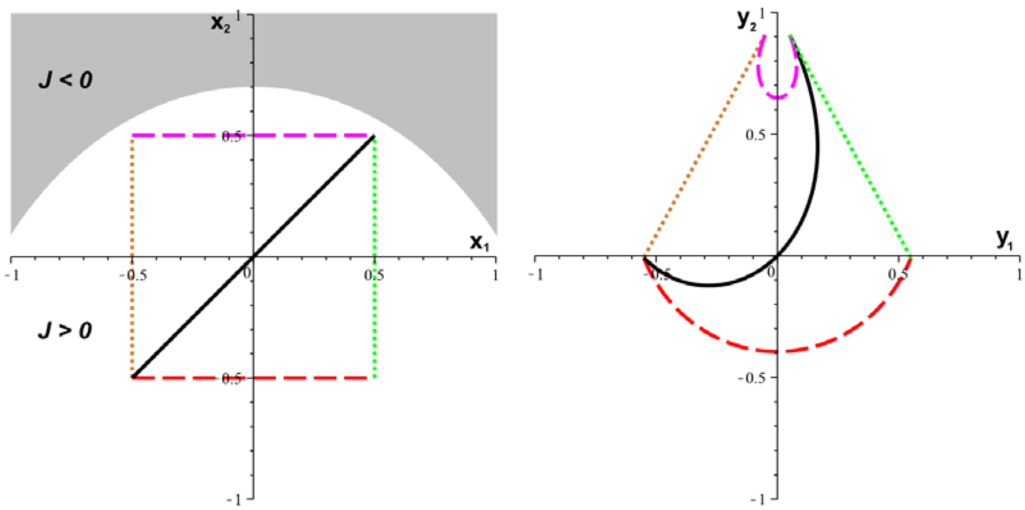

(A) (B)

Figure 2.1: (A) Contour plot of the Jacobian determinant J in (2.4.16) where the unshaded region $J > 0$, and the shaded region $J < 0$. An undeformed square of side length 1.0 centered at the origin. (B) Square after deformation induced by (2.4.13) which corresponds to a rotation field $\theta = 2x_1$.

Example 2.2

Consider a rotation field generated by the scalar function

$$\theta(x_1, x_2) = x_1^2 + x_2^2 \equiv r^2, \quad \hat{\theta}(z,\overline{z}) = z\overline{z}\,. \tag{2.4.18}$$

We will take $\hat{\rho}$ to be constant and $\tilde{h} = 0$, and construct a deformation that is one-to-one in a neighborhood N of a radius δ surrounding the point $(x_1^o, x_2^o) = (0,0)$, $z_0 = \overline{z}_0 = 0$. In N,

$$\hat{\theta}_{\overline{z}}(\zeta, \overline{z}) = z, \quad |\,\hat{\theta}_{\overline{z}}\,|_{\max} = \delta\,, \tag{2.4.19}$$

and inequality (2.4.5) becomes,

$$\delta^2 < \frac{1}{|e^{i\hat{\theta}(\zeta,\bar{z})}|_{\max}}. \tag{2.4.20}$$

To determine the maximum value of $|e^{i\hat{\theta}(\zeta,\bar{z})}|$ on the path of integration for this case, note that

$$\begin{aligned} &e^{i\hat{\theta}} = e^{i(\zeta\bar{z})} = e^{(x_2\zeta_1 - \zeta_2 x_1)}(\cos(\zeta_1 x_1 + \zeta_2 x_2) + i\sin(\zeta_1 x_1 + \zeta_2 x_2)) \\ &\Rightarrow |e^{i\hat{\theta}}| = e^{(x_2\zeta_1 - \zeta_2 x_1)} \end{aligned} \quad , \tag{2.4.21}$$

where $\zeta = \zeta_1 + i\zeta_2$. Since

$$x_2\zeta_1 - \zeta_2 x_1 \le 2\delta^2 , \tag{2.4.22}$$

for ζ and z in N ,

$$|e^{\hat{\theta}}|_{\max} = e^{2\delta^2} . \tag{2.4.23}$$

So (2.4.20) becomes

$$\delta^2 < \frac{1}{e^{2\delta^2}} , \tag{2.4.24}$$

and the neighborhood N for which there is definitely a one-to-one mapping of $\hat{y}$ occurs when $\delta < 0.652$. However, the deformation to be constructed will turn out to have a positive Jacobian in a neighborhood larger than this.

As in *Example 2.1*, we take $\hat{\rho} = \rho_0 = 1$ with $\hat{\theta} = z\bar{z}$ and $z_0 = 0$ in (2.4.6). Integrating (2.4.6) with these conditions provides the following deformation,

$$\hat{y}(z,z) = \frac{-i\left(e^{iz\bar{z}} - 1\right)}{\bar{z}}. \tag{2.4.25}$$

The components of the deformation in (2.4.25) are,

$$\begin{aligned} y_1(x_1,x_2) &= \frac{x_2\cos(r^2) - x_2 + x_1\sin(r^2)}{r^2}, \\ y_2(x_1,x_2) &= \frac{-x_2\cos(r^2) + x_1 + x_2\sin(r^2)}{r^2}, \end{aligned} \tag{2.4.26}$$

where $r = \sqrt{x_1^2 + x_2^2}$. The gradient of deformation can be found to be,

$$\boldsymbol{F} = \begin{bmatrix} \frac{-2x_1x_2}{r^4}[\cos(r^2)\text{-}1+r^2\sin(r^2)]+\frac{2x_1^2}{r^4}[r^2\cos(r^2)\text{-}\sin(r^2)]+\frac{\sin(r^2)}{r^2}, & \frac{2x_1x_2}{r^4}[r^2\cos(r^2)-\sin(r^2)]\text{-}\frac{2x_2^2}{r^4}[\cos(r^2)\text{-}1\text{-}r^2\sin(r^2)]+\frac{\cos(r^2)-1}{r^2} \\ \frac{2x_1x_2}{r^4}[r^2\cos(r^2)-\sin(r^2)]+\frac{2x_1^2}{r^4}[\cos(r^2)\text{-}1\text{-}r^2\sin(r^2)]+\frac{\cos(r^2)-1}{r^2}, & \frac{-2x_1x_2}{r^4}[\cos(r^2)\text{-}1+r^2\sin(r^2)]+\frac{2x_2^2}{r^4}[r^2\cos(r^2)\text{-}\sin(r^2)]+\frac{\sin(r^2)}{r^2} \end{bmatrix}, \tag{2.4.27}$$

and the Jacobian determinant is

$$J = \frac{2\left(r^2\sin(r^2) + \cos(r^2) - 1\right)}{r^4}, \tag{2.4.28}$$

which is positive for $0 \le r \le 1.53$.

Although the algebra is somewhat more involved than in *Example 2.1*, the rotation matrix of the polar decomposition for $\boldsymbol{F} = \boldsymbol{RU}$ is found to be

$$\boldsymbol{R} = \begin{bmatrix} \cos(r^2) & -\sin(r^2) \\ \sin(r^2) & \cos(r^2) \end{bmatrix}, \tag{2.4.29}$$

which confirms that the deformation in (2.4.25) has the desired rotation tensor field. In Figure 2.2 we show the deformation of a square with side length 2.0 centered at $(x_1^o, x_2^o) = (0,0)$.

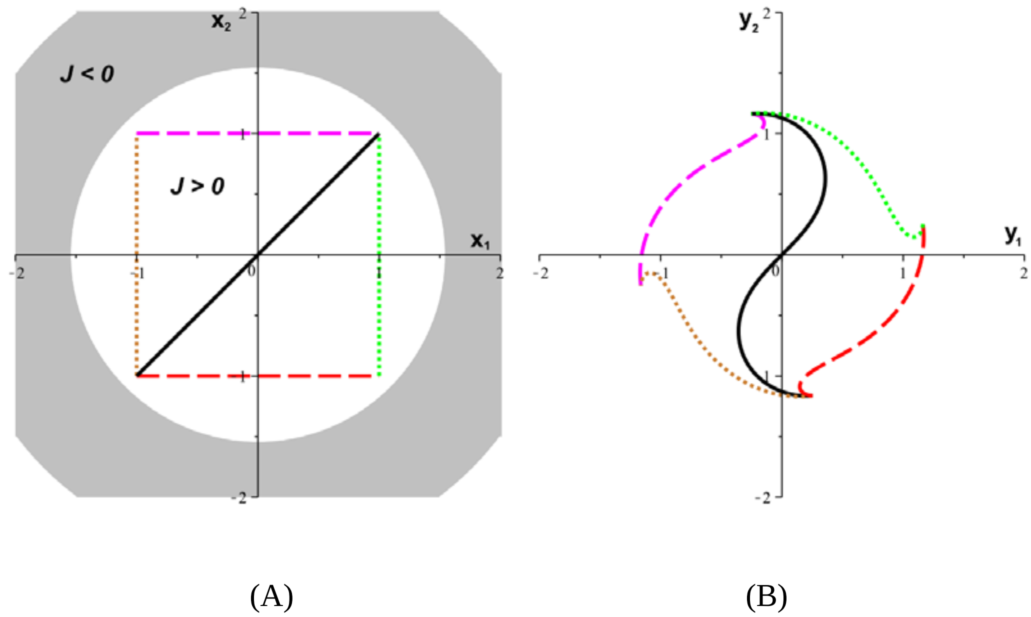

Figure 2.2: (A) Contour plot of the Jacobian determinant J in (2.4.28) where the unshaded region $J > 0$, and the shaded region $J < 0$. An undeformed square with side length 2.0 centered at the origin. (B) Square after deformation induced by (2.4.25) which corresponds to a rotation field $\theta = x_1^2 + x_2^2 = r^2$.

Example 2.3

Suppose again we define the rotation field with the same scalar function as in *Example 2.1*,

$$\theta(x_1, x_2) = 2x_1 \quad , \quad \hat{\theta}(z, \overline{z}) = z + \overline{z}. \tag{2.4.30}$$

To illustrate that the function $\hat{\rho}$ need not be constant to construct a generating deformation, take $\hat{\rho}(z, \overline{z}) = 1 + z\overline{z}$, and let $\tilde{h} = 0$. Taking $z_0 = 0$, we see that (2.4.1) becomes

$$\hat{y}(z,\overline{z}) = \int_{z_0}^{z} \hat{\rho}(\zeta,\overline{z}) e^{i\hat{\theta}(\zeta,\overline{z})} d\zeta = \int_0^z (\zeta\overline{z}+1) e^{i(\zeta+\overline{z})} d\zeta \ . \tag{2.4.31}$$

Although $\hat{\rho}$ is not constant, this does not affect the calculations in (2.4.8)-(2.4.12) in determining a minimum neighborhood N where $\hat{y}$ is one-to-one. So the region N is still bounded by the radius $\delta < 0.425$.

Integrating (2.4.31) gives the deformation

$$\hat{y}(z,\overline{z}) = \overline{z}(e^{i(z+\overline{z})} - e^{i\overline{z}} - zie^{i(z+\overline{z})}) + ie^{i\overline{z}}(e^{iz} - 1) \tag{2.4.32}$$

The components of the deformation are,

$$\begin{aligned} y_1(x_1,x_2) &= x_1\cos(2x_1) + \sin(2x_1)\{x_1^2 + x_2^2 + x_2 + 1\} \\ &\quad -e^{x_2}\{x_1\cos(x_1) + \sin(x_1)[x_2+1]\} \ , \\ y_2(x_1,x_2) &= x_1\sin(2x_1) - \cos(2x_1)\{x_1^2 + x_2^2 + x_2 + 1\} \\ &\quad -e^{x_2}\{x_1\sin(x_1) - \cos(x_1)[x_2+1]\} \ . \end{aligned} \tag{2.4.33}$$

The gradient of deformation $\boldsymbol{F}$ can be found to be,

$$\boldsymbol{F} = \begin{bmatrix} e^{x^2}[x_1\sin(x_1) - x_2\cos(x_1) - 2\cos(x_1)] + 2\cos(2x_1)[x_1^2 + x_2^2 + x_2 + 1] + \cos(2x_1), & -e^{x^2}[x_2\sin(x_1) + x_1\cos(x_1) + 2\sin(x_1)] + \sin(2x_1)[2x_2+1] \\ -e^{x^2}[x_2\sin(x_1) + x_1\cos(x_1) + 2\sin(x_1)] + 2\sin(2x_1)[x_1^2 + x_2^2 + x_2 + 1] + \sin(2x_1), & e^{x^2}[x_2\cos(x_1) - x_1\sin(x_1) + 2\cos(x_1)] - \cos(2x_1)[2x_2+1] \end{bmatrix} , \tag{2.4.34}$$

and the Jacobian determinant is,

$$\begin{aligned} J = \mathrm{e}^{x_2}\Big[& 4\sin(x_1)x_1 + 8\cos(x_1) + 12\cos(x_1)x_2 + 8\cos(x_1)x_2^2 + 4x_1^2\cos(x_1) + \\ & 2x_1^3\sin(x_1) + 2x_2^3\cos(x_1) + 4x_1x_2\sin(x_1) + 2x_1^2x_2\cos(x_1) + 2x_2^2x_1\sin(x_1)\Big] \\ & -\mathrm{e}^{(2x_2)}\left[x_1^2 + x_2^2 + 4x_2 + 4\right] - \left[4x_2^3 + 4x_2x_1^2 + 6x_2^2 + 2x_1^2 + 8x_2 + 3\right] \ , \end{aligned} \tag{2.4.35}$$

which is positive in a region bounded by a radius $\delta < 0.67$ around the point $(x_1^o, x_2^o) = (0,0)$. Although the algebra is somewhat more involved, the rotation matrix of the polar decomposition for $\boldsymbol{F} = \boldsymbol{RU}$ is found to be

$$\boldsymbol{R} = \begin{bmatrix} \cos(2x_1) & -\sin(2x_1) \\ \sin(2x_1) & \cos(2x_1) \end{bmatrix} \tag{2.4.36}$$

which is the same as the rotation matrix in *Example 2.1*.

In Figure 2.3 we show the deformation of a square with side length 1.0 centered at $(x_1^o, x_2^o) = (0,0)$, applying the same rotation field as in *Example 2.1*, except now the value of $\hat{\rho}(z,\overline{z}) = 1 + z\overline{z}$ in not constant.

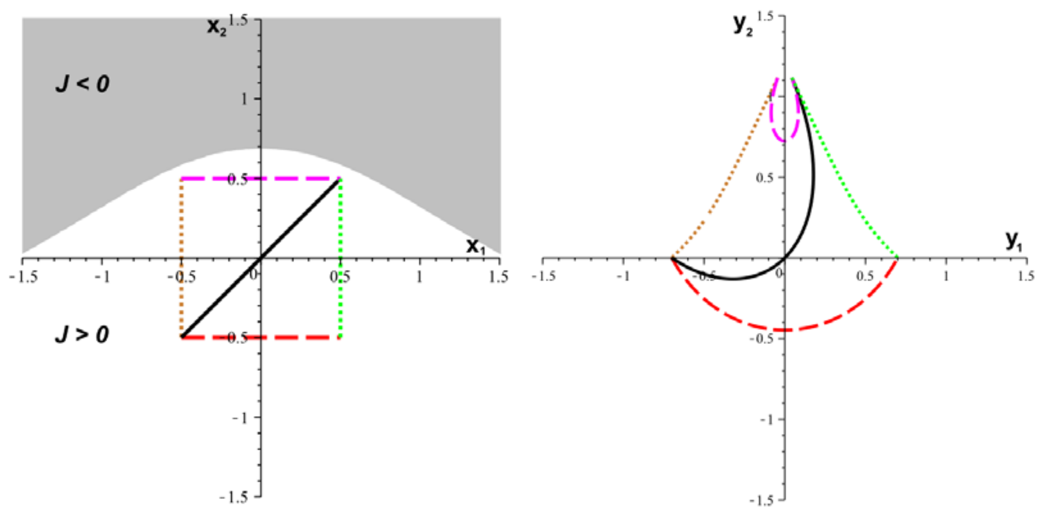

(A) (B)

Figure 2.3: (A) Contour plot of the Jacobian determinant J in (3.35) where the unshaded region $J > 0$, and the shaded region $J < 0$. An undeformed square with side length 1.0 centered at the origin. (B) Square after deformation induced by (3.32) which corresponds to a rotation field $\theta = 2x_1$, with $\hat{\rho} = 1 + z\overline{z}$.

2.5 Finite deformations which take on a prescribed value on a given curve

The results of the preceding derivation suggest that there may be many deformations that correspond to an arbitrarily prescribed rotation field. Next we will discuss the determination of generating a deformation in a region B from a prescribed rotation field that maps a prescribed curve C to another prescribed curve $C*$ in a neighborhood of any point along C.

Suppose again that a finite rotation field $\boldsymbol{R}$ is prescribed through a continuous scalar function $\theta(x_1, x_2)$, and let

$$\theta(x_1, x_2) = \hat{\theta}(z, \bar{z}) . \tag{2.5.1}$$

We seek a deformation $\boldsymbol{y}$ which gives rise to the rotation field defined by (2.5.1) and in addition maps the curve C to a curve $C*$. Let the curves C and $C*$ be parameterized as follows:

$$C : \boldsymbol{x} = \tilde{\boldsymbol{x}}(s) \ \ , \ C{*}: \ \ \boldsymbol{y} = \tilde{\boldsymbol{y}}(s) \ (0 < s < s_0) , \tag{2.5.2}$$

with s standing for arc-length along the curve, and s_0 is a constant defining the upper bound of the arc-length. The deformation $\boldsymbol{y}$ must map C onto $C*$, so that

$$\boldsymbol{y}(x_1, x_2) = \boldsymbol{y}(\tilde{x}_1(s), \tilde{x}_2(s)) = \tilde{\boldsymbol{y}}(s) \ \ , \quad (0 < s < s_0) . \tag{2.5.3}$$

Differentiating (4.3) with respect to s and using the polar decomposition for $\boldsymbol{F}$ expressed in (2.1) we find

$$\boldsymbol{F}\dot{\tilde{\boldsymbol{x}}} = \boldsymbol{R}\boldsymbol{U}\dot{\tilde{\boldsymbol{x}}} = \dot{\tilde{\boldsymbol{y}}}\,, \tag{2.5.4}$$

where the dots above $\tilde{\boldsymbol{x}}$ and $\tilde{\boldsymbol{y}}$ denote derivatives with respect to s. Since $\boldsymbol{U}$ is positive definite, the scalar function $\psi = \dot{\tilde{\boldsymbol{x}}} \cdot \boldsymbol{U}\dot{\tilde{\boldsymbol{x}}}$ is positive along C, so that (2.5.4) implies that the given rotation $\boldsymbol{R}$ and the curve parameterizations $\tilde{\boldsymbol{x}}$ and $\tilde{\boldsymbol{y}}$ must obey,

$$\begin{aligned}\psi &= \dot{\tilde{\boldsymbol{x}}} \cdot \boldsymbol{U}\dot{\tilde{\boldsymbol{x}}} = \dot{\tilde{\boldsymbol{y}}} \cdot \boldsymbol{R}\dot{\tilde{\boldsymbol{x}}} \\ &= \left(\dot{\tilde{x}}_1\dot{\tilde{y}}_1 + \dot{\tilde{x}}_2\dot{\tilde{y}}_2\right)\cos(\theta) + \left(\dot{\tilde{x}}_1\dot{\tilde{y}}_2 - \dot{\tilde{x}}_2\dot{\tilde{y}}_1\right)\sin(\theta) \\ &= \sqrt{\dot{\tilde{y}}_1^2 + \dot{\tilde{y}}_2^2}\,\cos(\theta - \varphi) > 0 \quad .\end{aligned} \tag{2.5.5}$$

Here, θ is the rotation angle associated with $\boldsymbol{R}$, and $\varphi = \varphi(s)$ is the angle subtended by the vectors $\dot{\tilde{\boldsymbol{x}}}$ and $\dot{\tilde{\boldsymbol{y}}}$, as measured from $\dot{\tilde{\boldsymbol{x}}}$. The inequality in (2.5.5) is a necessary condition for the existence of a deformation that maps the curve C onto C^* corresponding to a rotation field defined by the scalar function $\theta(x_1, x_2)$.

We show next that given any rotation field θ and curves C and C^* which conform to (2.5.5), one can produce a local deformation of a neighborhood of every point along C which carries C to C^* and has θ as its rotation field.

Before launching into this proof, it is useful to present some alternate characterizations of the curves C and C^* using complex notation. Shown in the Appendix, suitably smooth curves C and C^* can be fully defined in terms of the complex functions $\tilde{z}(\overline{z})$ and $\tilde{y}(\overline{z})$ such that

$$z = \tilde{z}(\overline{z}) = \tilde{x}_1(s) + i\tilde{x}_2(s)\,, \text{ on } C\,, \tag{2.5.6}$$

and

$$y = \tilde{y}(\overline{z}) = \tilde{y}_1(s) + i\tilde{y}_2(s), \text{ on } C^*. \tag{2.5.7}$$

Following the procedure in the previous section, the complex function $\hat{y}$ defined by

$$\hat{y}(z,\overline{z}) = y_1(x_1,x_2) + iy_2(x_1,x_2) = \int_{z_0}^{z} \hat{\rho}(\zeta,\overline{z})e^{i\hat{\theta}(\zeta,\overline{z})}d\zeta + \tilde{h}(\overline{z}), \tag{2.5.8}$$

generates the rotation field defined in (2.5.1), provided $\rho(x_1,x_2) = \hat{\rho}(z,\overline{z})$ is a positive real-valued function, $z_0 = x_1^0 + ix_2^0$ is a point on the curve C, and $\tilde{h}(\overline{z})$ is an analytic function of the complex variable $\overline{z}$. These must be determined to ensure that the Jacobian of the deformation gradient of (2.5.8) is positive in a neighborhood N surrounding z_0, and that the condition in (2.5.5) is met.

Let,

$$k(z,\overline{z}) = \int_{z_0}^{z} \hat{\rho}(\zeta,\overline{z})e^{i\hat{\theta}(\zeta,\overline{z})}d\zeta, \tag{2.5.9}$$

so that (2.5.8) can be rewritten as

$$\hat{y}(z,\overline{z}) = k(z,\overline{z}) + \tilde{h}(\overline{z}). \tag{2.5.10}$$

From (2.5.6) we see that on the curve C, (2.5.10) becomes

$$\hat{y}(\tilde{z}(\overline{z}),\overline{z}) = \tilde{y}(\overline{z}) = k(\tilde{z}(\overline{z}),\overline{z}) + \tilde{h}(\overline{z}), \tag{2.5.11}$$

where, recall (2.5.7), $\tilde{y}(\overline{z})$ describes the mapping of curve C onto the curve C^*. We can rewrite (2.5.11) as follows

$$\tilde{h}(\overline{z}) = \tilde{y}(\overline{z}) - k(\tilde{z}(\overline{z}), \overline{z}), \tag{2.5.12}$$

and substitute it into (2.5.10) which gives us the following representation of $\hat{y}$ on the curve C,

$$\hat{y}(z, \overline{z}) = k(z, \overline{z}) - k(\tilde{z}(\overline{z}), \overline{z}) + \tilde{y}(\overline{z}). \tag{2.5.13}$$

From (2.5.9) and (2.5.13), it can be seen that $\hat{y}(z, \overline{z})$ takes the form,

$$\hat{y}(z, \overline{z}) = \int_{\tilde{z}(\overline{z})}^{z} \hat{\rho}(\zeta, \overline{z}) e^{i\hat{\theta}(\zeta, \overline{z})} d\zeta + \tilde{y}(\overline{z}). \tag{2.5.14}$$

Next, $\hat{\rho}(z, \overline{z})$ must be determined such that the Jacobian determinant of the deformation $\hat{y}(z, \overline{z})$ is positive, at least in a neighborhood surrounding a point $z_0 = x_1^0 + i x_2^0$ along the curve C. As in the previous section, let $\hat{\rho}(z, \overline{z}) = \rho_0$ be a positive constant so that (2.5.14) becomes

$$\hat{y}(z, \overline{z}) = \rho_0 \int_{\tilde{z}(\overline{z})}^{z} e^{i\hat{\theta}(\zeta, \overline{z})} d\zeta + \tilde{y}(\overline{z}). \tag{2.5.15}$$

Differentiating (2.5.15) with respect to $\overline{z}$, we get

$$\hat{y}_{\overline{z}}(z, \overline{z}) = -\rho_0 e^{i\hat{\theta}(\tilde{z}(\overline{z}), \overline{z})} \tilde{z}'(\tilde{z}(\overline{z}), \overline{z}) + \rho_0 \int_{\tilde{z}(\overline{z})}^{z} i\hat{\theta}_{\overline{z}}(\zeta, \overline{z}) e^{i\hat{\theta}(\zeta, \overline{z})} d\zeta + \tilde{y}'(\overline{z}), \tag{2.5.16}$$

where the prime notation is defined as the derivative of the function with respect to $\overline{z}$ (same as in the previous section). Clearly, since $z = \tilde{z}(\overline{z})$ on the curve C, then (2.5.16) can be simplified to,

$$\hat{y}_{\overline{z}}(\tilde{z}(\overline{z}), \overline{z}) = -\rho_0 e^{i\hat{\theta}(\tilde{z}(\overline{z}), \overline{z})} \tilde{z}'(\overline{z}) + \tilde{y}'(\overline{z}). \tag{2.5.17}$$

As a consequence we have,

$$|\,\hat{y}_{\bar{z}}(\tilde{z}(\bar{z}),\bar{z})\,|^2 = \rho_0{}^2\,|\,\tilde{z}'(\bar{z})\,|^2 + |\,\tilde{y}'(\bar{z})\,|^2 - 2\rho_0\,\mathrm{Re}\left\{e^{-i\hat{\theta}(\tilde{z}(\bar{z}),\bar{z})}\,\overline{\tilde{z}'(\bar{z})}\tilde{y}'(\bar{z})\right\}, \quad (2.5.18)$$

and by taking the derivative of (2.5.6) with respect to s we find

$$\tilde{z}'(\bar{z}) \equiv \frac{d\tilde{z}}{d\bar{z}} = \frac{\dot{\tilde{x}}_1 + i\,\dot{\tilde{x}}_2}{\dot{\tilde{x}}_1 - i\,\dot{\tilde{x}}_2}\,, \text{ on } C, \quad (2.5.19)$$

so that

$$|\,\tilde{z}'(\bar{z})\,|^2 = \left|\frac{\dot{\tilde{x}}_1 + i\,\dot{\tilde{x}}_2}{\dot{\tilde{x}}_1 - i\,\dot{\tilde{x}}_2}\right|^2 = 1. \quad (2.5.20)$$

Substituting (2.5.20) into (2.5.18) we then reach

$$|\,\hat{y}_{\bar{z}}(\tilde{z}(\bar{z}),\bar{z})\,|^2 = \rho_0{}^2 + |\,\tilde{y}'(\bar{z})\,|^2 - 2\rho_0\,\mathrm{Re}\left\{e^{-i\hat{\theta}(\tilde{z}(\bar{z}),\bar{z})}\,\overline{\tilde{z}'(\bar{z})}\tilde{y}'(\bar{z})\right\}, \text{ on } C. \quad (2.5.21)$$

Also, from (2.5.20) we have

$$\left|\overline{\tilde{z}'(\bar{z})}\right| = 1, \quad \overline{\tilde{z}'(\bar{z})} = \frac{1}{\tilde{z}'(\bar{z})}, \quad (2.5.22)$$

so that (2.5.21) becomes,

$$|\,\hat{y}_{\bar{z}}(\tilde{z}(\bar{z}),\bar{z})\,|^2 = \rho_0{}^2 + |\,\tilde{y}'(\bar{z})\,|^2 - 2\rho_0\,\mathrm{Re}\left\{e^{-i\hat{\theta}(\tilde{z}(\bar{z}),\bar{z})}\tilde{y}'(\bar{z})\,/\,\tilde{z}'(\bar{z})\right\}, \text{ on } C. \quad (2.5.23)$$

Recalling the expression for the Jacobian determinant J in (2.3.13), we see that J is positive if and only if

$$\begin{aligned} J &= |\hat{y}_z|^2 - |\hat{y}_{\bar{z}}|^2 \\ &= {\rho_0}^2 - |\hat{y}_{\bar{z}}|^2 \\ &= 2\rho_0 \operatorname{Re}\left\{ e^{-i\hat{\theta}(\tilde{z}(\bar{z}),\bar{z})} \tilde{y}'(\bar{z}) / \tilde{z}'(\bar{z}) \right\} - |\tilde{y}'(\bar{z})|^2 > 0 \quad . \end{aligned} \tag{2.5.24}$$

Next we set

$$\hat{\psi} = \operatorname{Re}\left\{ e^{-i\hat{\theta}(\tilde{z}(\bar{z}),\bar{z})} \tilde{y}'(\bar{z}) / \tilde{z}'(\bar{z}) \right\} \quad , \quad \hat{\chi} = |\tilde{y}'(\bar{z})|^2 , \tag{2.5.25}$$

for a neighborhood N surrounding a point z_0 on C. Differentiating (2.5.7) with respect to s gives,

$$\tilde{y}'(\bar{z}) = \frac{\dot{\tilde{y}}_1 + i\,\dot{\tilde{y}}_2}{\dot{\tilde{x}}_1 - i\,\dot{\tilde{x}}_2} \text{ , on } C . \tag{2.5.26}$$

From this, along with (2.5.19) and the fact that $\dot{\tilde{x}}_1^2 + \dot{\tilde{x}}_2^2 = 1$ (arc length parameterization of C), it can be seen from (2.5.5) and (2.5.25) that $\psi = \hat{\psi}$ on C. Thus necessary that $\hat{\psi} > 0$ on C. By its definition, $\hat{\chi} \geq 0$. To assure positivity of the Jacobian J, the value of ρ_0 must be chosen such that,

$$\rho_0 > \frac{\hat{\chi}_{\max}}{2\hat{\psi}_{\min}} , \tag{2.5.27}$$

where $\hat{\chi}_{\max}$ and $\hat{\psi}_{\min}$ are the maximum and minimum values of the scalar functions $\hat{\chi}$ and $\hat{\psi}$ in the neighborhood of a point z_0 on C. The relationship in (2.5.27) assures the positivity of the Jacobian determinant J, in a neighborhood N surrounding point z_0 on C.

As in **Section 2.4**, it is also possible to generate deformations without the requirements that $\hat{\rho}$ be constant as long as the condition of (2.5.27) is met for all values of $\hat{\rho}$, which will be demonstrated in the following examples.

Example 2.4: Finite deformation around a curve

Suppose the rotation field is defined by the scalar function

$$\theta(x_1, x_2) = x_1 \quad , \quad \hat{\theta}(z, \overline{z}) = \frac{z + \overline{z}}{2} . \tag{2.5.28}$$

Let the curve C be the unit circle, which may be represented as

$$(x_1, x_2) = (\tilde{x}_1(s), \tilde{x}_2(s)) = (\cos(s), \sin(s)) \quad , \quad (0 \le s < 2\pi) , \tag{2.5.29}$$

where s is arc-length along C. This gives the following representation of the curve C in terms of a complex function analytic in $\overline{z}$

$$z = \tilde{z}(\overline{z}) = \frac{1}{\overline{z}} , \text{ on } C . \tag{2.5.30}$$

Further, suppose the deformation under consideration maps C onto itself $C^* = C$ so that

$$(y_1, y_2) = (x_1, x_2) = (\cos(s), \sin(s)) . \tag{2.5.31}$$

For this mapping of C to C^*, it follows that $\tilde{y}(\overline{z})$ in (2.5.7) is given by

$$\tilde{y}(\overline{z}) = \tilde{z}(\overline{z}) = \frac{1}{\overline{z}} , \text{ on } C . \tag{2.5.32}$$

Given (2.5.32), the following expressions for $\hat{\chi}$ and $\hat{\psi}$ in (2.5.25) for this example are

$$\hat{\chi} = |\,\tilde{y}'(\overline{z})\,|^2 = 1/\,|\,\overline{z}\,|^4, \tag{2.5.33}$$

$$2\hat{\psi} = 2\,\mathrm{Re}\left\{ e^{-i(\overline{z}+\frac{1}{\overline{z}})} \right\} = 2\cos(x_1)\,. \tag{2.5.34}$$

The desired deformation may be constructed in a neighborhood of any point on C for which the condition in (4.5) is met, where $\psi = \hat{\psi}$. Clearly looking at (2.5.34), $\hat{\psi} > 0$ everywhere on the unit circle. Along the curve C the values for x_1 are bounded by $(-1 \le x_1 \le 1)$ so that

$$2\hat{\psi}_{\min}(\overline{z}) = 2\cos(\pm 1) = 1.08, \tag{2.5.35}$$

for the minimum value of $\hat{\psi}$, and the maximum value of $\hat{\chi}$ on the curve C is

$$\hat{\chi}_{\max}(\overline{z}) = 1. \tag{2.5.36}$$

Using the values in (2.5.35) and (2.5.36), the condition for ρ_0 in (2.5.27) in order to assure the positivity of the Jacobian determinant J along the curve C is

$$\rho_0 > 1/1.08 = 0.93. \tag{2.5.37}$$

We take $\rho_0 = 1$, and carry out the integration in (2.5.15),

$$\hat{y}(z,\overline{z}) = 2i\left(e^{\frac{i(\overline{z}^2+1)}{2}} - e^{\frac{i(\overline{z}+z)}{2}} - \frac{i}{2\overline{z}} \right). \tag{2.5.38}$$

The real and imaginary parts of (2.5.38) give the components of the deformation, but these are long and complicated expressions. The Jacobian determinant of the deformation algebraically reduces to

$$J = 2\cos(x_1) - 1, \tag{2.5.39}$$

and shown in Figure 2.4(A) are the regions where J is positive, negative and zero. The rotation matrix of the polar decomposition of the deformation gradient $\boldsymbol{F} = \boldsymbol{RU}$ is found to be

$$\boldsymbol{R} = \begin{bmatrix} \cos(x_1) & -\sin(x_1) \\ \sin(x_1) & \cos(x_1) \end{bmatrix}. \tag{2.5.40}$$

From (2.5.39), the constructed deformation in (2.5.38) has a positive Jacobian, and is one-to-one and invertible in a neighborhood surrounding any point along the unit circle shown in Figure 2.4(A). It is worth noting that the neighborhood surrounding the unit circle does not include the entire inside of the unit circle for this example, meaning that the one-to-oneness of the deformation is lost is the shaded region inside the unit circle. The deformation in (2.5.38) is also illustrated in Figure 2.4 below, where a square centered at the origin surrounding the curve C is deformed.

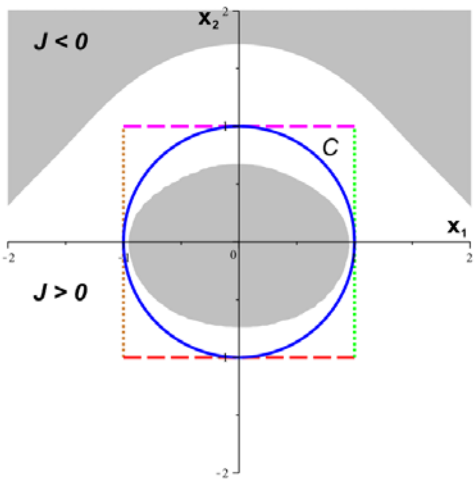

(A)

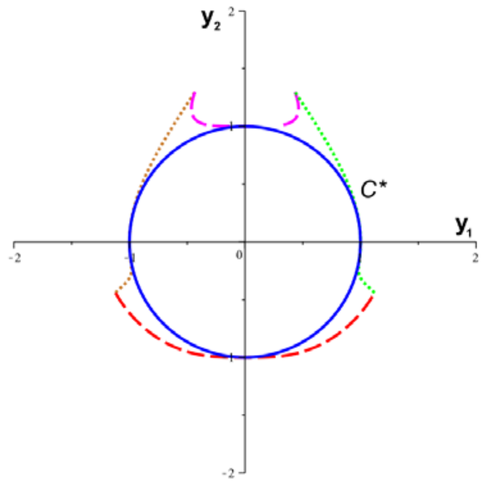

(B)

Figure 2.4: (A) Contour plot of the Jacobian determinant J in (2.5.39) and the curve C defined as the unit circle, where the unshaded regions $J > 0$, and the shaded regions $J < 0$. An undeformed square of side length 2.0 centered at the origin. (B) Square after deformation defined in (2.5.38) which corresponds to a rotation field $\theta = x_1$, and the unit circle mapped to itself.

Example 2.5

In this example, we use the same rotation field as in the preceding case:

$$\theta(x_1, x_2) = x_1 \quad , \quad \hat{\theta}(z, \overline{z}) = \frac{z + \overline{z}}{2} . \tag{2.5.41}$$

This time, we take a non-constant function $\hat{\rho}$ defined by,

$$\hat{\rho}(z, \overline{z}) = 1 + z\overline{z} \quad , \quad \rho(x_1, x_2) = 1 + x_1^2 + x_2^2 , \tag{2.5.42}$$

which is positive everywhere. As in the previous example, we seek a deformation that maps the unit circle onto itself. Thus,

$$\tilde{z}(\overline{z}) = \tilde{y}(\overline{z}) = \frac{1}{\overline{z}}, \text{ on } C. \tag{2.5.43}$$

For non-constant $\hat{\rho}$, the equivalent condition to (2.5.27) is $\hat{\rho} > \hat{\chi}_{\max} / 2\hat{\psi}_{\min}$. This condition is satisfied since from the previous example we know for this rotation field in (2.5.41) and the curves C, C^*, both defined as the unit circle, our choice of $\hat{\rho}$ must agree with the condition $\rho > 0.93$. For this choice of $\hat{\theta}$, $\hat{\rho}$, C, and C^*, the integration in (2.5.14) gives the following deformation

$$\hat{y}(z,\overline{z}) = 4e^{\frac{i(\overline{z}^2+1)}{2}}\left(i-\overline{z}\right) + 2e^{\frac{i(\overline{z}+z)}{2}}\left(2\overline{z} - z\overline{z}i - i\right) + \frac{1}{\overline{z}}. \tag{2.5.44}$$

The expression for the Jacobian is long and complicated, but regions in which it is positive, negative and zero are shown in Figure 2.5(A). The rotation matrix of the polar decomposition of $\boldsymbol{F}$ is still the same as in the previous example. In Figure 2.5, a square centered at the origin with side length 2.0 is deformed by the deformation in (2.5.44).

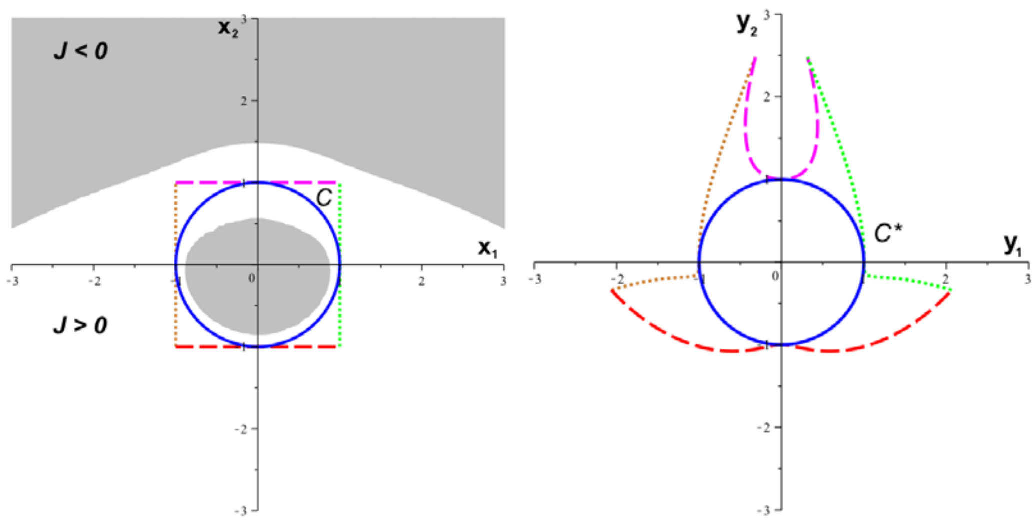

(A) (B)

Figure 2.5: (A) Contour plot of the Jacobian determinant J for the deformation (4.44) and curve C defined as the unit circle, where the unshaded regions $J > 0$, and the shaded regions $J < 0$. An undeformed square of side length 2.0 centered at the origin. (B) Square after deformation defined in (4.44) which corresponds to a rotation field $\theta = x_1$, and the unit circle mapped to itself.

Example 2.6

In the final example of this chapter, we look at a case where the given initial curve C and the curve C^* differ from each other. Suppose the rotation field is defined by the scalar function,

$$\theta(x_1, x_2) = x_1^2 + x_2^2 \equiv r^2 \quad , \quad \hat{\theta}(z, \overline{z}) = z\overline{z} \, , \tag{2.5.45}$$

which is the same scalar function used to define the rotation matrix $\boldsymbol{R}$ in *Example 2.2*. Let the initial curve C be a vertical line on the x_2-axis defined as

$$(x_1, x_2) = (\tilde{x}_1(s), \tilde{x}_2(s)) = (0, s) \quad , \quad (-\pi \le s < \pi) \, . \tag{2.5.46}$$

This gives the following representation of the curve C in terms $\tilde{z}(\overline{z})$,

$$z = \tilde{z}(\overline{z}) = -\overline{z} \text{ , on } C . \tag{2.5.47}$$

Further, suppose the deformation under consideration maps C onto the unit circle, given by

$$(y_1(s), y_2(s)) = (\cos(s), \sin(s)) \quad , \quad (-\pi \le s < \pi) . \tag{2.5.48}$$

For this mapping of C to $C*$, of a vertical line to the unit circle, it follows that $\tilde{y}(\overline{z})$ in (2.5.7) is given by

$$\tilde{y}(\overline{z}) = e^{-\overline{z}} . \tag{2.5.49}$$

Given (2.5.47) and (2.5.49), the values of $\hat{\chi}$ and $\hat{\psi}$ in (2.5.25) for this example are,

$$\hat{\chi} = | \tilde{y}'(\overline{z}) |^2 = | -e^{\overline{z}} |^2 , \tag{2.5.50}$$

$$2\hat{\psi} = 2 \operatorname{Re}\left\{ e^{\overline{z}(i\overline{z}+1)} \right\} . \tag{2.5.51}$$

On the prescribed curve C, $x_1 = 0$ which simplifies the above equations to,

$$\chi = | -(\cos(x_2) + i \sin(x_2)) |^2 = 1 , \tag{2.5.52}$$

$$2\psi = 2 \cos(x_2^2 + x_2) . \tag{2.5.53}$$

As stated before, the desired deformation may be constructed in a neighborhood of any point on C for which the conditions in (2.5.5) and (2.5.27) are met. Looking at (2.5.53), on C we see that $\psi > 0$ wherever $-0.85 < x_2 < 1.85$, which means that for this example only a portion of the curve C meets these conditions. Along the curve C, we will bound the values of x_2 : $\left(-\pi/4 \le x_2 \le \pi/4\right)$, so that (2.5.53) yields

$$2\hat{\psi}_{\min} = 0.336\,, \tag{2.5.54}$$

for the minimum value of $\hat{\psi}$. Clearly, the maximum value of $\hat{\chi}$ on the curve C is

$$\hat{\chi}_{\max} = 1\,. \tag{2.5.55}$$

Using the values in (2.5.54) and (2.5.55), the condition for ρ_0 in (2.5.27) that ensures the positivity of the Jacobian determinant J along the curve C is

$$\rho_0 > 2.98\,. \tag{2.5.56}$$

We take $\rho_0 = 3$, and carry out the integration in (2.5.15) for this example:

$$\hat{y}(z,\overline{z}) = \frac{3ie^{-i\overline{z}^2}}{\overline{z}}\left(1 - e^{i(\overline{z}+z)\overline{z}}\right) + e^{-\overline{z}}\,. \tag{2.5.57}$$

Again, the real and imaginary parts of (2.5.57) give the components of the deformation, but these are long and complicated expressions. The Jacobian determinant J will not be shown for the same reason, but in Figure 2.6(A) it is shown where J is positive, negative and zero. From Figure 2.6(A), it can be seen that the range of values $\left\{x_1 = 0 \;,\; (-\pi/4 \le x_2 \le \pi/4)\right\}$ for the curve C does correspond to a positive Jacobian. The rotation matrix of the polar decomposition of $\boldsymbol{F} = \boldsymbol{RU}$ is found to be

$$\boldsymbol{R} = \begin{bmatrix} \cos(r^2) & -\sin(r^2) \\ \sin(r^2) & \cos(r^2) \end{bmatrix}. \tag{2.5.58}$$

In Figure 2.6, a square centered at the origin with side length 0.4 is deformed by the prescribed rotation $\theta = x_1^2 + x_2^2 \equiv r^2$.

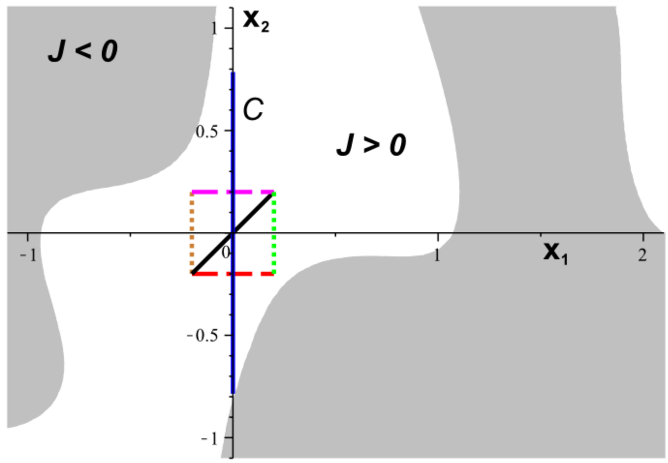

(A)

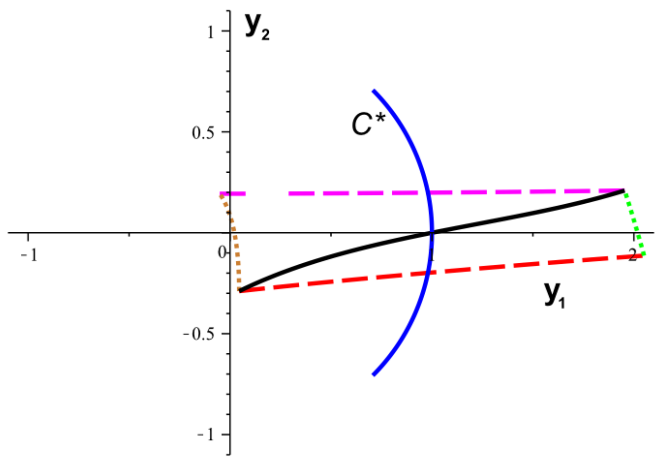

(B)

Figure 2.6: (A) Contour plot of the Jacobian determinant J for the deformation (4.57) and the curve C: $\{x_1 = 0 \;,\; (-\pi/4 \le x_2 \le \pi/4)\}$, where $J > 0$ in the unshaded regions, and $J < 0$ in the shaded regions. An undeformed square of side length 0.4 centered at the origin. (B) Square after the deformation (4.57) which corresponds to a rotation field $\theta = x_1^2 + x_2^2 \equiv r^2$, and the curve C mapped to an arc of the unit circle C^*: $\{x_1 = \cos(s)\,, x_2 = \sin(s) \;\; (-\pi/4 \le s \le \pi/4)\}$.

CHAPTER 3

TWINNED FINITE PLANE DEFORMATIONS GENERATED BY PRESCRIBED ROTATION FIELDS

3.1 Introduction

In the previous chapter, we showed that any planar proper orthogonal tensor field may serve as a rotation field, for generating a plane finite, one-to-one deformation. Now we will look at these results in the context of twinning, and show that a pair of plane rotation fields defined on either side of a prescribed twin boundary curve can generate a twin finite deformation field in a neighborhood surrounding such curve.

In **Section 3.2**, a brief summary of some key concepts presented in the previous chapter are reviewed as a prelude to the main works of this chapter.

In **Section 3.3**, the kinematics associated with twinning are reviewed. We present results for twin deformations where either the stretch field or the rotation field is continuous across the twin boundary. A methodology is given for generating a plane finite twin deformation field in the neighborhood of a prescribed curve which separates two different given rotation fields. In generating a twin deformation, the Jacobian determinants can be either continuous or discontinuous across the twin boundary. This is discussed in detail, and some examples of these deformations are shown.

In **Section 3.4**, the kinematics of twin deformation in an elastic region is reviewed. An in-depth analysis of the constraints on the pair of rotation fields that must be upheld in order to generate a twin deformation that maps a prescribed twin boundary curve to another are discussed in detail. Some example problems are shown for various twin elastic deformations.

3.2 Constructing a plane finite deformation field that maps one prescribed curve to another given a rotation field

If $\theta(x_1, x_2)$ is a given scalar field that is continuous on a region B, then a rotation field $\boldsymbol{R}$ can be fully determined through (2.3.2). With $\boldsymbol{R}$ as defined, a generated mapping $\boldsymbol{y}(\boldsymbol{x})$ can be constructed in terms of a complex valued function $\hat{y}$. Let $\rho(x_1, x_2) = \hat{\rho}(z, \overline{z})$ be an arbitrary positive, real valued function of its arguments, and $\tilde{h}(\overline{z})$ be a function analytic in $\overline{z}$. If $\theta(x_1, x_2) = \hat{\theta}(z, \overline{z})$,

$$\hat{y}(z, \overline{z}) = \int_{z_0}^{z} \hat{\rho}(\zeta, \overline{z}) e^{i\hat{\theta}(\zeta, \overline{z})} d\zeta + \tilde{h}(\overline{z}), \tag{3.2.1}$$

then the following constructs a deformation, where $z_0 = x_1^0 + ix_2^0$ is a point of interest in region B, and $\zeta = \zeta_1 + i\zeta_2$ is the complex variable of integration. This relationship comes from integrating (2.3.10) with respect to z. It was shown in the previous chapter that it is possible to assign functions to $\hat{\rho}(z,\overline{z})$ and $\tilde{h}(\overline{z})$ so that the deformation in (3.2.1) satisfies (2.3.14) for a neighborhood N surrounding a point of interest (x_1^0, x_2^0).

Suppose now we are given a rotation field $\boldsymbol{R}$, and wish to find a plane deformation field $\boldsymbol{y}(\boldsymbol{x})$ that corresponds to $\boldsymbol{R}$ and also maps a prescribed curve onto another prescribed curve. Define the initial prescribed curve as C and the curve to which C maps to as C^*.

Let the prescribed curves C and C^* be parameterized as followed:

$$C: \ \boldsymbol{x} = \tilde{\boldsymbol{x}}(s), \ \ (0 < s < s_0), \tag{3.2.2}$$

$$C^*: \ \boldsymbol{y} = \tilde{\boldsymbol{y}}(s), \ \ (0 < s < s_0), \tag{3.2.3}$$

such that the deformation $\boldsymbol{y}(\boldsymbol{x})$ maps C to C^*,

$$\boldsymbol{y}(x_1(s), x_2(s)) = \tilde{\boldsymbol{y}}(s), \tag{3.2.4}$$

where s is defined as arc-length along the curve C, and s_0 is a constant defining the upper bound of the arc-length. Differentiating (3.2.4) with respect to s and using the definition of the polar decomposition of $\boldsymbol{F}$ in (2.3.1) we get the expression:

$$\boldsymbol{F}\dot{\tilde{\boldsymbol{x}}} = \boldsymbol{R}\boldsymbol{U}\dot{\tilde{\boldsymbol{x}}} = \dot{\tilde{\boldsymbol{y}}} \ \text{ on } C, \tag{3.2.5}$$

which can be rewritten to give,

$$\boldsymbol{U}\dot{\tilde{\boldsymbol{x}}} = \boldsymbol{R}^T \dot{\tilde{\boldsymbol{y}}}, \tag{3.2.6}$$

where dots above $\tilde{\boldsymbol{x}}$ and $\tilde{\boldsymbol{y}}$ imply derivatives with respect to s. Because the stretch tensor $\boldsymbol{U}$ is symmetric and positive definite, the scalar function ψ defined as,

$$\begin{aligned}\psi &= \dot{\tilde{\boldsymbol{x}}} \cdot \boldsymbol{U} \dot{\tilde{\boldsymbol{x}}} = \dot{\tilde{\boldsymbol{y}}} \cdot \boldsymbol{R} \dot{\tilde{\boldsymbol{x}}} \\ &= \left(\dot{\tilde{x}}_1 \dot{\tilde{y}}_1 + \dot{\tilde{x}}_2 \dot{\tilde{y}}_2 \right) \cos(\theta) + \left(\dot{\tilde{x}}_1 \dot{\tilde{y}}_2 - \dot{\tilde{x}}_2 \dot{\tilde{y}}_1 \right) \sin(\theta) \ > \ 0 \ ,\end{aligned} \tag{3.2.7}$$

must be positive. Described in (3.2.7) is a condition that must be met by the two prescribed curves C, C^* and the angle θ.

As discussed in the previous chapter, the curves C and C^*, if infinitely smooth, can be represented in terms of functions $\tilde{z}(\overline{z})$ and $\tilde{y}(\overline{z})$, both analytic in $\overline{z}$, such that,

$$z = \tilde{z}(\overline{z}) = \tilde{x}_1(s) + i\tilde{x}_2(s), \ \text{ on } C, \tag{3.2.8}$$

$$y = \tilde{y}(\overline{z}) = \tilde{y}_1(s) + i\tilde{y}_2(s), \ \ z = \tilde{z}(\overline{z}) \ \text{ on } C^*. \tag{3.2.9}$$

Using this representation of C and C^*, a deformation $\boldsymbol{y}$ may be generated from a prescribed $\theta(x_1, x_2) = \hat{\theta}(z, \overline{z})$ which maps C to C^*,

$$\hat{y}(z, \overline{z}) = \int_{\tilde{z}(\overline{z})}^{z} \hat{\rho}(\zeta, \overline{z}) e^{i\hat{\theta}(\zeta, \overline{z})} d\zeta + \tilde{y}(\overline{z}), \tag{3.2.10}$$

where again $\zeta = \zeta_1 + i\zeta_2$ is the complex variable of integration and $\rho(x_1, x_2) = \hat{\rho}(z, \overline{z})$ is a positive, real valued function of its arguments, chosen so that the deformation in (3.2.10) satisfies (2.3.14).

To see that it is possible to find a $\hat{\rho}(z,\overline{z})$ which agrees with (2.3.14), we differentiate (3.2.10) and evaluate the results on C, noting that on C $z = \tilde{z}(\overline{z})$. Thus (2.3.13) gives:

$$\begin{aligned} J &= \left|\hat{y}_z\right|^2 - \left|\hat{y}_{\overline{z}}\right|^2 \\ &= \hat{\rho}(\tilde{z}(\overline{z}),\overline{z})^2 - \left|\hat{y}_{\overline{z}}\right|^2 \\ &= 2\hat{\rho}(\tilde{z}(\overline{z}),\overline{z})\,\mathrm{Re}\left\{e^{-i\hat{\theta}(z,\overline{z})}\tilde{y}'(\overline{z})/\tilde{z}'(\overline{z})\right\} - \left|\tilde{y}'(\overline{z})\right|^2 \quad \text{, on } C, \end{aligned} \tag{3.2.11}$$

where apostrophes represent derivates with respect to $\overline{z}$. Let the terms in (3.2.11) be represented by real scalar functions,

$$\hat{\psi} = \mathrm{Re}\left\{e^{-i\hat{\theta}(z,\overline{z})}\tilde{y}'(\overline{z})/\tilde{z}'(\overline{z})\right\}, \tag{3.2.12}$$

$$\hat{\chi} = \left|\tilde{y}'(\overline{z})\right|^2, \tag{3.2.13}$$

such that $J = 2\hat{\rho}(\tilde{z}(\overline{z}),\overline{z})\hat{\psi} - \hat{\chi}$ on C. It was shown that $\hat{\psi} = \psi$ as defined in (3.2.7). Therefore, $\hat{\psi} > 0$ and by the definition of our problem $\hat{\chi} \geq 0$ such that the following condition for $\hat{\rho}(\tilde{z}(\overline{z}),\overline{z})$ can be concluded,

$$\hat{\rho}(\tilde{z}(\overline{z}),\overline{z}) > \frac{\hat{\chi}}{2\hat{\psi}} \quad \text{, on } C. \tag{3.2.14}$$

So for (2.3.14) to hold, $\hat{\rho}(\tilde{z}(\overline{z}),\overline{z})$ must satisfy,

$$\hat{\rho}(\tilde{z}(\overline{z}),\overline{z})_{min} > \frac{\hat{\chi}_{max}}{2\hat{\psi}_{min}} \quad \text{, on } C, \tag{3.2.15}$$

where $\hat{\chi}_{max}$ and $\hat{\psi}_{min}$ are the maximum and minimum values of their respective functions on C, and $\hat{\rho}(\tilde{z}(\overline{z}),\overline{z})_{min}$ is the minimum possible positive value taken by the function $\hat{\rho}(\tilde{z}(\overline{z}),\overline{z})$ on C. Thus, as long as $\hat{\rho}(z,\overline{z})$ is taken so that (3.2.15) holds on C, then it is possible to find a plane deformation represented as $\hat{y}$ that corresponds to $\boldsymbol{R}$ fully determined by $\hat{\theta}$ and maps a prescribed curve C onto C^* in a neighborhood N surrounding C on B.

3.3 Generating Twin Finite Deformations from Prescribed Rotation Fields

Kinematics of twin deformation

The kinematics of twinning, shear banding, and two-phase deformations have been studied quite thoroughly by James (1981, 1987), Pitteri (1985), Parry (1986), Gurtin (1983), and Ericksen (1985), among others. Before we begin our analysis of a means of computing a twin finite plane deformation from arbitrarily assigned rotation fields defined on regions separated by a prescribed curve (twin boundary), we will review the kinematics involved in twin deformation.

A plane deformation $\boldsymbol{y} = \boldsymbol{y}(\boldsymbol{x})$ represents twinning if there exists a curve C across which the deformation $\boldsymbol{y}$ is continuous, but its gradient field $\boldsymbol{F}$ is discontinuous. The Maxwell condition [2] asserts that this jump in $\boldsymbol{F}$ across C admits the representation:

$$\boldsymbol{F}^{+} - \boldsymbol{F}^{-} = \boldsymbol{a} \otimes \boldsymbol{n}, \tag{3.3.1}$$

where $\boldsymbol{n}$ is a unit normal vector to C, $\boldsymbol{a}$ is a vector, and $\boldsymbol{F}^{+}$ and $\boldsymbol{F}^{-}$ are the deformation fields taken on by $\boldsymbol{F}$ on either side of C with $(+)$ and $(-)$ indicating each side of the twin deformation (See Figure 3.1).

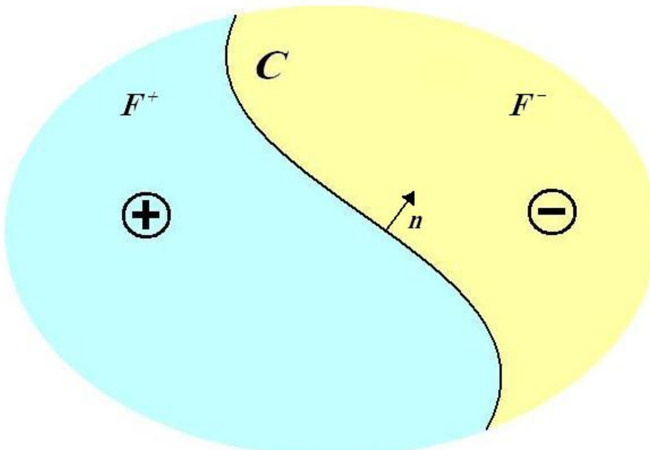

Figure 3.1: Schematic of a twin deformation with the twin boundary defined as C .

The polar decomposition of the deformation gradients on either side of C are defined as,

$$\boldsymbol{F}^{+} = \boldsymbol{R}^{+}\boldsymbol{U}^{+} = \boldsymbol{V}^{+}\boldsymbol{R}^{+}, \tag{3.3.2}$$

$$\boldsymbol{F}^{-} = \boldsymbol{R}^{-}\boldsymbol{U}^{-} = \boldsymbol{V}^{-}\boldsymbol{R}^{-}. \tag{3.3.3}$$

Substituting (3.3.2) and (3.3.3) into (3.3.1) gives,

$$\boldsymbol{R}^{+}\boldsymbol{U}^{+} - \boldsymbol{R}^{-}\boldsymbol{U}^{-} = \boldsymbol{a} \otimes \boldsymbol{n}, \tag{3.3.4}$$

representing the jump condition across C in terms of the stretch and rotation tensors corresponding to the regions on either side of C.

*Result 3.1: If either stretch field **U** or **V** is continuous across the twin boundary **C**, then **R** and therefore **F** are continuous across **C** as well.*

We will now examine a special case of twinning where,

$$\boldsymbol{U}^{+} = \boldsymbol{U}^{-} = \boldsymbol{U}\,, \tag{3.3.5}$$

on a twin boundary. If the right polar decomposition factor (or left, since this result can be shown using either form of the polar decomposition of the deformation gradient) is continuous across the twin boundary, then the rotation field is continuous as well, and therefore the deformation gradient is continuous across a twin boundary.

To see this assume (3.3.5), and note that (3.3.4) can be rewritten as:

$$\boldsymbol{R}^{+}\boldsymbol{U} - \boldsymbol{R}^{-}\boldsymbol{U} = \boldsymbol{a} \otimes \boldsymbol{n}\,, \tag{3.3.6}$$

which simplifies to,

$$\boldsymbol{R}^{+} - \boldsymbol{R}^{-} = \boldsymbol{a} \otimes \boldsymbol{U}^{-1}\boldsymbol{n} \quad \text{on } C\,. \tag{3.3.7}$$

Multiplying the transpose of $\boldsymbol{R}^{+}$ to (3.3.7) gives:

$$(\boldsymbol{R}^{+})^{T}\boldsymbol{R}^{-} = \boldsymbol{1} - (\boldsymbol{R}^{+})^{T}\boldsymbol{a} \otimes \boldsymbol{U}^{-1}\boldsymbol{n}\,, \tag{3.3.8}$$

where $\boldsymbol{1}$ is defined as the identity matrix. Let the left hand side of (3.3.8) be defined as,

$$\boldsymbol{T} = \boldsymbol{1} - (\boldsymbol{R}^{+})^{T}\boldsymbol{a} \otimes \boldsymbol{U}^{-1}\boldsymbol{n}\,, \tag{3.3.9}$$

where $\boldsymbol{T} \equiv (\boldsymbol{R}^{+})^{T}\boldsymbol{R}^{-}$ is proper orthogonal. Let $\boldsymbol{b} \equiv (\boldsymbol{R}^{+})^{T}\boldsymbol{a}$ and $\boldsymbol{c} \equiv \boldsymbol{U}^{-1}\boldsymbol{n}$ so that (3.3.9) becomes:

$$\boldsymbol{T} = \boldsymbol{1} - \boldsymbol{b} \otimes \boldsymbol{c}\,. \tag{3.3.10}$$

Multiply (3.3.10) by $\boldsymbol{T}^{T}$ and then substitute the transpose of (3.3.10) into the new equation. This gives:

$$\begin{aligned} \boldsymbol{T}\boldsymbol{T}^{T} &= \boldsymbol{T}^{T} - \boldsymbol{b} \otimes \boldsymbol{T}\boldsymbol{c} \\ \boldsymbol{1} &= (\boldsymbol{1} - \boldsymbol{b} \otimes \boldsymbol{c})^{T} - \boldsymbol{b} \otimes (\boldsymbol{1} - \boldsymbol{b} \otimes \boldsymbol{c})\boldsymbol{c} \\ &= \boldsymbol{1} - \boldsymbol{c} \otimes \boldsymbol{b} - \boldsymbol{b} \otimes \boldsymbol{c} + \left|\boldsymbol{c}^{2}\right| \boldsymbol{b} \otimes \boldsymbol{b}\,, \end{aligned} \tag{3.3.11}$$

simplifying to the form,

$$\boldsymbol{0} = -\boldsymbol{c} \otimes \boldsymbol{b} - \boldsymbol{b} \otimes \boldsymbol{c} + \left|\boldsymbol{c}^{2}\right| \boldsymbol{b} \otimes \boldsymbol{b}\,. \tag{3.3.12}$$

Looking at (3.3.12), it is easily seen that both $\boldsymbol{b} = \boldsymbol{0}$ and $\boldsymbol{c} = \boldsymbol{0}$ are possible solutions.

The other possible solution for $\boldsymbol{b}$ and $\boldsymbol{c}$ that makes (3.3.12) true can be found by taking the trace of (3.3.12),

$$0 = -2\boldsymbol{b}\cdot\boldsymbol{c} + \left|\boldsymbol{c}^{2}\right|\left|\boldsymbol{b}^{2}\right|, \tag{3.3.13}$$

which can be rewritten as,

$$\boldsymbol{b}\cdot\boldsymbol{c} = \frac{1}{2}\left|\boldsymbol{b}^{2}\right|\left|\boldsymbol{c}^{2}\right|. \tag{3.3.14}$$

Multiplying (3.3.12) by $\boldsymbol{b}$ gives:

$$\begin{aligned}\boldsymbol{0} &= \left(-\boldsymbol{c}\otimes\boldsymbol{b}-\boldsymbol{b}\otimes\boldsymbol{c}+\left|\boldsymbol{c}^2\right|\boldsymbol{b}\otimes\boldsymbol{b}\right)\boldsymbol{b} \\ &= -\left|\boldsymbol{b}^2\right|\boldsymbol{c}-\left(\boldsymbol{c}\cdot\boldsymbol{b}\right)\boldsymbol{b}+\left|\boldsymbol{c}^2\right|\left|\boldsymbol{b}^2\right|\boldsymbol{b}\ .\end{aligned} \tag{3.3.15}$$

Substituting the relationship from (3.3.14) into (3.3.15) gives,

$$\begin{aligned}\boldsymbol{0} &= -\left|\boldsymbol{b}^2\right|\boldsymbol{c}-\frac{1}{2}\left|\boldsymbol{c}^2\right|\left|\boldsymbol{b}^2\right|\boldsymbol{b}+\left|\boldsymbol{c}^2\right|\left|\boldsymbol{b}^2\right|\boldsymbol{b} \\ &= -\left|\boldsymbol{b}^2\right|\boldsymbol{c}+\frac{1}{2}\left|\boldsymbol{c}^2\right|\left|\boldsymbol{b}^2\right|\boldsymbol{b}\ ,\end{aligned} \tag{3.3.16}$$

and since we are looking for non-zero solutions for $\boldsymbol{b}$ and $\boldsymbol{c}$, (3.3.16) reduces to the form:

$$\boldsymbol{b} = 2\boldsymbol{c}/\left|\boldsymbol{c}^2\right|. \qquad (3.3.17)[2]$$

If we substitute $\boldsymbol{b} = 2\boldsymbol{c}/\left|\boldsymbol{c}^2\right|$ into (3.3.10) we get,

$$\begin{aligned}\boldsymbol{T} &= \boldsymbol{1}-2\boldsymbol{c}/\left|\boldsymbol{c}^2\right|\otimes\boldsymbol{c} \\ &= \boldsymbol{1}-2\left(\frac{\boldsymbol{c}}{|\boldsymbol{c}|}\otimes\frac{\boldsymbol{c}}{|\boldsymbol{c}|}\right) \\ &= \boldsymbol{1}-2\boldsymbol{m}\otimes\boldsymbol{m}\ ,\end{aligned} \tag{3.3.18}$$

where $\boldsymbol{m}$ is a unit vector. However, (3.3.18) implies that $\det\boldsymbol{T} = -1$, which contradicts the requirement that $\boldsymbol{T}$ be proper orthogonal.

Thus the only possible solutions for $\boldsymbol{b}$ and $\boldsymbol{c}$ that hold are $\boldsymbol{b}=\boldsymbol{0}$ or $\boldsymbol{c}=\boldsymbol{0}$, which in turn implies that both $\boldsymbol{R}^+ = \boldsymbol{R}^-$ and $\boldsymbol{F}^+ = \boldsymbol{F}^-$ on C as well. A similar derivation to the

[2] It can be shown that (3.3.17) can also be written in the form $\boldsymbol{c} = 2\boldsymbol{b}/\left|\boldsymbol{b}^2\right|$.

one shown here can be performed with the same results using the left stretch tensor $\boldsymbol{V}$ for the case of $\boldsymbol{V}^+ = \boldsymbol{V}^-$ on C.

Result 3.2: If a rotation field ***R*** *is continuous across the twin boundary C, then the vector* ***a*** *in (3.3.1) must have the form* $\boldsymbol{a} = \alpha \boldsymbol{R}\boldsymbol{n}$.

Now we will examine the special case where,

$$\boldsymbol{R}^+ = \boldsymbol{R}^- = \boldsymbol{R}, \tag{3.3.19}$$

on a twin boundary. If a twin deformation has continuous rotation fields $\boldsymbol{R}^+ = \boldsymbol{R}^-$ across the twin boundary, then $\boldsymbol{F}^+ - \boldsymbol{F}^- = \alpha \boldsymbol{R}\boldsymbol{n} \otimes \boldsymbol{n}$ where α is a scalar and $\boldsymbol{n}$ is a vector normal to the twin boundary.

Assuming (3.3.19), (3.3.4) becomes:

$$\boldsymbol{R}\boldsymbol{U}^+ - \boldsymbol{R}\boldsymbol{U}^- = \boldsymbol{a} \otimes \boldsymbol{n}, \tag{3.3.20}$$

which can be rewritten as,

$$\boldsymbol{U}^+ - \boldsymbol{U}^- = \boldsymbol{R}^T \boldsymbol{a} \otimes \boldsymbol{n}. \tag{3.3.21}$$

Let the left hand side of (3.3.21) be defined as:

$$\boldsymbol{S} = \boldsymbol{R}^T \boldsymbol{a} \otimes \boldsymbol{n}, \tag{3.3.22}$$

where $\boldsymbol{S} \equiv \boldsymbol{U}^+ - \boldsymbol{U}^-$, is symmetric since it is made up of the difference between two symmetric tensors. Since $\boldsymbol{S}$ is symmetric, then (3.3.22) must have the form,

$$\boldsymbol{S} = \alpha \boldsymbol{n} \otimes \boldsymbol{n}, \tag{3.3.23}$$

where,

$$\boldsymbol{R}^T \boldsymbol{a} = \alpha \boldsymbol{n}, \tag{3.3.24}$$

must be true. Using (3.3.24), we get the following expression for $\boldsymbol{a}$,

$$\boldsymbol{a} = \alpha \boldsymbol{R} \boldsymbol{n} \tag{3.3.25}$$

such that (3.3.1) becomes,

$$\boldsymbol{F}^+ - \boldsymbol{F}^- = \alpha \boldsymbol{R} \boldsymbol{n} \otimes \boldsymbol{n}. \tag{3.3.26}$$

*Construction of a twin deformation corresponding to pre-assigned rotation fields, a twin boundary curve C, and its image C**

We assume that the prescribed twin boundary C and its image C^* are infinitely smooth curves that are parameterized as described in (3.2.2) and (3.2.3). As in (3.2.8) and (3.2.9), C and C^* may be represented by functions $\tilde{z}(\overline{z})$ and $\tilde{y}(\overline{z})$, which are analytic functions of $\overline{z}$.

The rotation fields $\boldsymbol{R}^+$ and $\boldsymbol{R}^-$ are respectively defined on either side of C, where $\boldsymbol{R}^+$ is defined on one side of C in a region B^+ and $\boldsymbol{R}^-$ is defined on the other side of C in a region B^-, such that region $B = B^+ \cup B^-$. Both $\boldsymbol{R}^+$ and $\boldsymbol{R}^-$ are fully determined by scalar functions θ^+ and θ^- (see Figure 3.2).

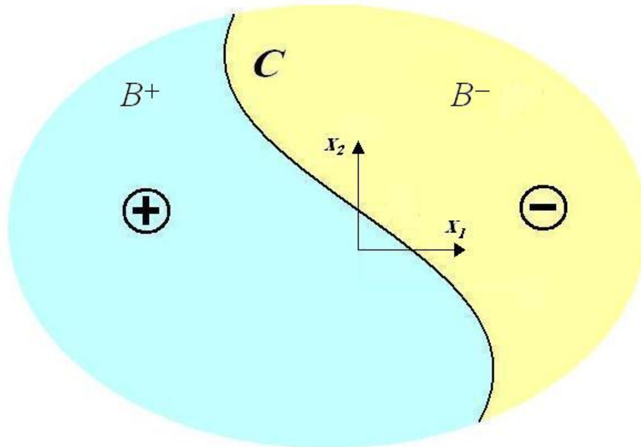

(A)

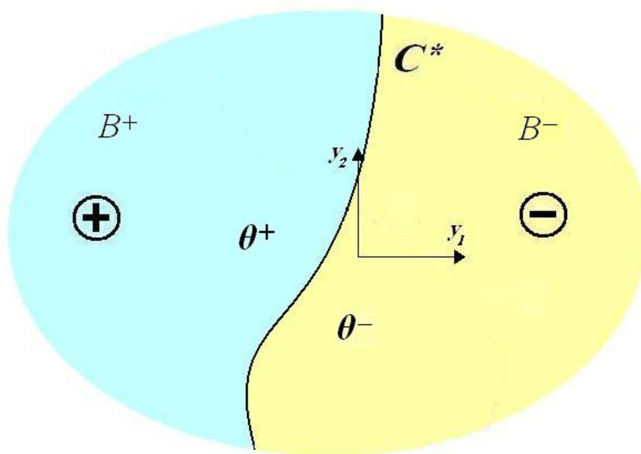

(B)

Figure 3.2: **(A)** The undeformed configuration of a region $B = B^{+} \cup B^{-}$ divided by a curve C defined as the twin boundary. **(B)** Twin deformation of the region $B = B^{+} \cup B^{-}$ generated by the rotation fields $\boldsymbol{R}^{+}$ and $\boldsymbol{R}^{-}$ defined on either side of the curve C, which are fully determined by scalar functions θ^{+} and θ^{-} . The curve C is mapped to the curve $C*$ defined as the twin boundary in the deformed configuration.

Let $\hat{\rho}^{+}(z,\overline{z})$ and $\hat{\rho}^{-}(z,\overline{z})$ be real-valued functions that each obeys (3.2.15) on C. Setting $\hat{\rho}^{+}(z,\overline{z}) = \hat{\rho}^{+}$ and $\hat{\rho}^{-}(z,\overline{z}) = \hat{\rho}^{-}$ as constants, the integral in (3.2.10) that defines a deformation in a neighborhood of C takes the form for each side of the twin boundary as,

$$\hat{y}^{+}(z,\overline{z}) = \hat{\rho}^{+}\int_{\tilde{z}(\overline{z})}^{z} e^{i\hat{\theta}^{+}(\zeta,\overline{z})}d\zeta + \tilde{y}(\overline{z}), \text{ on } B^{+}, \tag{3.3.27}$$

$$\hat{y}^{-}(z,\overline{z}) = \hat{\rho}^{-}\int_{\tilde{z}(\overline{z})}^{z} e^{i\hat{\theta}^{-}(\zeta,\overline{z})}d\zeta + \tilde{y}(\overline{z}), \text{ on } B^{-}, \tag{3.3.28}$$

where the $(+)$ and $(-)$ indicate the regions on either side of C as shown in Fig 2. Similar to the untwined case, (3.3.27) and (3.3.28) generate, from prescribed rotation fields $\boldsymbol{R}^{+}$ and $\boldsymbol{R}^{-}$ determined by $\hat{\theta}^{+}$ and $\hat{\theta}^{-}$, plane deformations represented as $\hat{y}^{+}(z,\overline{z})$ and $\hat{y}^{-}(z,\overline{z})$ that are continuous on C, and map a prescribed curve C onto C^{*} in a neighborhood N^{+} and N^{-} contained in B with positive Jacobian.

In general, for this type of deformation, the Jacobian J is discontinuous across the twin boundary C. Later, we will show that it is possible to generate a twin deformation for which the Jacobian J is continuous across C if it is assumed that $e^{i\hat{\theta}^{+}(z,\overline{z})}$ may be continuously extended across C onto N^{-}. Both these cases are discussed next, in which several examples are given.

Example 3.1: Discontinuous Jacobian across twin boundary

Suppose the rotation fields on either side of the twin boundary are determined by the scalar functions,

$$\theta^{+}(x_1,x_2)=2x_1\ ,\qquad \hat{\theta}^{+}(z,\overline{z})=z+\overline{z}\ , \tag{3.3.29}$$

$$\theta^{-}(x_1,x_2)=2x_2\ ,\qquad \hat{\theta}^{-}(z,\overline{z})=-i(z-\overline{z})\ . \tag{3.3.30}$$

Let the twin boundary C in the undeformed configuration be a vertical line on the x_2-axis defined as,

$$\left(x_1,x_2\right)=\left(\tilde{x}_1(s),\tilde{x}_2(s)\right)=\left(0,s\right)\ ,\quad \left(-1\le s\le 1\right), \tag{3.3.31}$$

(See Figure 3(A)). Referring to (3.2.8), this curve can be defined by the analytic function,

$$\tilde{z}(\overline{z})=-\overline{z}\ ,\ \text{ on } C\ , \tag{3.3.32}$$

which implies a curve of $x_1=0$ so that $z=\tilde{z}(\overline{z})=-\overline{z}$ on C.

The image C^* of C is the unit circle,

$$\left(y_1,y_2\right)=\left(\tilde{y}_1(s),\tilde{y}_2(s)\right)=\left(\cos(s),\sin(s)\right)\ ,\quad \left(-\pi\le s\le\pi\right). \tag{3.3.33}$$

Referring to (3.2.9), C^* can be defined by the analytic function $\tilde{y}(\overline{z})$ for this example as,

$$y=\tilde{y}(\overline{z})=e^{-\overline{z}}\ ,\quad z=\tilde{z}(\overline{z})=-\overline{z}\ , \tag{3.3.34}$$

for the case of a vertical line mapped to the unit circle. This is shown below.

If C is defined as a vertical line along the x_2-axis, then $x_1 = 0$ such that $z = ix_2$ and $\overline{z} = -ix_2$, which gives the representation of C in (3.3.32). Thus finding a function analytic in $\overline{z}$ given (3.3.32) where C maps to the unit circle is done by,

$$\begin{aligned} y(0, x_2) &= y_1(x_2) + iy_2(x_2) \\ &= \cos(x_2) + i\sin(x_2) \\ &= e^{ix_2} \ . \end{aligned} \tag{3.3.35}$$

To see that these functions define C and C^*, note that $z = \tilde{z}(\overline{z}) = -\overline{z}$ on C such that $x_1 = 0$, therefore $z = -\overline{z} = ix_2$ on C. From (2.3.9), it can be seen that (3.3.35) is equivalent to (3.3.34).

To construct the deformation, let $\hat{\rho}^+$ and $\hat{\rho}^-$ be prescribed as,

$$\hat{\rho}^+ = 7, \tag{3.3.36}$$

$$\hat{\rho}^- = 1, \tag{3.3.37}$$

where it can be seen that $\hat{\rho}^+$ and $\hat{\rho}^-$ defined this way both agree with the condition for $\hat{\rho}(\tilde{z}(\overline{z}), \overline{z})$ in (3.2.15) for our prescribed curves C and C^*. This is seen by solving for ψ^+ and ψ^-, and for $\hat{\chi}$. For this example $\psi^+ = \psi^- = \psi$ such that from (3.2.12) and (3.2.13), we get:

$$\hat{\psi} = \psi = \cos(x_2), \tag{3.3.38}$$

$$\hat{\chi} = 1. \tag{3.3.39}$$

For C defined in (3.3.31), (3.2.15) becomes,

$$\hat{\rho}_{min} > 0.93, \text{ on } C, \tag{3.3.40}$$

in which both (3.3.36) and (3.3.37) agree.

Substituting (3.3.29), (3.3.30), (3.3.32), (3.3.34), (3.3.36) and (3.3.37) into (3.3.27) and (3.3.28), and carrying out the integrations, lead to:

$$\hat{y}^{+}(z,\overline{z}) = -i\left(7e^{i(z+\overline{z})} + ie^{-\overline{z}} - 7\right), \text{ in } B^{+}, \tag{3.3.41}$$

$$\hat{y}^{-}(z,\overline{z}) = e^{(z-\overline{z})} - e^{-2\overline{z}} + e^{-\overline{z}}, \text{ in } B^{-}. \tag{3.3.42}$$

Stated in (2.3.8), the components of the deformation for each side of the twin boundary can be found by taking the real and imaginary parts of (3.3.41) and (3.3.42), but these are long expressions and thus will be omitted. The Jacobain determinants J^{+} and J^{-} will not be shown for the same reason, but in Figure 3.3(A) the discontinuity between the determinants across the twin boundary defined as the x_2-axis can be seen.

As seen in Figure 3.3(A), the range of values $\{x_1 = 0,\ (-1 \le x_2 \le 1)\}$ for the curve C does correspond to positive J^{+} and J^{-}. The rotation matrices for the twin deformation are:

$$\boldsymbol{R}^{+} = \begin{bmatrix} \cos(2x_1) & -\sin(2x_1) \\ \sin(2x_1) & \cos(2x_1) \end{bmatrix}, \text{ in } B^{+}, \tag{3.3.43}$$

$$\boldsymbol{R}^{-} = \begin{bmatrix} \cos(2x_2) & -\sin(2x_2) \\ \sin(2x_2) & \cos(2x_2) \end{bmatrix}, \text{ in } B^{-}. \tag{3.3.44}$$

The twin deformation in (3.3.41) and (3.3.42) is illustrated in Figure 3.3, where a square centered at the origin with a side length of 0.5 is deformed by the rotations in (3.3.43) and (3.3.44).

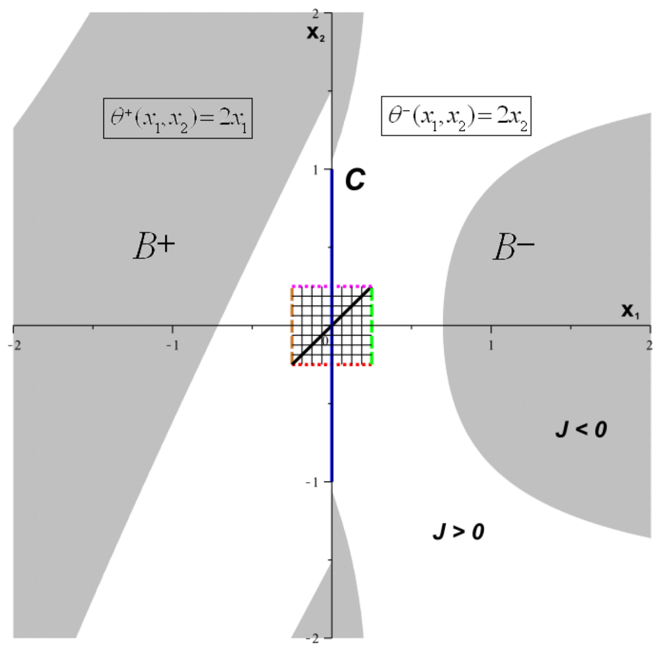

(A)

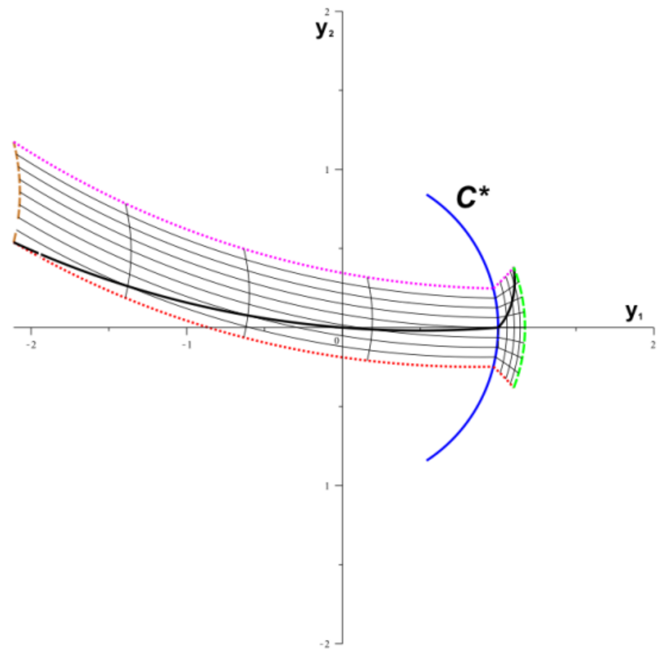

(B)

Figure 3.3: **(A)** Contour plot of the Jacobian determinants J^+ and J^- for the deformation (3.3.41) and (3.3.42), and twin boundary $C : \{x_1{=}0,\ (-1{\le}x_2{\le}1)\}$. In the unshaded regions $J^+ > 0$ or $J^- > 0$ depending on which side of the twin boundary is being examined, and in the shaded region $J^+ < 0$ or $J^- < 0$. A square of side length 0.5 centered at the origin is shown as well. **(B)** The deformation generated from rotations $\theta^+(x_1, x_2) = 2x_1$ and $\theta^-(x_1, x_2) = 2x_2$, with the square mapped to its image, and the twin boundary mapped to the unit circle $C*$.

Example 3.2

In this example, let the rotation fields be described by scalar functions,

$$\theta^+(x_1, x_2) = 2x_1 \ , \qquad \hat{\theta}^+(z, \overline{z}) = z + \overline{z} \ , \tag{3.3.45}$$

$$\theta^-(x_1, x_2) = x_1^2 + x_2^2 \ , \qquad \hat{\theta}^-(z, \overline{z}) = z\overline{z} \ . \tag{3.3.46}$$

Let the twin boundary C be a horizontal line along the x_1-axis defined as,

$$\left(x_1, x_2\right) = \left(\tilde{x}_1(s), \tilde{x}_2(s)\right) = \left(s, 0\right) \ , \quad \left(-0.5 \le s \le 0.5\right). \tag{3.3.47}$$

Referring to (3.2.8), C can be defined by the analytic function,

$$z = \tilde{z}(\overline{z}) = \overline{z}\ , \text{ on } C\ . \tag{3.3.48}$$

Let the twin boundary C map to a sine wave given by,

$$\left(y_1, y_2\right) = \left(\tilde{y}_1(s), \tilde{y}_2(s)\right) = \left(s, a\sin(ks)\right)\ , \quad \left(-0.5 \le s \le 0.5\right), \tag{3.3.49}$$

where a and k are scalar values related to the sine wave's amplitude and period. For our example let $a = 1/10$ and $k = 10$, such that referring to (3.2.9), $C*$ can be defined by the analytic function $\tilde{y}(\overline{z})$ such that,

$$y = \tilde{y}(\overline{z}) = \overline{z} + i\frac{1}{10}\sin(10\overline{z})\,. \tag{3.3.50}$$

It can be easily shown that this representation in (3.3.50) gives,

$$y_1 + iy_2 = x_1 + i\frac{1}{10}\sin(10x_1)\,, \text{ with } z = \overline{z} = x_1\,. \tag{3.3.51}$$

To construct the deformation, let $\hat{\rho}^+$ and $\hat{\rho}^-$ be prescribed as,

$$\hat{\rho}^+ = 4\,, \tag{3.3.52}$$

$$\hat{\rho}^- = 2\,. \tag{3.3.53}$$

As in the previous example, it can be seen that $\hat{\rho}^+$ and $\hat{\rho}^-$ defined this way do satisfy (3.2.15), and the derivation showing this is similar to that done in the previous example.

Carrying out the integration in (3.3.27) and (3.3.28) for this example gives,

$$\hat{y}^{+}(z,\overline{z}) = i\left(4e^{2i\overline{z}} - 4e^{i(z+\overline{z})} + \frac{1}{10}\sin(10\overline{z}) - i\overline{z}\right), \text{ in } B^{+}, \tag{3.3.54}$$

$$\hat{y}^{-}(z,\overline{z}) = 2ze^{iz\overline{z}} - 2\overline{z}e^{iz\overline{z}} + zb + \frac{1}{10}i\sin(10\overline{z}), \text{ in } B^{-}. \tag{3.3.55}$$

As before, the components of the deformation on each side of the twin boundary can be found by taking the real and imaginary parts of (3.3.54) and (3.3.55), but they are long expressions. The Jacobain determinants J^{+} and J^{-} will not be shown for the same reason, but in Fig 4(A) it can be seen where they are positive, negative and zero for this twin deformation.

In Figure 3.4(A), it can be seen that the range of values $\{(-1 \le x_1 \le 1)\ , x_2 = 0\}$ for the curve C do correspond to positive J^{+} and J^{-}, which confirms that our choices for ρ^{+} and ρ^{-} do agree with (3.2.15). As expected, the rotation matrices derived from (3.3.45) and (3.3.46) for the twin deformation are:

$$\boldsymbol{R}^{+} = \begin{bmatrix} \cos(2x_1) & -\sin(2x_1) \\ \sin(2x_1) & \cos(2x_1) \end{bmatrix}, \text{ in } B^{+}, \tag{3.3.56}$$

$$\boldsymbol{R}^{-} = \begin{bmatrix} \cos(x_1^2 + x_2^2) & -\sin(x_1^2 + x_2^2) \\ \sin(x_1^2 + x_2^2) & \cos(x_1^2 + x_2^2) \end{bmatrix}, \text{ in } B^{-}. \tag{3.3.57}$$

The twin deformation in (3.3.54) and (3.3.55) is shown in Figure 3.4, where a rectangle centered at the origin with side lengths 0.1 and 0.6 is deformed by the rotations in (3.3.56) and (3.3.57).

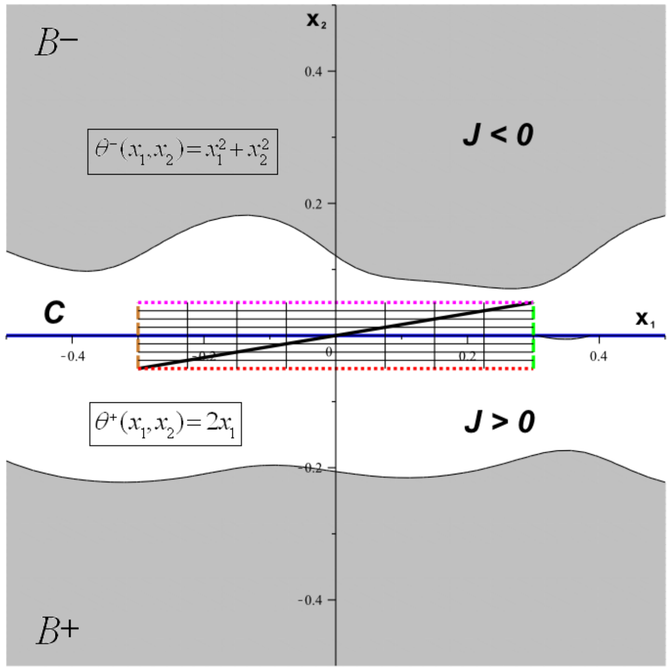

B−
x₂
0.4
J < 0
$\theta^-(x_1,x_2)=x_1^2+x_2^2$
0.2
C
x₁
-0.4
0
0.2
0.4
$\theta^+(x_1,x_2)=2x_1$
J > 0
-0.2
-0.4
B+

(A)

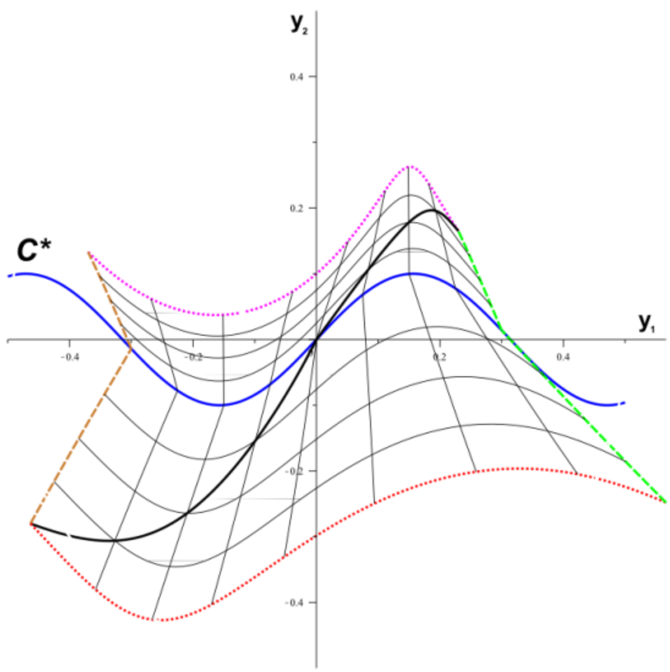

y₂
0.4
0.2
C*
y₁
-0.4
-0.2
0.2
0.4
-0.2
-0.4

(B)

Figure 3.4: **(A)** Contour plot of the Jacobian determinants J^+ and J^- for the deformation (3.3.54) and (3.3.55), and twin boundary $C:\{x_2=0,\ (-0.5\le x_1\le 0.5)\}$. In the unshaded regions $J^+>0$ or $J^->0$ depending on which side of the twin boundary is being examined, and in the shaded region $J^+<0$ or $J^-<0$. Also, a rectangle with side lengths 0.1 and 0.6 centered at the origin. **(B)** The deformation generated from rotations $\theta^+(x_1,x_2)=2x_1$ and $\theta^-(x_1,x_2)=x_1^2+x_2^2$, with the rectangle mapped to its image, and the twin boundary mapped to a sine wave $C*$.

Continuous Jacobians across twin boundary

In order to produce a twin deformation where the Jacobian J is continuous across the twin boundary ($J^+=J^-$, on C), and maps C to $C*$, let the integral in (3.2.10) that describes the deformation around C take the following form for each side of the twin boundary,

$$\hat{y}^+(z,\overline{z})=\int_{\tilde{z}(\overline{z})}^{z}\hat{\rho}^+(\zeta,\overline{z})e^{i\hat{\theta}^+(\zeta,\overline{z})}d\zeta+\tilde{y}(\overline{z}) \quad , \tag{3.3.58}$$

$$\hat{y}^-(z,\overline{z})=\int_{\tilde{z}(\overline{z})}^{z}\hat{\rho}^-(\zeta,\overline{z})e^{i\hat{\theta}^-(\zeta,\overline{z})}d\zeta+\tilde{y}(\overline{z}) \quad . \tag{3.3.59}$$

In these equations, $\hat{\theta}^+(z,\overline{z})$, $\hat{\theta}^-(z,\overline{z})$, $\tilde{z}(\overline{z})$ and $\tilde{y}(\overline{z})$ are prescribed. The real valued functions $\hat{\rho}^+(z,\overline{z})$ and $\hat{\rho}^-(z,\overline{z})$ must be determined so that the Jacobians are positive in a neighborhood N^+ and N^- and continuous across C. Setting $J^+=J^-$ across C, we get the following relationship from (3.2.11),

$$\begin{aligned}&2\hat{\rho}^+(\tilde{z}(\overline{z}),\overline{z})\,\mathrm{Re}\left\{e^{-i\hat{\theta}^+(\tilde{z}(\overline{z}),\overline{z})}\tilde{y}'(\overline{z})/\tilde{z}'(\overline{z})\right\}+\left|\tilde{y}'(\overline{z})\right|^2\\&\quad=2\hat{\rho}^-(\tilde{z}(\overline{z}),\overline{z})\,\mathrm{Re}\left\{e^{-i\hat{\theta}^-(\tilde{z}(\overline{z}),\overline{z})}\tilde{y}'(\overline{z})/\tilde{z}'(\overline{z})\right\}+\left|\tilde{y}'(\overline{z})\right|^2 \quad ,\end{aligned} \tag{3.3.60}$$

on C. This is satisfied if,

$$\hat{\rho}^{+}(z,\overline{z}) = \hat{\gamma}(z,\overline{z})\left(e^{-i\hat{\theta}^{-}(z,\overline{z})}\tilde{y}'(\overline{z}) / \tilde{z}'(\overline{z}) + e^{i\hat{\theta}^{-}(z,\overline{z})}\widehat{y}'(z) / \widehat{z}'(z)\right), \qquad (3.3.61)$$

$$\hat{\rho}^{-}(z,\overline{z}) = \hat{\gamma}(z,\overline{z})\left(e^{-i\hat{\theta}^{+}(z,\overline{z})}\tilde{y}'(\overline{z}) / \tilde{z}'(\overline{z}) + e^{i\hat{\theta}^{+}(z,\overline{z})}\widehat{y}'(z) / \widehat{z}'(z)\right), \qquad (3.3.62)$$

on C, where $\widehat{y}'(z) = \overline{\tilde{y}'(\overline{z})}$ and $\widehat{z}'(z) = \overline{\tilde{z}'(\overline{z})}$, and $\hat{\gamma}(z,\overline{z})$ is a function defined on B that is real-valued on C.

Thus a twin deformation with continuous Jacobian across the twin boundary can be constructed from,

$$\hat{y}^{+}(z,\overline{z}) = \int_{\tilde{z}(\overline{z})}^{z} \hat{\gamma}(\zeta,\overline{z})\left(e^{-i\hat{\theta}^{-}(\zeta,\overline{z})}\tilde{y}'(\overline{z}) / \tilde{z}'(\overline{z}) + e^{i\hat{\theta}^{-}(\zeta,\overline{z})}\widehat{y}'(\zeta) /' \widehat{z}(\zeta)\right) e^{i\hat{\theta}^{+}(\zeta,\overline{z})} d\zeta + \tilde{y}(\overline{z}) \ , \qquad (3.3.63)$$

$$\hat{y}^{-}(z,\overline{z}) = \int_{\tilde{z}(\overline{z})}^{z} \hat{\gamma}(\zeta,\overline{z})\left(e^{-i\hat{\theta}^{+}(\zeta,\overline{z})}\tilde{y}'(\overline{z}) / \tilde{z}'(\overline{z}) + e^{i\hat{\theta}^{+}(\zeta,\overline{z})}\widehat{y}'(\zeta) / \widehat{z}'(\zeta)\right) e^{i\hat{\theta}^{-}(\zeta,\overline{z})} d\zeta + \tilde{y}(\overline{z}) \ , \qquad (3.3.64)$$

for a neighborhood N^{+} and N^{-} surrounding C, where $e^{\pm i\theta^{+}}$ can be continuously extended into N^{-}, and $e^{\pm i\theta^{-}}$ can be continuously extended into N^{+}. The function $\hat{\gamma}(z,\overline{z})$ must be defined so that J^{+} and J^{-} are positive in N^{+} and N^{-}, and is real-valued on C.

Example 3.3: Continuous Jacobian across twin boundary

For this example, let the twin rotation fields be fully determined by the following scalar functions,

$$\theta^{+}(x_1,x_2)=2x_1\ , \qquad \hat{\theta}^{+}(z,\overline{z})=z+\overline{z}\ , \tag{3.3.65}$$

$$\theta^{-}(x_1,x_2)=2x_2\ , \qquad \hat{\theta}(z,\overline{z})=-i(z-\overline{z})\,. \tag{3.3.66}$$

Let the twin boundary C in the undeformed configuration, be a horizontal line on the x_1-axis defined as,

$$\left(x_1,x_2\right)=\left(\tilde{x}_1(s),\tilde{x}_2(s)\right)=\left(s,0\right)\ , \quad \left(-1\le s\le 1\right). \tag{3.3.67}$$

Referring to (3.2.8), this curve can be defined by the analytic function,

$$z=\tilde{z}(\overline{z})=\overline{z}\ \text{, on } C\,. \tag{3.3.68}$$

For the mapping of the twin boundary C to its image C^*, let C^* be a parabola defined as,

$$\left(y_1,y_2\right)=\left(\tilde{y}_1(s),\tilde{y}_2(s)\right)=\left(s,s^2\right)\ , \quad \left(-1\le s\le 1\right), \tag{3.3.69}$$

where referring to (3.2.9), C^* can be defined by the analytic function $\tilde{y}(\overline{z})$ such that,

$$y=\tilde{y}(\overline{z})=\overline{z}+i\overline{z}^{2}\,. \tag{3.3.70}$$

Given $\hat{\theta}^{+}$, $\hat{\theta}^{-}$, $\tilde{z}(\overline{z})$, and $\tilde{y}(\overline{z})$ defined this way, then equations (3.3.61) and (3.3.62) for $\hat{\rho}^{+}(z,\overline{z})$ and $\hat{\rho}^{-}(z,\overline{z})$ take on the following forms for this example,

$$\hat{\rho}^{+}(z,\overline{z})=5\Big(e^{-2ix_2}\left(1+2x_2+2ix_1\right)+e^{2ix_2}\left(1+2x_2-2ix_1\right)\Big), \tag{3.3.71}$$

$$\hat{\rho}^{-}(z,\overline{z})=5\Big(e^{-2ix_1}\left(1+2x_2+2ix_1\right)+e^{2ix_1}\left(1+2x_2-2ix_1\right)\Big), \tag{3.3.72}$$

where the scalar function $\hat{\gamma}(z,\overline{z})$ is taken to be $\hat{\gamma}(z,\overline{z})=5$. Performing the same type of derivation as in *Example 3.1*, it can seen be that $\hat{\rho}^{+}(z,\overline{z})$ and $\hat{\rho}^{-}(z,\overline{z})$ defined this way do agree with the condition in (3.2.15) on twin boundary C as defined.

Substituting these prescribed terms into (3.3.58) and (3.3.59) respectively, and carrying out the integration, we get the following deformation:

$$\begin{aligned}\hat{y}^{+}(z,\overline{z}) = \frac{1}{2} i \Big\{ & e^{2i\overline{z}}\left(10+10i+20\overline{z}\right) - e^{(1+i)(z+\overline{z}i)}\left(5+15i-10z-10iz\right) \\ & - e^{(1-i)(\overline{z}i-z)}\left(5-5i+10\overline{z}+10i\overline{z}\right)+2\overline{z}^{2}-2i\overline{z}\Big\} \quad , \text{ in } B^{+},\end{aligned} \tag{3.3.73}$$

$$\begin{aligned}\hat{y}^{-}(z,\overline{z}) = \frac{1}{2}(1+i)\Big\{\Big[& -e^{4i\overline{z}}\left(5-10i-10\overline{z}\right)+e^{(1+i)(z+\overline{z}+2i\overline{z})}\left(+5-10i-10z\right) \\ & + e^{(1-i)(z-\overline{z})}\left(5+10i\overline{z}\right)-5-10i\overline{z}\Big]e^{-2i\overline{z}}+\overline{z}^{2}\left(1+i\right)+\overline{z}\left(1-i\right)\Big\} \quad , \\ & \text{in } B^{-}.\end{aligned} \tag{3.3.74}$$

Stated in (2.3.8), the components of the deformation for each side of the twin boundary can be found by taking the real and imaginary parts of (3.3.73) and (3.3.74), but these are long expressions and such will be omitted. For the same reason, the Jacobian determinants J^{+} and J^{-} will not be shown as well, but it can be shown that on the twin boundary C defined as the x_1-axis, the twin determinants are equal. Also, seen in Figure 3.5(A), the twin boundary C described as $\{x_2=0,\ (-1\le x_1\le 1)\}$ does correspond to positive J^{+} and J^{-} further demonstrating that our choice of $\hat{\rho}^{+}(z,\overline{z})$ and $\hat{\rho}^{-}(z,\overline{z})$ does agree with (3.2.15).

The twin deformation in (3.3.73) and (3.3.74) is represented in Figure 3.5, where a rectangle centered at the origin with side lengths 0.2 and 0.4 is deformed by the rotations prescribed in (3.3.65) and (3.3.66).

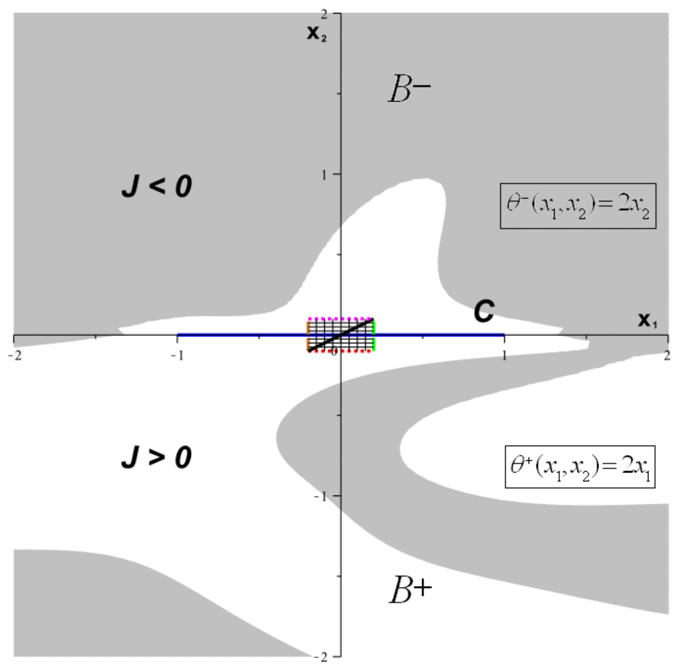

(A)

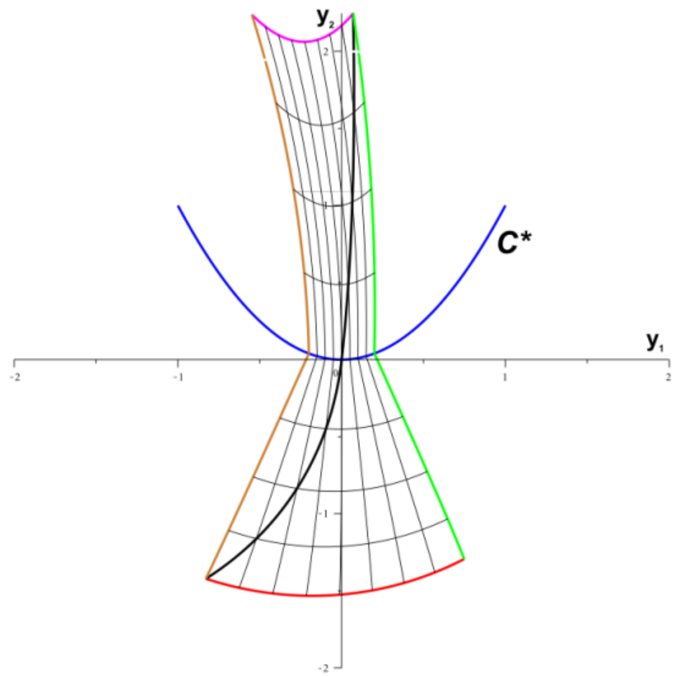

(B)

Figure 3.5: **(A)** Contour plot of the Jacobian determinants J^+ and J^- for the deformation (3.3.73) and (3.3.74), which are continuous across the twin boundary $C:\{x_2=0, (-1\le x_1 \le 1)\}$. In the unshaded regions $J^+>0$ or $J^->0$ depending on which side of the twin boundary is being examined, and in the shaded region $J^+<0$ or $J^-<0$. Also, a rectangle with side lengths 0.2 and 0.4 centered at the origin. **(B)** The deformation generated from rotations $\theta^+(x_1,x_2)=2x_1$ and $\theta^-(x_1,x_2)=2x_2$, with the rectangle mapped to its image, and the twin boundary mapped to a parabola $C*$.

Example 3.4

Let the twin rotation fields be fully determined by the same scalar functions as in the previous example,

$$\theta^+(x_1,x_2)=2x_1\ , \qquad \hat{\theta}^+(z,\overline{z})=z+\overline{z}\ , \tag{3.3.75}$$

$$\theta^-(x_1,x_2)=2x_2\ , \qquad \hat{\theta}(z,\overline{z})=-i(z-\overline{z})\,. \tag{3.3.76}$$

The twin boundary C in the undeformed configuration, is a vertical line on the x_2-axis defined as,

$$\left(x_1, x_2\right) = \left(\tilde{x}_1(s), \tilde{x}_2(s)\right) = \left(0, s\right) \ , \quad \left(-1 \le s \le 1\right). \tag{3.3.77}$$

Referring to (3.2.8), C can be defined by the analytic function,

$$z = \tilde{z}(\overline{z}) = -\overline{z} \text{ , on } C. \tag{3.3.78}$$

We take C^* as the unit circle like in Ex. 4.1,

$$\left(y_1, y_2\right) = \left(\tilde{y}_1(s), \tilde{y}_2(s)\right) = \left(\cos(s), \sin(s)\right) \ , \quad \left(-1 \le s \le 1\right), \tag{3.3.79}$$

where referring to (3.2.9), C^* can be defined by the analytic function $\tilde{y}(\overline{z})$ such that,

$$y = \tilde{y}(\overline{z}) = e^{-\overline{z}}. \tag{3.3.80}$$

As stated thus far, this example is exactly the same as Ex. 4.1. In Ex. 4.1, both $\hat{\rho}^+$ and $\hat{\rho}^-$ were constants, which led to a discontinuous Jacobian across the twin boundary. In this example, we will build a twin deformation with a continuous Jacobian across the twin bounday by defining these terms as,

$$\hat{\rho}^+(z, \overline{z}) = 5\left(e^{-z} + e^{-\overline{z}}\right), \tag{3.3.81}$$

$$\hat{\rho}^-(z, \overline{z}) = 5\left(e^{-i(z+\overline{z})-\overline{z}} + e^{i(z+\overline{z})-z}\right), \tag{3.3.82}$$

where as in the previous example, $\hat{\gamma}(z, \overline{z}) = 5$. Defining $\hat{\rho}^+(z, \overline{z})$ and $\hat{\rho}^-(z, \overline{z})$ this way does agree with the condition in (3.2.15) on twin boundary C where $z = \tilde{z}(\overline{z})$.

Using these prescribed parameters, a twin deformation can generated from (3.3.58) and (3.3.59), which takes the form:

$$\hat{y}^{+}(z,\overline{z}) = \frac{1}{2}(1+i)e^{-\overline{z}}\left\{5\left(e^{2\overline{z}} - e^{-(1-i)(z-\overline{z}i)} - (1+i)e^{i(z+\overline{z})}\right) + 6 + 4i\right\}, \text{ in } B^{+}, \quad (3.3.83)$$

$$\hat{y}^{-}(z,\overline{z}) = 5ie^{-3\overline{z}}\left\{e^{2\overline{z}} - e^{i(z+\overline{z}-2i\overline{z})} + \frac{1}{2}(1+i)\left(e^{(1-i)(z+\overline{z})} - 1\right)\right\} + e^{-\overline{z}}, \text{ in } B^{-}. \quad (3.3.84)$$

The twin deformation in (3.3.83) and (3.3.84) is shown in Figure 3.6, where a rectangle centered at the origin with side lengths 1.0 and 0.2 is deformed by the rotations prescribed in (3.3.75) and (3.3.76). Also shown in Figure 3.6(A) are the regions where J^{+} and J^{-} are positive, negative and zero corresponding to a twin boundary C described as $\{x_1 = 0, \ (-1 \le x_2 \le 1)\}$.

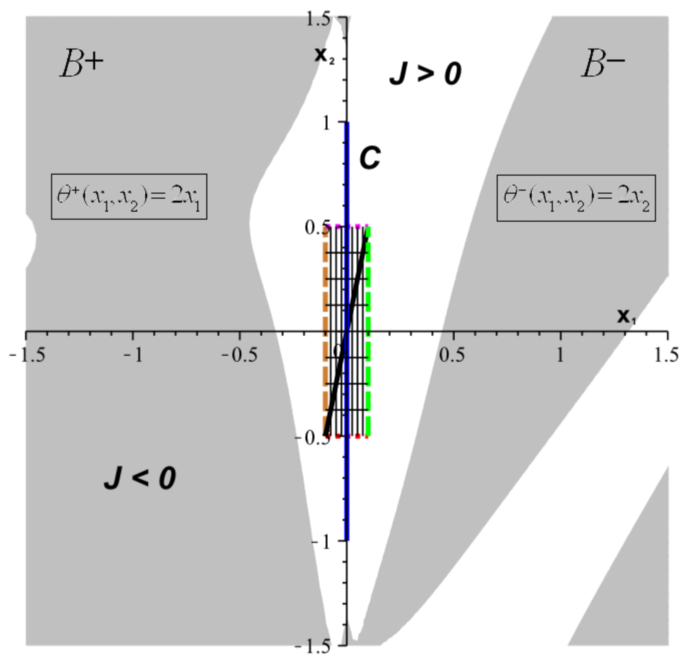

(A)

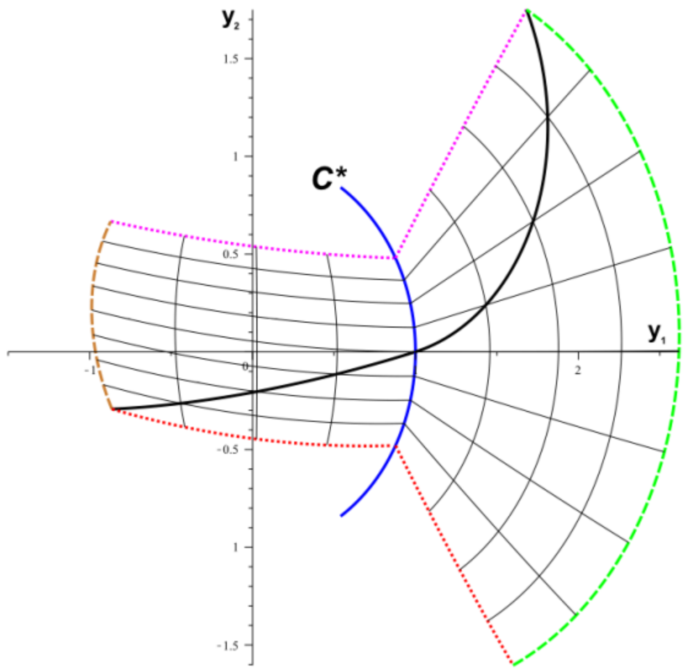

(B)

Figure 3.6: **(A)** Contour plot of the Jacobian determinants J^+ and J^- for the deformation (3.3.83) and (3.3.84), and twin boundary $C: \{x_1{=}0,\ (-1{\le}x_2{\le}1)\}$. In the unshaded regions $J^+ > 0$ or $J^- > 0$ depending on which side of the twin boundary is being examined, and in the shaded region $J^+ < 0$ or $J^- < 0$. Also, a rectangle of side lengths 1.0 and 0.2 centered at the origin. **(B)** The deformation generated from rotations $\theta^+(x_1, x_2) = 2x_1$ and $\theta^-(x_1, x_2) = 2x_2$, with the rectangle mapped to its image, and the twin boundary mapped to the unit circle $C*$

3.4 Twin elastic deformations

Here we present some general results concerning twin deformations of an elastic material. Suppose now that the twin deformation is located in a region defined as hyperelastic in the sense that the material's constitutive relation is characterized by the stored energy function $W(\boldsymbol{F})$ across the twin boundary (James, 1981) such that the following relationship between the deformation gradients occurs

$$F^{+} = QF^{-}H \text{ on } C. \quad (3.4.1)$$

In (3.4.1), Q is a proper-orthogonal tensor such that objectivity necessitates $W(F) = W(QF)$ for all tensors F, and H is a member of the participating elastic region's material symmetry group such that $W(F) = W(FH)$ for all tensors F. Hence, $W(F) = W(QFH)$ for all tensors F.

As the material symmetry group for an elastic material is a subset of the orthogonal group, H itself is proper-orthogonal as well. This relationship in (3.4.1) is given from (James, 1981, Pitteri, 1985, Ball and James, 1987).

A consequence of (3.4.1), is that $\det F^{+} = \det F^{-}$ on C, showing that the Jacobian of the defined deformation gradient must be continuous across the twin boundary in an elastic region. James also showed in (James, 1981) that the determinant of (3.3.1) gives,

$$\begin{aligned} Det(F^{+}) &= Det(F^{-} + a \otimes n) \\ &= Det(F^{-}) Det(1 + (F^{-})^{-1} a \otimes n) \\ &= Det(F^{-}) \left(1 + \left[(F^{-})^{-1} a\right] \cdot n\right), \end{aligned} \quad (3.4.2)$$

and substituting the equality of the Jacobians on C $\left(\det F^{+} = \det F^{-}\right)$ into (3.4.2), leads to the expression:

$$0 = \left[(F^{-})^{-1} a\right] \cdot n \text{ on } C. \quad (3.4.3)$$

Therefore, the condition in (3.4.3) must hold true on C for all elastic twinning.

We will discuss now the effect (3.4.1) has on the components of the polar decomposition of F^{+} and F^{-}. As in the previous section on kinematics of twinning, we substitute the polar decompositions of the deformation gradient on each side of the twin boundary shown in (3.3.2) and (3.3.3) into (3.4.1):

$$\boldsymbol{R}^{+}\boldsymbol{U}^{+} = \boldsymbol{Q}\boldsymbol{R}^{-}\boldsymbol{U}^{-}\boldsymbol{H} \text{ on } C. \tag{3.4.4}$$

Since $\boldsymbol{H}\boldsymbol{H}^{T} = \boldsymbol{1}$, (3.4.4) can be rewritten as:

$$\boldsymbol{R}^{+}\boldsymbol{U}^{+} = \boldsymbol{Q}\boldsymbol{R}^{-}\boldsymbol{H}\boldsymbol{H}^{T}\boldsymbol{U}^{-}\boldsymbol{H}. \tag{3.4.5}$$

From (3.4.5), it can be seen that the following relationships may be constructed between the rotation tensors on either side of the twin boundary and the stretch tensors on either side of the twin boundary,

$$\boldsymbol{R}^{+} = \boldsymbol{Q}\boldsymbol{R}^{-}\boldsymbol{H}, \tag{3.4.6}$$

$$\boldsymbol{U}^{+} = \boldsymbol{H}^{T}\boldsymbol{U}^{-}\boldsymbol{H}. \tag{3.4.7}$$

Result 3.3: Rotation angles θ^{+} and θ^{-} must be related through $\theta^{+} = \theta^{-}$ (3.4.19) or $\theta^{+} = -\theta^{-} + 2\phi$ (3.4.20) for twinning in an elastic region

We will now show how we arrive at the above relationships between the previously defined scalar functions θ^{+} and θ^{-}, where ϕ is a scalar function prescribed by the angle formed between C and $C*$, for twinning in a plane elastic region.

Note that across the twin boundary C, (3.2.5) gives,

$$\boldsymbol{F}^{+}\dot{\boldsymbol{x}} = \boldsymbol{F}^{-}\dot{\boldsymbol{x}} = \dot{\boldsymbol{y}}, \tag{3.4.8}$$

where $\dot{\tilde{\boldsymbol{x}}}$ and $\dot{\tilde{\boldsymbol{y}}}$ are the parameterizations of C and C^* defined in (3.2.2) and (3.2.3), and the dot above each term denotes derivatives with respect to the tracing parameter s (See Figure 3.7).

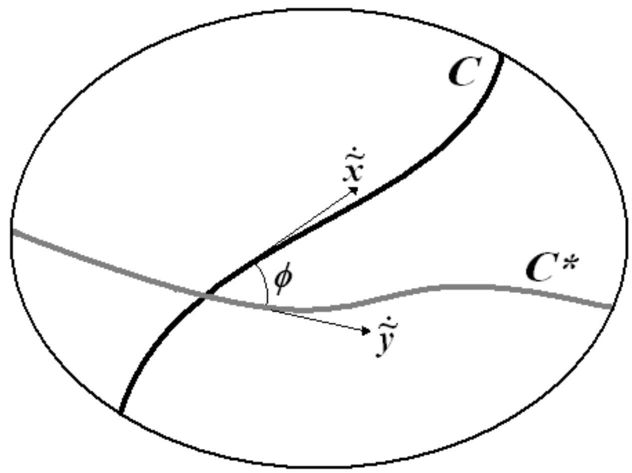

Figure 3.7: Schematic of the twin boundary C and its image C^* separated by an angle ϕ, measured from $\dot{\tilde{\boldsymbol{x}}}$ to $\dot{\tilde{\boldsymbol{y}}}$.

From (3.3.2), (3.3.3), and (3.4.8),

$$\boldsymbol{U}^{+}\dot{\tilde{\boldsymbol{x}}} = [\boldsymbol{R}^{+}]^{T}\,\dot{\tilde{\boldsymbol{y}}}, \tag{3.4.9}$$

$$\boldsymbol{U}^{-}\dot{\tilde{\boldsymbol{x}}} = [\boldsymbol{R}^{-}]^{T}\,\dot{\tilde{\boldsymbol{y}}}, \tag{3.4.10}$$

which in turn leads to:

$$\dot{\tilde{\boldsymbol{x}}}\cdot[\boldsymbol{U}^{+}]^{2}\,\dot{\tilde{\boldsymbol{x}}} = \dot{\tilde{\boldsymbol{x}}}\cdot[\boldsymbol{U}^{-}]^{2}\,\dot{\tilde{\boldsymbol{x}}} = \left|\dot{\tilde{\boldsymbol{y}}}\right|^{2}. \tag{3.4.11}$$

Now substituting (3.4.7) into (3.4.11) implies,

$$\dot{\tilde{\boldsymbol{x}}} \cdot [\boldsymbol{U}^+]^2 \, \dot{\tilde{\boldsymbol{x}}} = \dot{\tilde{\boldsymbol{x}}} \cdot \boldsymbol{H}^T [\boldsymbol{U}^-]^2 \, \boldsymbol{H} \dot{\tilde{\boldsymbol{x}}} \\ = \boldsymbol{t} \cdot [\boldsymbol{U}^-]^2 \boldsymbol{t} = \dot{\tilde{\boldsymbol{x}}} \cdot [\boldsymbol{U}^-]^2 \, \dot{\tilde{\boldsymbol{x}}} \ , \tag{3.4.12}$$

where $\boldsymbol{t} \equiv \boldsymbol{H} \dot{\tilde{\boldsymbol{x}}}$. Applying the two-dimensional version of the Cayley-Hamilton theorem[3] to the right hand side of (3.4.12) gives:

$$\boldsymbol{t} \cdot [\boldsymbol{U}^-]^2 \boldsymbol{t} = \dot{\tilde{\boldsymbol{x}}} \cdot [\boldsymbol{U}^-]^2 \, \dot{\tilde{\boldsymbol{x}}} \\ I^- \boldsymbol{t} \cdot \boldsymbol{U}^- \boldsymbol{t} - J^- \left| \boldsymbol{t} \right|^2 = I^- \dot{\tilde{\boldsymbol{x}}} \cdot \boldsymbol{U}^- \dot{\tilde{\boldsymbol{x}}} - J^- \left| \dot{\tilde{\boldsymbol{x}}} \right|^2 \ , \tag{3.4.13}$$

where I^- and J^- are the trace and determinant of $\boldsymbol{U}^-$[4]. By substituting $\boldsymbol{t} = \boldsymbol{H} \dot{\tilde{\boldsymbol{x}}}$ into (3.4.13), it can be shown that,

$$\dot{\tilde{\boldsymbol{x}}} \cdot \boldsymbol{H}^T \boldsymbol{U}^- \boldsymbol{H} \dot{\tilde{\boldsymbol{x}}} = \dot{\tilde{\boldsymbol{x}}} \cdot \boldsymbol{U}^- \dot{\tilde{\boldsymbol{x}}} \ , \tag{3.4.14}$$

or equivalently,

$$\dot{\tilde{\boldsymbol{x}}} \cdot \boldsymbol{U}^+ \dot{\tilde{\boldsymbol{x}}} = \dot{\tilde{\boldsymbol{x}}} \cdot \boldsymbol{U}^- \dot{\tilde{\boldsymbol{x}}} \ . \tag{3.4.15}$$

Using (3.4.15), we substitute (3.4.9) and (3.4.10) to get a similar type of relationship relating the twin rotation tensors as such,

$$\dot{\tilde{\boldsymbol{x}}} \cdot [\boldsymbol{R}^+]^T \, \dot{\tilde{\boldsymbol{y}}} = \dot{\tilde{\boldsymbol{x}}} \cdot [\boldsymbol{R}^-]^T \, \dot{\tilde{\boldsymbol{y}}} . \tag{3.4.16}$$

Applying (2.3.2) to (3.4.16) and noting that $\left| \dot{\tilde{\boldsymbol{x}}} \right|^2 = 1$, the relationship between the right and left sides of the twin deformation takes the form:

$$\left| \dot{\tilde{\boldsymbol{y}}} \right| \left(\cos(\theta^+) \cos(\phi) + \sin(\theta^+) \sin(\phi) \right) = \left| \dot{\tilde{\boldsymbol{y}}} \right| \left(\cos(\theta^-) \cos(\phi) + \sin(\theta^-) \sin(\phi) \right) \ , \tag{3.4.17}$$

---

[3] For a two-dimensional square matrix $\boldsymbol{A}$, the Cayley-Hamilton theorem states, $\boldsymbol{A}^2 = tr(\boldsymbol{A})\boldsymbol{A} - \det(\boldsymbol{A})\boldsymbol{1}$.

[4] It can be shown easily that the invariants $I^+ = I^-$ and $J^+ = J^-$ on C for twin elastic deformation.

where ϕ represents the angle subtended by the vectors $\dot{\boldsymbol{x}}$ and $\dot{\boldsymbol{y}}$ measured from $\dot{\boldsymbol{x}}$. The above equality can be simplified to the form,

$$\cos(\theta^{+} - \phi) = \cos(\theta^{-} - \phi)\,, \text{ on } C\,. \tag{3.4.18}$$

This relationship holds true for all twinning in an elastic region.

However, a consequence of (3.4.18) is that the rotation angles θ^{+} and θ^{-} must be related through either of the following:

$$\theta^{+} = \theta^{-}, \text{ or} \tag{3.4.19}$$

$$\theta^{+} = -\theta^{-} + 2\phi\,, \text{ across } C\,[5]. \tag{3.4.20}$$

Examples of each case are shown next. Note that if C maps to itself $(C = C^{*})$, then $\phi = 0$ such that the rotation angles θ^{+} and θ^{-} can either be equal to each other or the negative of each other to be representative of elastic twinning.

Example 3.5: Elastic twinning for $\theta^{+} = \theta^{-}$ on $C = C^{*}$

In this example $\theta^{+} = \theta^{-}$ on the twin boundary C. Let the rotation fields be fully determined by the scalar functions,

$$\theta^{+}(x_1, x_2) = 2\left(x_1 + x_2\right)\,, \qquad \hat{\theta}^{+}(z, \bar{z}) = \left(1 + i\right) z + \left(1 - i\right) \bar{z}\,, \tag{3.4.21}$$

[5] Note that an additive integer multiple of 2π is suppressed in both (3.4.19) and (3.4.20) without loss of generality.

$$\theta^{-}(x_1,x_2)=2x_2\ , \qquad \hat{\theta}^{-}(z,\overline{z})=\left(\overline{z}-z\right)i\,. \tag{3.4.22}$$

Let the twin boundary be defined as a fixed vertical line on the x_2-axis,

$$(x_1,x_2)=\left(\tilde{x}_1(s),\tilde{x}_2(s)\right)=(0,s)\ , \quad \left(-0.5\le s\le 0.5\right), \tag{3.4.23}$$

such that C maps to itself. Referring to (3.2.8), this curve can be defined by the analytic function,

$$z=\tilde{z}(\overline{z})=-\overline{z}\ , \tag{3.4.24}$$

and since $C=C^{*}$, then $y=\tilde{y}(\overline{z})=-\overline{z}$ as well.

As explained previously in the description of equation (3.4.1) for twinning in an elastic region, the Jacobian determinants must be equal across C. Thus $\hat{\rho}^{+}(z,\overline{z})$ and $\hat{\rho}^{-}(z,\overline{z})$ must be related by (3.3.60), which means they will each take the form in (3.3.61) and (3.3.62) respectively. We take $\hat{\gamma}(z,\overline{z})=1$, such that $\hat{\rho}^{+}(z,\overline{z})$ and $\hat{\rho}^{-}(z,\overline{z})$ are,

$$\hat{\rho}^{+}(z,\overline{z})=2\cosh\left(\overline{z}-z\right), \tag{3.4.25}$$

$$\hat{\rho}(z,\overline{z})=2\cos\left(\left(1+i\right)z+\left(1-i\right)\overline{z}\right). \tag{3.4.26}$$

Substituting the above parameters into (3.3.58) and (3.3.59), the following deformation is generated around the twin boundary:

$$\hat{y}^{+}(z,\overline{z})=\frac{1}{5}i\left\{\left(5e^{4\overline{z}}-5e^{i\left(z+\overline{z}-4i\overline{z}\right)}-\left(2i+1\right)e^{(2+i)(z+\overline{z})}+1+2i\right)e^{-4\overline{z}}\right\}-\overline{z}\ , \text{ in } B^{+}, \tag{3.4.27}$$

$$\hat{y}^{-}(z,\bar{z}) = \frac{1}{5} i \left\{ \left(5\left(e^{4\bar{z}} - e^{i(z+\bar{z}-4i\bar{z})} \right) + 2ie^{i(z+\bar{z})} - (2i+1) e^{(2+i)(z+\bar{z})} + e^{i(z+\bar{z})} \right) e^{-i(z+\bar{z}-4i\bar{z})} \right\} - \bar{z}\ , \text{ in } B^{-}. \tag{3.4.28}$$

As stated in previous examples, the components of the deformation for each side of the twin boundary can be found by taking the real and imaginary parts of the above equations.

Shown in Figure 3.8 is the twin deformation described by (3.4.27) and (3.4.28), where a rectangle of side lengths 0.6 and 0.1 centered at the origin is deformed. Also shown in Figure 3.8(A) are the regions where the Jacobian determinants are positive, negative and zero for the twin boundary C defined as $\{x_1 = 0,\ \ (-0.5 \le x_2 \le 0.5)\}$.

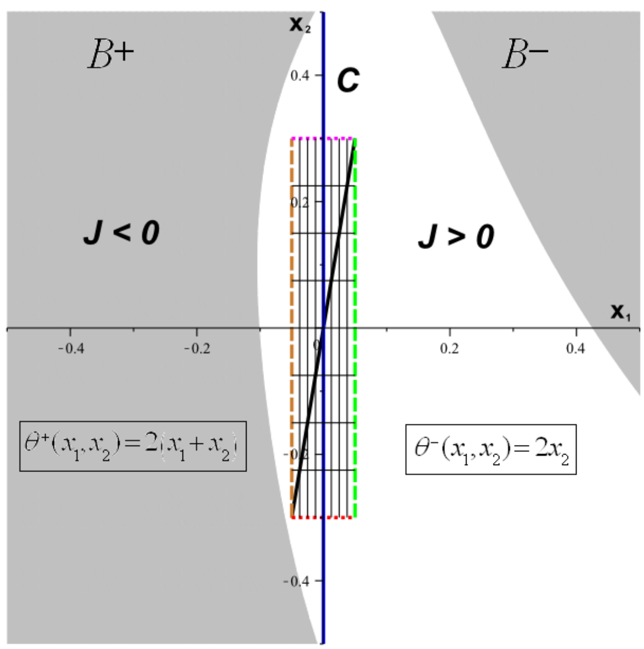

(A)

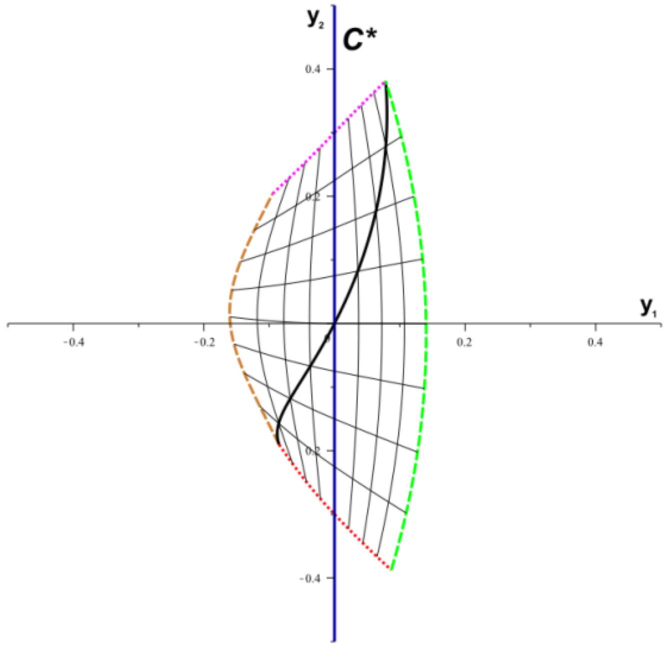

(B)

Figure 3.8 **(A)** Contour plot of the Jacobian determinants J^+ and J^- for the deformation (3.4.27) and (3.4.28), and the twin boundary $C:\{x_1=0,\ (-0.5\leq x_2\leq 0.5)\}$. In the unshaded regions $J^+>0$ or $J^->0$ depending on which side of the twin boundary is being examined, and in the shaded region $J^+<0$ or $J^-<0$. Also, a rectangle of side lengths 0.6 and 0.1 centered at the origin. **(B)** The deformation generated from rotations $\theta^+(x_1,x_2)=2(x_1+x_2)$ and $\theta^-(x_1,x_2)=2x_2$, with the rectangle mapped to its image, and the twin boundary mapped to itself.

Example 3.6: Elastic twinning for $\theta^+=\theta^-$ on $C\neq C^*$

In this example, we will keep θ^+ and θ^- as defined in (3.4.21) and (3.4.22) with the same twin boundary C as a vertical line on the x_2-axis $(x_1=0)$, such that $\theta^+=\theta^-$ across the twin boundary. This problem varies from *Example 3.5* in that twin boundary C will no longer map to itself, but to the unit circle. Referring to (3.2.8) and (3.2.9), the twin boundary and its image can be defined by the analytic functions $\tilde{z}(\overline{z})$ and $\tilde{y}(\overline{z})$ as:

$$z = \tilde{z}(\overline{z}) = -\overline{z} \ , \tag{3.4.29}$$

$$y = \tilde{y}(\overline{z}) = e^{-\overline{z}} \ . \tag{3.4.30}$$

Given these prescribed functions, $\hat{\rho}^{+}(z,\overline{z})$ and $\hat{\rho}^{-}(z,\overline{z})$ are found from (3.3.61) and (3.3.62) with $\hat{\gamma}(z,\overline{z}) = 1$:

$$\hat{\rho}^{+}(z,\overline{z}) = e^{-z} + e^{-\overline{z}} \ , \tag{3.4.31}$$

$$\hat{\rho}^{-}(z,\overline{z}) = e^{-(z+i(z+\overline{z}))} + e^{-z+i(z+\overline{z})} \ . \tag{3.4.32}$$

Substituting the above expressions for $\hat{\rho}^{+}(z,\overline{z})$ and $\hat{\rho}^{-}(z,\overline{z})$ along with our prescribed rotation fields and twin boundary into (3.3.58) and (3.3.59), the twin deformation generated is,

$$\begin{aligned} \hat{y}^{+}(z,\overline{z}) = \Bigg\{ & i\left(e^{2\overline{z}} - e^{-i\left(z+\overline{z}-2i\overline{z}\right)} + \frac{1}{2} \right) \\ & + \frac{1}{2}\left(1-i\right) e^{(1+i)(z+\overline{z})} - \frac{1}{2} \Bigg\} e^{-3\overline{z}} + e^{-\overline{z}} \ , \ \text{in } B^{+}, \end{aligned} \tag{3.4.33}$$

$$\begin{aligned} \hat{y}^{-}(z,\overline{z}) = \frac{1}{2} \Big\{ & \left(i-1\right) e^{i(z+\overline{z})} + \left(1-i\right) e^{(1+2i)(z+\overline{z})} \\ & + 2e^{2\overline{z}} - 2e^{i\left(z+\overline{z}-2i\overline{z}\right)} \Big\} e^{-i\left(z+\overline{z}-3i\overline{z}\right)} + e^{-\overline{z}} \ , \ \text{in } B^{-}. \end{aligned} \tag{3.4.34}$$

Figure 3.9 shows the twin deformation described above, where a rectangle of side lengths 0.6 and 0.15 centered at the origin is deformed. Shown in Figure 3.9(A) are the regions in which the Jacobian determinants are positive, negative and zero, such that the Jacobian determinants are equal across the twin boundary C defined as $\left\{ x_1 = 0, \ \left(-1 \le x_2 \le 1\right) \right\}$.

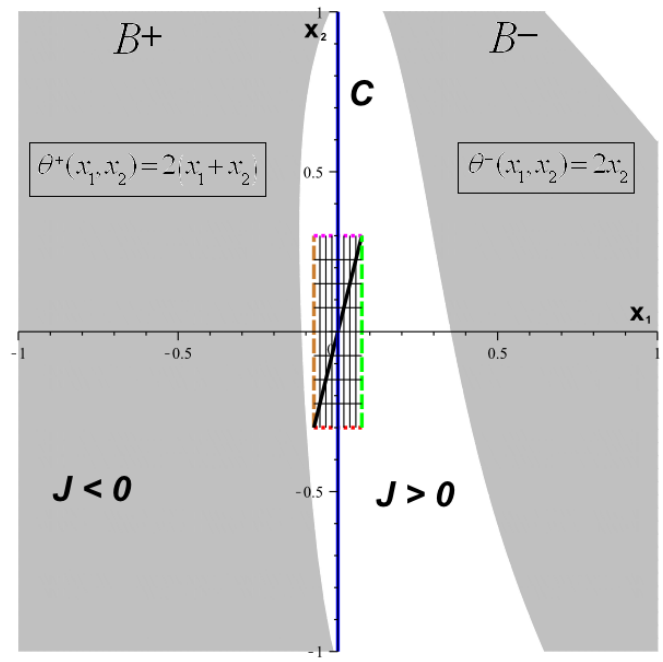

(A)

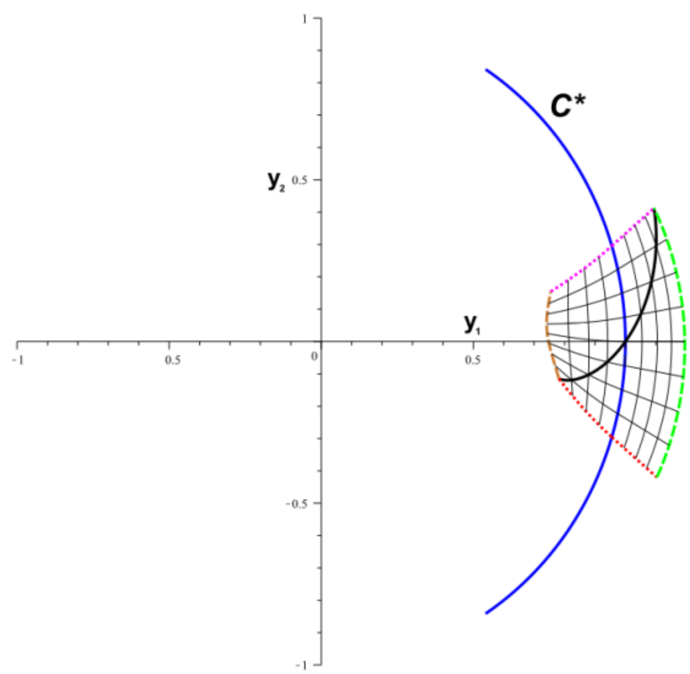

(B)

Figure 3.9 **(A)** Contour plot of the Jacobian determinants J^+ and J^- for the deformation (3.4.33) and (3.4.34), and the twin boundary $C:\{x_1{=}0,\ (-1{\le}x_2{\le}1)\}$. In the unshaded regions $J^+>0$ or $J^->0$ depending on which side of the twin boundary is being examined, and in the shaded region $J^+<0$ or $J^-<0$. Also, a rectangle of side lengths 0.6 and 0.15 centered at the origin. **(B)** The deformation generated from rotations $\theta^+(x_1,x_2)=2(x_1+x_2)$ and $\theta^-(x_1,x_2)=2x_2$, with the rectangle mapped to its image, and the twin boundary mapped to the unit circle C^*.

Example 3.7: Elastic twinning for $\theta^+ = \text{-}\theta^- + 2\phi$ on $C \neq C^*$

We now consider an example in which,

$$\theta^+(x_1,x_2) = -\theta^-(x_1,x_2) + 2\phi(x_1,x_2)\,, \tag{3.4.35}$$

on the twin boundary C, where $\phi(x_1,x_2)$ is the angle subtended by C and its image C^* at (x_1,x_2). Let the twin boundary C be defined as a horizontal line on the x_1-axis,

$$\left(x_1,x_2\right) = \left(\tilde{x}_1(s),\tilde{x}_2(s)\right) = \left(s,0\right)\ , \quad \left(-1.5\le s\le 1.5\right), \tag{3.4.36}$$

which maps to C^* defined as,

$$\left(y_1,y_2\right) = \left(\tilde{y}_1(s),\tilde{y}_2(s)\right) = \left(s,s\right)\ , \quad \left(-1.5\le s\le 1.5\right), \tag{3.4.37}$$

where C^* is a slanted line of slope 1. Referring to (3.2.8) and (3.2.9), the twin boundary and its image can be defined by the analytic functions $\tilde{z}(\overline{z})$ and $\tilde{y}(\overline{z})$ as:

$$z = \tilde{z}(\overline{z}) = \overline{z}\ , \tag{3.4.38}$$

$$y = \tilde{y}(\overline{z}) = (1+i)\overline{z}\ , \tag{3.4.39}$$

thus $\phi(x_1,x_2) = \pi/4$.

We will prescribe the rotation field around the twin boundary to be determined by,

$$\theta^{-}(x_1,x_2)=2x_2\ ,\qquad \hat{\theta}^{-}(z,\overline{z})=-i\left(z-\overline{z}\right), \tag{3.4.40}$$

$$\theta^{+}(x_1,x_2)=-2x_2+\frac{\pi}{2}\ ,\qquad \hat{\theta}^{+}(z,\overline{z})=i\left(z-\overline{z}\right)+\frac{\pi}{2}. \tag{3.4.41}$$

Note that θ^{+} and θ^{-} conform to (3.4.20) (and likewise (3.4.35)).

Since the Jacobian determinant must be positive and continuous across the twin boundary, let $\hat{\rho}^{+}(z,\overline{z})$ and $\hat{\rho}^{-}(z,\overline{z})$ be described by (3.3.61) and (3.3.62) respectively with $\hat{\gamma}(z,\overline{z})=1$,

$$\hat{\rho}^{+}(z,\overline{z})=(1+i)e^{\overline{z}-z}+(1-i)e^{z-\overline{z}}, \tag{3.4.42}$$

$$\hat{\rho}^{-}(z,\overline{z})=(1+i)e^{z-\overline{z}-i\pi/2}+(1-i)e^{-z+\overline{z}+i\pi/2}. \tag{3.4.43}$$

Substituting the above problem definitions into (3.3.58) and (3.3.59) generates the following twin deformation:

$$\hat{y}^{+}(z,\overline{z})=\left\{\left(1+i\right)\left(z-\overline{z}+\frac{i}{2}\right)e^{2z}+\frac{1}{2}\left(1-i\right)e^{2\overline{z}}\right\}e^{-2z}+\left(1+i\right)\overline{z}\ ,\ \text{ in } B^{+}, \tag{3.4.44}$$

$$\hat{y}^{-}(z,\overline{z})=\frac{1}{2}\left(1-i\right)\left\{i\left(2z-2\overline{z}+1\right)e^{2\overline{z}}+e^{2z}\right\}e^{-2\overline{z}}+\left(1+i\right)\overline{z}\ ,\ \text{ in } B^{-}. \tag{3.4.45}$$

Given the above twin deformation, a rectangle centered at the origin with side lengths 0.6 and 1.0 is deformed as shown in Figure 3.10. Also shown in Figure 3.10 is the mapping of the twin boundary from a horizontal line to a slanted line as prescribed in

(3.4.36) and (3.4.37). In Figure 3.10(A), the regions where the Jacobian determinant is postitive, negative and zero are given as well.

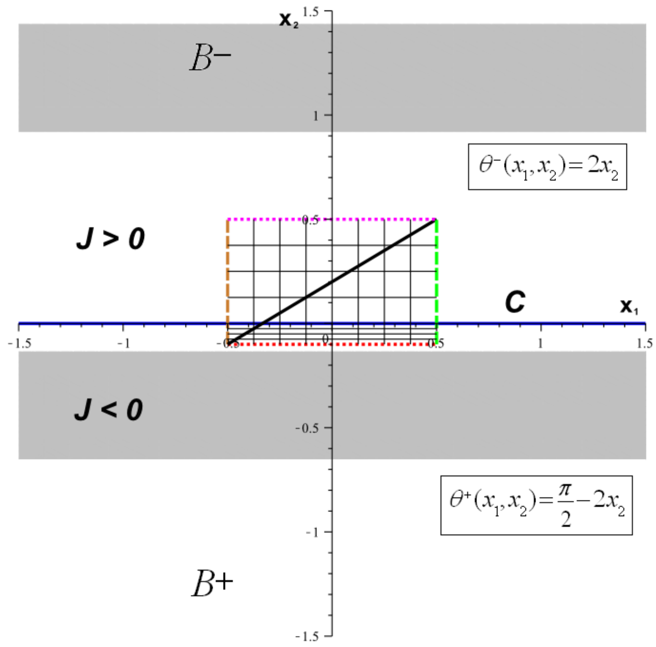

(A)

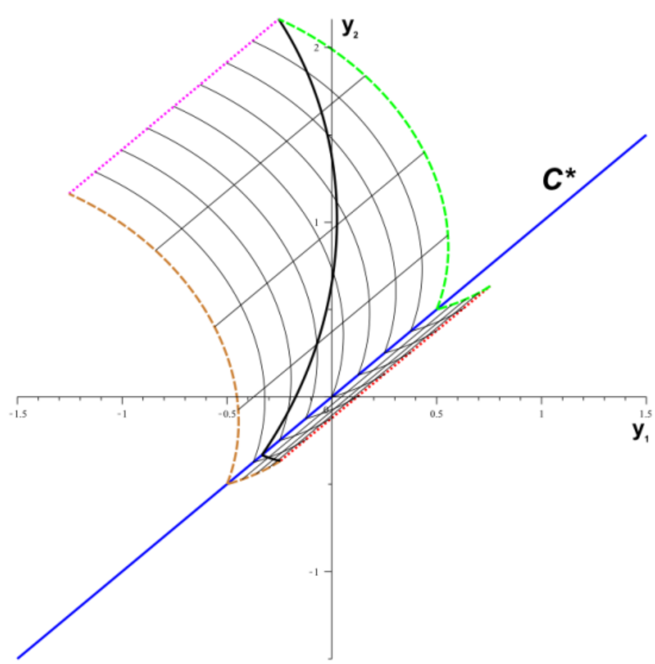

(B)

Figure 3.10 **(A)** Contour plot of the Jacobian determinants J^+ and J^- for the deformation (3.4.44) and (3.4.45), and the twin boundary $C:\{x_2{=}0,\ (-1.5{\le}x_1{\le}1.5)\}$. In the unshaded regions $J^+>0$ or $J^->0$ depending on which side of the twin boundary is being examined, and in the shaded region $J^+<0$ or $J^-<0$. Also, a rectangle of side lengths 0.6 and 1.0 centered at the origin. **(B)** The deformation generated from the rotation fields fully determined by (3.4.40) and (3.4.41), with the rectangle mapped to its image, and the twin boundary mapped to a slanted line C^* with slope 1 corresponding to an angle $\phi=\pi/4$.

Example 3.8: Elastic twinning for $\theta^+ = -\theta^- + 2\phi$ on $C \neq C^*$

Let the twin boundary C be defined as a horizontal line on the x_1-axis,

$$\left(x_1, x_2\right)=\left(\tilde{x}_1(s), \tilde{x}_2(s)\right)=\left(s, 0\right), \quad \left(-1 \leq s \leq 1\right), \tag{3.4.46}$$

which referring to (3.2.8), C can be defined by the analytic function,

$$z=\tilde{z}(\bar{z})=\bar{z}\,. \tag{3.4.47}$$

Let C map to parabola defined as,

$$\left(y_1, y_2\right)=\left(\tilde{y}_1(s), \tilde{y}_2(s)\right)=\left(s, s\tan(\tilde{\phi})\right), \quad \left(-1 \leq s \leq 1\right), \tag{3.4.48}$$

where,

$$\phi(x_1, x_2)=\tilde{\phi}(s)=\frac{s}{10}, \tag{3.4.49}$$

is the angle subtended by C and C^* at (x_1, x_2). Given our range of s, $\phi(x_1, x_2)$ is small enough such that we can approximate (3.4.48) to be,

$$\left(\tilde{y}_1(s), \tilde{y}_2(s)\right)=\left(s, s\tilde{\phi}\right)=\left(s, \frac{s^2}{10}\right), \quad \left(-1 \leq s \leq 1\right). \tag{3.4.50}$$

This approximation is done to get an explicit solution to the integral equations (3.3.58) and (3.3.59) which gives the generating deformation. However, neglecting this approximation still results in a generated deformation, but the mapping would not be in such a simplified form. Referring to (3.2.9), this approximation of $C*$ can be defined by the analytic function $\tilde{y}(\overline{z})$ such that,

$$\tilde{y}(\overline{z}) = \overline{z}\left(1+\frac{1}{10}\overline{z}\right), \quad z = \tilde{z}(\overline{z}) = \overline{z} \,. \tag{3.4.51}$$

We take the rotation fields as:

$$\theta^{-}(x_1,x_2) = 2x_2 \;, \qquad \hat{\theta}^{-}(z,\overline{z}) = -i\left(z-\overline{z}\right), \tag{3.4.52}$$

$$\theta^{+}(x_1,x_2) = -2x_2 + \frac{x_1}{10} \;, \qquad \hat{\theta}^{+}(z,\overline{z}) = i\left(z-\overline{z}\right) + \frac{1}{10}\left(z+\overline{z}\right), \tag{3.4.53}$$

which are of the form presented in (3.4.35) .

Given the $\theta^{+}(x_1,x_2)$, $\theta^{-}(x_1,x_2)$, and C defined this way with the image $C*$ approximated by (3.4.50), we will prescribe $\hat{\rho}^{+}(z,\overline{z})$ and $\hat{\rho}^{-}(z,\overline{z})$ in the form presented in (3.3.61) and (3.3.62) with $\hat{\gamma}(z,\overline{z}) = 1$,

$$\hat{\rho}^{+}(z,\overline{z}) = e^{\overline{z}-z}\left(1+\frac{i}{5}\overline{z}\right) + e^{z-\overline{z}}\left(1-\frac{i}{5}z\right), \tag{3.4.54}$$

$$\hat{\rho}^{-}(z,\overline{z}) = \left(1+\frac{i}{5}\overline{z}\right)e^{-i[z/10+\overline{z}/10+i(z-\overline{z})]} + \left(1-\frac{i}{5}z\right)e^{i[z/10+\overline{z}/10+i(z-\overline{z})]}. \tag{3.4.55}$$

Substituting (3.4.54) and (3.4.55) along with the other problem parameters into (3.3.58) and (3.3.59), we get the following twin deformation:

$$\hat{y}^{+}(z,\overline{z}) = \frac{1}{401}\left(2+\frac{i}{10}\right)\Big\{\left(400+6000i+400\overline{z}\right)e^{i\overline{z}/5}$$
$$-\left(300+6000i+400z-20iz\right)e^{i/10(z+\overline{z})}$$
$$-\left(100+20i\overline{z}\right)e^{1/401(2-i/10)(399\overline{z}-401z+40i\overline{z})} \tag{3.4.56}$$
$$+\overline{z}^{2}+200\overline{z}+20i\overline{z}^{2}-10i\overline{z}\Big\} \;,\; \text{ in } B^{+},$$

$$\hat{y}^{-}(z,\overline{z}) = -\frac{1}{401}\Big\{\left(200+10i-2\overline{z}+40i\overline{z}\right)e^{-i\overline{z}/5}$$
$$+\left(200+10i-2\overline{z}+40i\overline{z}\right)e^{1/401(i/10-2)(399\overline{z}-401z+40i\overline{z})}\Big\} \tag{3.4.57}$$
$$+\left(30i+2\overline{z}\right)e^{i\overline{z}/5}-\left(30i+2z\right)e^{i/10(z+\overline{z})}+\overline{z}+\frac{i}{10}\overline{z}^{2} \;,\; \text{ in } B^{-}.$$

The twin deformation in (3.4.56) and (3.4.57) is illustrated in Figure 3.11, where a rectangle centered at the origin of side lengths 0.6 and 1.5 is deformed by the rotation field determined from (3.4.52) and (3.4.53). In Figure 3.11, the twin boundary C maps to its image $C*$ defined as a parabola approximated by (3.4.50). The regions in which the Jacobian determinant is positive, negative and zero are shown in Figure 3.11(A) as well.

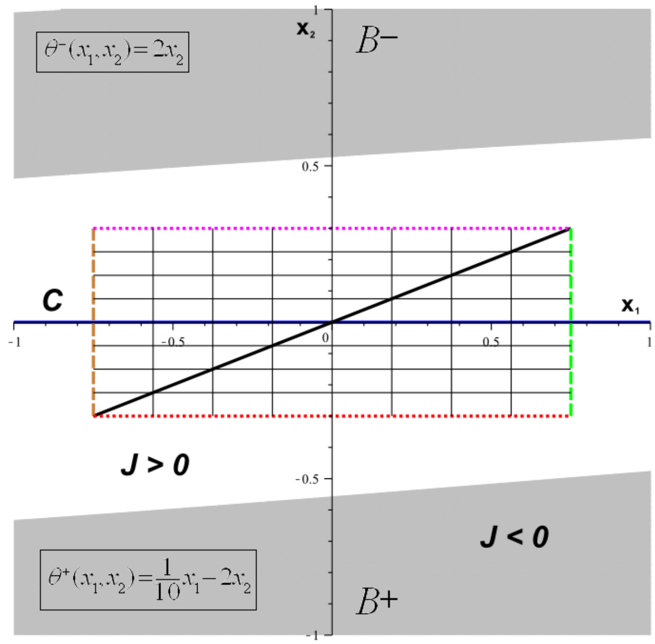

(A)

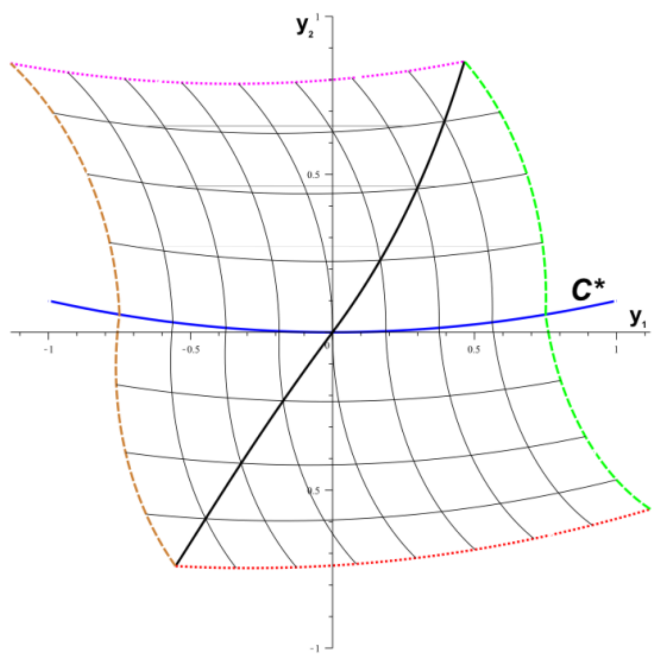

(B)

Figure 3.11 **(A)** Contour plot of the Jacobian determinants J^+ and J^- for the deformation (3.4.56) and (3.4.57), and the twin boundary $C:\{x_2=0,\ (-1\le x_1\le 1)\}$. In the unshaded regions $J^+>0$ or $J^->0$ depending on which side of the twin boundary is being examined, and in the shaded region $J^+<0$ or $J^-<0$. Also, a rectangle of side lengths 0.6 and 1.5 centered at the origin. **(B)** The deformation generated from rotations fields fully determined by (3.4.52) and (3.4.53), with the rectangle mapped to its image, and the twin boundary mapped to a parabola C^* approximated by (3.4.50).

CHAPTER 4

AREA PRESERVING PLANE DEFORMATIONS GENERATED FROM A GIVEN ROTATION FIELD ALONG A PRESCRIBED CURVE

4.1 Introduction

For our final analysis, we look at generating a deformation, which is locally area preserving in the neighborhood of a curve, given a rotation field and a prescribed curve and its mapping.

In **Section 4.2**, the case of locally area preserving infinitesimal plane deformation is reviewed in a similar method to **Section 2.2**, differing with the application of the constraint of area preservation on the generated displacement field. An example for this case is shown.

In **Section 4.3**, the kinematics associated with plane finite deformations are reviewed with the application of the constraint that the deformation is locally area preserving.

In **Section 4.4**, a plane finite deformation is constructed that is locally area preserving, given a prescribed rotation field, a curve, and its mapping, in the form of a

Taylor Series, using the Cauchy-Kovalevskaya procedure. An example demonstrating this is shown.

In **Section 4.5**, a plane finite deformation is constructed using the same Cauchy-Kovalevskaya procedure as in the previous section, with the Jacobian determinant no longer being set equal to one, but defined as a positive scalar function. An example is shown for this case as well.

4.2 Infinitesimal plane deformations that are locally area preserving

Let $\boldsymbol{u}$ be a locally area preserving infinitesimal plane displacement field on a planar region B. The infinitesimal strain and rotation fields $\boldsymbol{E}$ and $\boldsymbol{W}$ are respectively given by

$$\boldsymbol{E} = \frac{1}{2}\left(\nabla\boldsymbol{u} + \nabla\boldsymbol{u}^T\right),\ \boldsymbol{W} = \frac{1}{2}\left(\nabla\boldsymbol{u} - \nabla\boldsymbol{u}^T\right). \tag{4.2.1}$$

The tensor field $\boldsymbol{W}$, being skew-symmetric, is determined by the single scalar field

$$\theta = W_{12} = -W_{21} = \frac{1}{2}\left(u_{1,2} - u_{2,1}\right)\ \ ,\ (W_{11} = W_{22} = 0)\,. \tag{4.2.2}$$

If the infinitesimal deformation is locally area preserving, then the displacement field $\boldsymbol{u}$ satisfies,

$$0 = u_{1,1} + u_{2,2}\,. \tag{4.2.3}$$

For a simply connected region B, there exists a scalar function $v(x_1, x_2)$ such that

$$u_1 = v_{,2} \quad , \quad u_2 = -v_{,1} . \tag{4.2.4}$$

Substituting (4.2.4) into (4.2.2) yields the following relationship between the rotation and scalar field $\boldsymbol{v}$:

$$2\theta = v_{,11} + v_{,22} , \tag{4.2.5}$$

which takes the form of the Poisson Equation for a given θ determined by the rotation field (originally named for S. D. Poisson, 1813).

To produce an area preserving deformation that corresponds to a given rotation θ, (4.2.5) must be solved for $\boldsymbol{v}$ (Courant and Hilbert, 1962). The displacement field is then given by (4.2.5).

Example 4.1: Small plane deformation in an area preserving region

Suppose the rotation field is defined by the scalar function

$$\theta(x_1, x_2) = \frac{x_1 + x_2}{100} . \tag{4.3.1}$$

Given θ prescribed this way, it is easily shown that a solution to (4.2.5) is

$$v(x_1, x_2) = \frac{x_1^3 + x_2^3}{300} . \tag{4.3.2}$$

Differentiating (4.3.2) with respect to x_1 and x_2, and using the relationship in (4.2.4), the following displacement field is generated:

$$u_1 = \frac{x_2^2}{100} \quad , \quad u_2 = -\frac{x_1^2}{100}. \tag{4.3.3}$$

It is easily seen that the displacement field in (4.3.3) agrees with the condition in (4.2.3). Using (4.3.3), we get the following deformation which is area preserving for infinitesimal displacements

$$y_1 = \frac{x_2^2}{100} + x_1, \tag{4.3.4}$$

$$y_2 = -\frac{x_1^2}{100} + x_2. \tag{4.3.5}$$

In Figure 4.1, a square of side length 2 is deformed by the deformation field in (4.3.4) and (4.3.5).

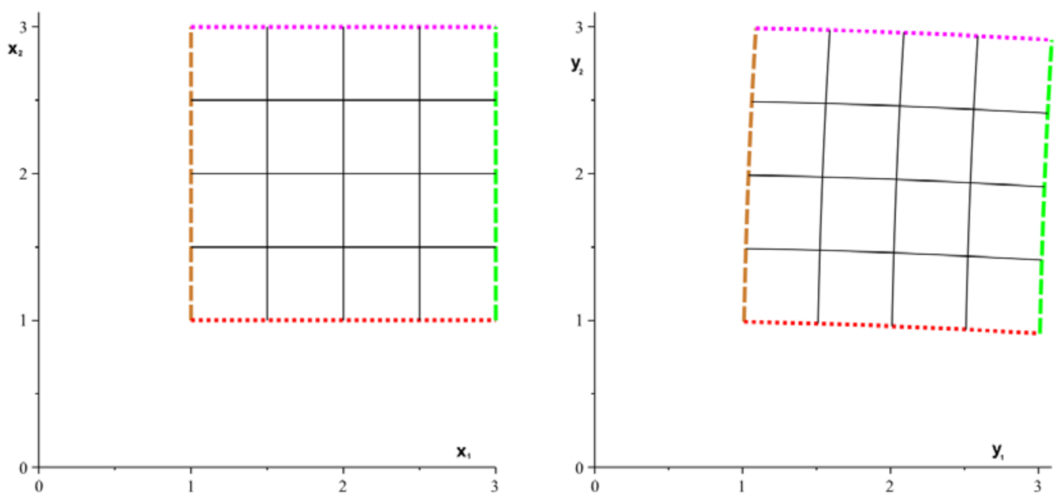

(A) (B)

Figure 4.1: (A) An undeformed square of side length 2 located in the first quadrant of the x_1, x_2 axes. (B) Square after deformation which corresponds to the prescribed θ in (4.3.1).

4.3 Kinematics of locally area preserving finite plane deformations

Let $\boldsymbol{y} = \boldsymbol{y}(\boldsymbol{x})$ be a deformation on a plane region B. The deformation gradient tensor is defined as $\boldsymbol{F} = \nabla \boldsymbol{y}$, and the left and right polar decompositions for $\boldsymbol{F}$ are

$$\boldsymbol{F} = \boldsymbol{R}\boldsymbol{U} = \boldsymbol{V}\boldsymbol{R}, \quad \boldsymbol{U} = \sqrt{\boldsymbol{F}^{T}\boldsymbol{F}}, \quad \boldsymbol{V} = \sqrt{\boldsymbol{F}\boldsymbol{F}^{T}}, \quad \boldsymbol{R} = \boldsymbol{F}\boldsymbol{U}^{-1}. \tag{4.3.6}$$

The mapping $\boldsymbol{y} = \boldsymbol{y}(\boldsymbol{x})$ is one-to-one, continuously differentiable, and has a Jacobian determinant of $J = 1$ for a plane region B. Thus

$$1 = F_{11}F_{22} - F_{12}F_{21}, \text{ on } B, \tag{4.3.7}$$

given by the derivatives of the deformation $\boldsymbol{y} = \boldsymbol{y}(\boldsymbol{x})$.

The left and right stretch tensors $\boldsymbol{U}$ and $\boldsymbol{V}$ are both symmetric and positive definite, and the rotation tensor $\boldsymbol{R}$ is proper orthogonal. The rotation field is fully determined by a single scalar field θ, corresponding to a right-handed rotation through θ about an out-of-plane axis:

$$\boldsymbol{R} = \begin{bmatrix} \cos\theta & -\sin\theta \\ \sin\theta & \cos\theta \end{bmatrix}. \tag{4.3.8}$$

From (4.3.6),

$$\boldsymbol{U} = \boldsymbol{R}^{T}\boldsymbol{F} \quad , \quad \boldsymbol{V} = \boldsymbol{F}\boldsymbol{R}^{T}, \tag{4.3.9}$$

such that,

$$[\boldsymbol{U}] = [\boldsymbol{U}]^T = \begin{bmatrix} \cos(\theta) & \sin(\theta) \\ -\sin(\theta) & \cos(\theta) \end{bmatrix} \begin{bmatrix} F_{11} & F_{12} \\ F_{21} & F_{22} \end{bmatrix}$$
$$= \begin{bmatrix} F_{11}\cos(\theta) + F_{21}\sin(\theta) & F_{12}\cos(\theta) + F_{22}\sin(\theta) \\ F_{21}\cos(\theta) - F_{11}\sin(\theta) & F_{22}\cos(\theta) - F_{12}\sin(\theta) \end{bmatrix}, \text{ on } B, \tag{4.3.10}$$

(note a similar matrix equation can be constructed for $\boldsymbol{V}$). Due to the symmetry of the stretch tensor $\boldsymbol{U}$, the following expression can be constructed from (4.3.10) relating the components of the of the deformation gradient tensor $\boldsymbol{F}$ to the rotation field

$$0 = (F_{11} + F_{22})\sin(\theta) + (F_{12} - F_{21})\cos(\theta), \text{ on } B. \tag{4.3.11}$$

4.4 Constructing a locally area preserving deformation corresponding to a given rotation field and maps a prescribed curve to another

In order to construct an area preserving plane deformation in the neighborhood of a curve which maps the said prescribed curve to another in a region B, we will make use of the Cauchy-Kovalevskaya Theorem (A Cauchy characteristic problem named for by being first proved by S. V. Kovalevskaya, 1875).

Given a rotation field $\boldsymbol{R}$, we wish to find a plane deformation field $\boldsymbol{y}(\boldsymbol{x})$ that corresponds to $\boldsymbol{R}$ and also maps a prescribed curve onto another prescribed curve. Define the initial prescribed curve as C and the curve to which C maps to as C^* (the same as in Ch. 3). Let the prescribed curves C and C^* be parameterized as followed:

$$C: \ \boldsymbol{x} = \tilde{\boldsymbol{x}}(s), \ (0 < s < s_0), \tag{4.4.1}$$

$$C^*: \ \boldsymbol{y} = \tilde{\boldsymbol{y}}(s), \ (0 < s < s_0), \tag{4.4.2}$$

such that the deformation $\boldsymbol{y}(\boldsymbol{x})$ maps C to C^*,

$$\boldsymbol{y}(x_1(s), x_2(s)) = \tilde{\boldsymbol{y}}(s)\,, \tag{4.4.3}$$

where s is defined as arc-length along the curve C, and s_0 is a constant defining the upper bound of the arc-length. Differentiating (4.4.3) with respect to s gives

$$\dot{\tilde{\boldsymbol{y}}} = \tilde{\boldsymbol{F}}\dot{\tilde{\boldsymbol{x}}} \;\rightarrow\; \begin{cases} \dot{\tilde{y}}_1 = \tilde{F}_{11}\dot{\tilde{x}}_1 + \tilde{F}_{12}\dot{\tilde{x}}_2 \\ \dot{\tilde{y}}_2 = \tilde{F}_{21}\dot{\tilde{x}}_1 + \tilde{F}_{22}\dot{\tilde{x}}_2 \end{cases}, \text{ on } C, \tag{4.4.4}$$

where the dots above $\tilde{\boldsymbol{x}}$ and $\tilde{\boldsymbol{y}}$ represent derivates with respect to s, and $\tilde{\boldsymbol{F}} \equiv \boldsymbol{F}(\boldsymbol{s})$ is defined as the deformation gradient $\boldsymbol{F}$ on C. Substituting (4.4.4) into the polar decomposition of $\boldsymbol{F}$ in (4.3.6) gives the expression:

$$\dot{\tilde{\boldsymbol{y}}} = \tilde{\boldsymbol{F}}\dot{\tilde{\boldsymbol{x}}} = \tilde{\boldsymbol{R}}\tilde{\boldsymbol{U}}\dot{\tilde{\boldsymbol{x}}}\,, \text{ on } C, \tag{4.4.5}$$

which can be written as

$$\tilde{\boldsymbol{U}}\dot{\tilde{\boldsymbol{x}}} = \tilde{\boldsymbol{R}}^T \dot{\tilde{\boldsymbol{y}}}\,, \text{ on } C. \tag{4.4.6}$$

Because $\boldsymbol{U}$ is positive definite, this leads to the following condition, which must be met by the prescribed curves and rotation field:

$$\begin{aligned} \psi &= \dot{\tilde{\boldsymbol{x}}}\cdot\tilde{\boldsymbol{U}}\dot{\tilde{\boldsymbol{x}}} = \dot{\tilde{\boldsymbol{y}}}\cdot\tilde{\boldsymbol{R}}\dot{\tilde{\boldsymbol{x}}} \\ &= \left(\dot{\tilde{x}}_1\dot{\tilde{y}}_1 + \dot{\tilde{x}}_2\dot{\tilde{y}}_2\right)\cos(\theta) + \left(\dot{\tilde{x}}_1\dot{\tilde{y}}_2 - \dot{\tilde{x}}_2\dot{\tilde{y}}_1\right)\sin(\theta) \;>\; 0\,, \text{ on } C, \end{aligned} \tag{4.4.7}$$

where ψ is a positive scalar function (as shown before in the Ch 2 and 3), noting that ~ above indicate the values of these terms defined along C. We assume that the prescribed rotation angle and curves C and C^* are consistent with this necessary condition. We also assume that θ, $\tilde{\boldsymbol{x}}$, and $\tilde{\boldsymbol{y}}$ have continuous derivatives of all orders.

Constructing an area preserving deformation in the neighborhood of a prescribed curve C that maps the curve C to its image C^* using the Cauchy-Kovalevskaya Theorem:

Following the Cauchy-Kovalevskaya Theorem, we will construct a deformation $\boldsymbol{y}(\boldsymbol{x})$ in the form of a Taylor series (Evans, 2010), in a neighborhood of points on C,

$$\boldsymbol{y}(\boldsymbol{x}) = \tilde{\boldsymbol{y}}(s) + \left(\boldsymbol{x} - \tilde{\boldsymbol{x}}(s)\right)\tilde{\boldsymbol{F}} + \frac{1}{2!}\left[\left(\boldsymbol{x} - \tilde{\boldsymbol{x}}(s)\right)^2 \nabla\tilde{\boldsymbol{F}}\right] + \frac{1}{3!}\left[\left(\boldsymbol{x} - \tilde{\boldsymbol{x}}(s)\right)^3 \nabla\nabla\tilde{\boldsymbol{F}}\right] + \ \ldots. \qquad (4.4.8)$$

Thus to construct the deformation $\boldsymbol{y}(\boldsymbol{x})$ which maps a prescribed curve C to its image C^*, we must determine $\boldsymbol{F}$ and its derivatives on C. To do this we will setup linear systems of equations to solve for $\boldsymbol{F}$ and its higher order derivates defined on the curve C.

To create a system of linear equations, define a vector field $\boldsymbol{h}$ such that,

$$h_\alpha = \tilde{F}_{\alpha 2}\dot{\tilde{x}}_1 - \tilde{F}_{\alpha 1}\dot{\tilde{x}}_2. \qquad (4.4.9)$$

Using (4.4.9) and (4.4.4), we solve for the components of $\boldsymbol{F}$ on C in terms of $\dot{\tilde{\boldsymbol{y}}}$ and $\boldsymbol{h}$ as,

$$\tilde{\boldsymbol{F}} \rightarrow \begin{cases} \tilde{F}_{11} = \dot{\tilde{y}}_1\dot{\tilde{x}}_1 - h_1\dot{\tilde{x}}_2 \\ \tilde{F}_{12} = \dot{\tilde{y}}_1\dot{\tilde{x}}_2 + h_1\dot{\tilde{x}}_2 \\ \tilde{F}_{21} = \dot{\tilde{y}}_2\dot{\tilde{x}}_1 - h_2\dot{\tilde{x}}_2 \\ \tilde{F}_{22} = \dot{\tilde{y}}_2\dot{\tilde{x}}_2 - h_2\dot{\tilde{x}}_1 \end{cases}, \text{ on } C. \tag{4.4.10}$$

Substituting these expressions into (4.3.7) gives,

$$1 = \left(\dot{\tilde{y}}_1\dot{\tilde{x}}_1 - h_1\dot{\tilde{x}}_2\right)\left(\dot{\tilde{y}}_2\dot{\tilde{x}}_2 - h_2\dot{\tilde{x}}_1\right) - \left(\dot{\tilde{y}}_1\dot{\tilde{x}}_2 + h_1\dot{\tilde{x}}_1\right)\left(\dot{\tilde{y}}_2\dot{\tilde{x}}_1 - h_2\dot{\tilde{x}}_2\right), \text{ on } C. \tag{4.4.11}$$

Simplifying (4.4.11),

$$1 = \dot{\tilde{y}}_1 h_2\left(\dot{\tilde{x}}_1^2 + \dot{\tilde{x}}_2^2\right) - \dot{\tilde{y}}_2 h_1\left(\dot{\tilde{x}}_1^2 + \dot{\tilde{x}}_2^2\right) = \dot{\tilde{y}}_1 h_2 - \dot{\tilde{y}}_2 h_1, \text{ on } C, \tag{4.4.12}$$

which after substituting the expression in (4.4.9) in for the components of $\boldsymbol{h}$, gives the linear equation for the components of $\boldsymbol{F}$ on C:

$$1 = \dot{\tilde{y}}_1(\dot{\tilde{x}}_1\tilde{F}_{22} - \dot{\tilde{x}}_2\tilde{F}_{21}) - \dot{\tilde{y}}_2(\dot{\tilde{x}}_1\tilde{F}_{12} - \dot{\tilde{x}}_2\tilde{F}_{11}), \text{ on } C, \tag{4.4.13}$$

noting that $\dot{\tilde{\boldsymbol{x}}}$ and $\dot{\tilde{\boldsymbol{y}}}$ are both known from the prescribed curve C and its mapping C^*.

Given the equations (4.3.11), (4.4.4), and (4.4.13), we can now construct a linear system of equations for which we can solve for the components of deformation gradient tensor $\boldsymbol{F}$ on the curve C,

$$\underbrace{\begin{bmatrix} \sin(\theta) & \cos(\theta) & -\cos(\theta) & \sin(\theta) \\ \dot{\tilde{x}}_1 & \dot{\tilde{x}}_2 & 0 & 0 \\ 0 & 0 & \dot{\tilde{x}}_1 & \dot{\tilde{x}}_2 \\ \dot{\tilde{x}}_2\dot{\tilde{y}}_2 & -\dot{\tilde{x}}_1\dot{\tilde{y}}_2 & -\dot{\tilde{x}}_2\dot{\tilde{y}}_1 & \dot{\tilde{x}}_1\dot{\tilde{y}}_1 \end{bmatrix}}_{[\boldsymbol{A}]} \underbrace{\begin{bmatrix} \tilde{F}_{11} \\ \tilde{F}_{12} \\ \tilde{F}_{21} \\ \tilde{F}_{22} \end{bmatrix}}_{[\boldsymbol{f}]} = \underbrace{\begin{bmatrix} 0 \\ \dot{\tilde{y}}_1 \\ \dot{\tilde{y}}_2 \\ 1 \end{bmatrix}}_{[\boldsymbol{b}]}, \text{ on } C. \tag{4.4.14}$$

The linear system of equations expressed in matrix form in (4.4.14) will have a solution for the components of $\tilde{\boldsymbol{F}}$ if and only if the determinant of the matrix $[\boldsymbol{A}]$ is non-zero. Taking the determinant of matrix $[\boldsymbol{A}]$ gives

$$Det\{[\boldsymbol{A}]\} = \left(\dot{\tilde{x}}_1\dot{\tilde{y}}_1 + \dot{\tilde{x}}_2\dot{\tilde{y}}_2\right)\cos(\theta) + \left(\dot{\tilde{x}}_1\dot{\tilde{y}}_2 - \dot{\tilde{x}}_2\dot{\tilde{y}}_1\right)\sin(\theta) \text{ , on } C. \qquad (4.4.15)$$

Because we assume that the given angle θ and the curves $\tilde{\boldsymbol{x}}$ and $\tilde{\boldsymbol{y}}$ satisfy (4.4.7) , the determinant of $[\boldsymbol{A}]$ is positive. Therefore a unique solution does exist for the components of $\boldsymbol{F}$ on the curve C.

To acquire the higher order derivatives of $\boldsymbol{F}$ along the curve C, we take derivates of equations (4.3.11) and (4.3.7) with respect to $\boldsymbol{x}$, and the derivatives of (4.4.4) with respect to s, to achieve a system of linear equations for the first partial derivatives of $\boldsymbol{F}$ on C. We construct the following linear system of equations, again in matrix form, for which we can solve for the first partial derivatives of $\boldsymbol{F}$ on the curve C,

$$\underbrace{\begin{bmatrix} \sin(\theta) & \cos(\theta) & 0 & -\cos(\theta) & \sin(\theta) & 0 \\ 0 & \sin(\theta) & \cos(\theta) & 0 & -\cos(\theta) & \sin(\theta) \\ \dot{\tilde{x}}_1^2 & 2\dot{\tilde{x}}_1\dot{\tilde{x}}_2 & \dot{\tilde{x}}_2^2 & 0 & 0 & 0 \\ 0 & 0 & 0 & \dot{\tilde{x}}_1^2 & 2\dot{\tilde{x}}_1\dot{\tilde{x}}_2 & \dot{\tilde{x}}_2^2 \\ \tilde{F}_{22} & -\tilde{F}_{21} & 0 & -\tilde{F}_{12} & \tilde{F}_{11} & 0 \\ 0 & \tilde{F}_{22} & -\tilde{F}_{21} & 0 & -\tilde{F}_{12} & \tilde{F}_{11} \end{bmatrix}}_{[\boldsymbol{A}_2]} \underbrace{\begin{bmatrix} \tilde{F}_{11,1} \\ \tilde{F}_{11,2} \\ \tilde{F}_{12,2} \\ \tilde{F}_{21,1} \\ \tilde{F}_{21,2} \\ \tilde{F}_{22,2} \end{bmatrix}}_{[\boldsymbol{f}_2]}$$

$$= \underbrace{\begin{bmatrix} -\tilde{F}_{12}\theta_{,1}\sin(\theta) + \tilde{F}_{22}\theta_{,1}\cos(\theta) + \tilde{F}_{11}\theta_{,1}\cos(\theta) + \tilde{F}_{21}\theta_{,1}\sin(\theta) \\ -\tilde{F}_{12}\theta_{,2}\sin(\theta) + \tilde{F}_{22}\theta_{,2}\cos(\theta) + \tilde{F}_{11}\theta_{,2}\cos(\theta) + \tilde{F}_{21}\theta_{,2}\sin(\theta) \\ \tilde{F}_{11}\ddot{\tilde{x}}_1 + \tilde{F}_{12}\ddot{\tilde{x}}_2 - \ddot{\tilde{y}}_1 \\ \tilde{F}_{21}\ddot{\tilde{x}}_1 + \tilde{F}_{22}\ddot{\tilde{x}}_2 - \ddot{\tilde{y}}_2 \\ 0 \\ 0 \end{bmatrix}}_{[\boldsymbol{b}_2]}, \text{ on } C. \qquad (4.4.16)$$

Taking the determinant of matrix $[\boldsymbol{A}_2]$ gives

$$Det\{[\boldsymbol{A}_2]\} = \left\{\left(\dot{\tilde{x}}_1\dot{\tilde{y}}_1 + \dot{\tilde{x}}_2\dot{\tilde{y}}_2\right)\cos(\theta) + \left(\dot{\tilde{x}}_1\dot{\tilde{y}}_2 - \dot{\tilde{x}}_2\dot{\tilde{y}}_1\right)\sin(\theta)\right\}^2, \text{ on } C, \qquad (4.4.17)$$

which is (4.4.15) squared, where by assuring the determinant of matrix $[\boldsymbol{A}_2]$ to be positive. Therefore a unique solution does exist for the first partial derivatives of $\boldsymbol{F}$ on the curve C.

Generalizing the above calculations for solving for higher order derivatives,

$$[\boldsymbol{A}_m]^{nxn}[\boldsymbol{f}_m]^n = [\boldsymbol{b}_m]^n \ , \ n = 2(m+1), \text{ on } C. \qquad (4.4.18)$$

where m is the order of derivative with (4.4.14) having an order of $m=1$, and n corresponds to the size of the system, it appears that the determinant of the matrix $[\boldsymbol{A}_m]$ takes the following form:

$$Det\{[\boldsymbol{A}_m]\} = \left\{\left(\dot{\tilde{x}}_1\dot{\tilde{y}}_1 + \dot{\tilde{x}}_2\dot{\tilde{y}}_2\right)\cos(\theta) + \left(\dot{\tilde{x}}_1\dot{\tilde{y}}_2 - \dot{\tilde{x}}_2\dot{\tilde{y}}_1\right)\sin(\theta)\right\}^m, \text{ on } C. \quad (4.4.19)$$

However, we have only verified this relation for $m=1,2,3,4$. It therefore appears possible to solve for higher order derivatives of $\boldsymbol{F}$ on C, enabling the deformation $\boldsymbol{y}$ to be determined through (4.4.8). An example of this is shown below. (Note that we do not address convergence of the series (4.4.8))

Example 4.2: Area preserving finite deformation

Suppose the rotation field is defined by the function

$$\theta(x_1,x_2) = \arcsin\left(\frac{x_1}{\sqrt{1+x_1^2}}\right) \;,\; \sin(\theta) = \frac{x_1}{\sqrt{1+x_1^2}}. \quad (4.4.20)$$

Let the curve C be defined as a horizontal line along the x_1-axis, which may be represented by

$$\left(x_1,x_2\right) = \left(\tilde{x}_1(s),\tilde{x}_2(s)\right) = \left(s,0\right) \;,\quad \left(0 \le s \le 5\right), \quad (4.4.21)$$

(See Figure 4.2(A)). The image C^* of C is a parabola,

$$\left(y_1,y_2\right) = \left(\tilde{y}_1,\tilde{y}_2\right) = \left(s,s^2+s\right) \;,\quad \left(0 \le s \le 5\right) \quad (4.4.22)$$

Given θ, $\tilde{\boldsymbol{x}}$, and $\tilde{\boldsymbol{y}}$, defined this way, we will substitute them into (4.4.7) to check that our eventual matrix $[\boldsymbol{A}]$ and its higher orders are all positive:

$$\dot{\tilde{\boldsymbol{y}}} \cdot \tilde{\boldsymbol{R}} \dot{\tilde{\boldsymbol{x}}} = \frac{\left(2s^2 + s + 1\right)}{\sqrt{1+s^2}} > 0 \quad , \quad 0 \le s \le 5 \text{, on } C . \qquad (4.4.23)$$

From (4.4.23), we see that positivity of matrix $[\boldsymbol{A}]$ and its higher orders will hold for our whole range of s.

In constructing our deformation, will limit our region B to the first quadrant such that $(x_1, x_2) \ge 0$. Using the Cauchy-Kovalevskaya procedure, we will now construct a deformation $\boldsymbol{y}(\boldsymbol{x})$ for our given θ, $\tilde{\boldsymbol{x}}$, and $\tilde{\boldsymbol{y}}$, in the form of a Taylor Series described in (4.4.8). As explained previously, we do this by solving for the components of $\boldsymbol{F}$ and its higher order derivatives on the curve C.

For this example in can be shown that the linear system in (4.4.14) takes the form

$$\underbrace{\begin{bmatrix} 0 & -(2s+1) & 0 & 1 \\ 1 & 0 & 0 & 0 \\ 0 & 0 & 1 & 0 \\ \frac{s}{\sqrt{1+s^2}} & \frac{1}{\sqrt{1+s^2}} & \frac{-1}{\sqrt{1+s^2}} & \frac{s}{\sqrt{1+s^2}} \end{bmatrix}}_{[\boldsymbol{A}]} \underbrace{\begin{bmatrix} \tilde{F}_{11} \\ \tilde{F}_{12} \\ \tilde{F}_{21} \\ \tilde{F}_{22} \end{bmatrix}}_{[\boldsymbol{f}]} = \underbrace{\begin{bmatrix} 1 \\ 1 \\ 2s+1 \\ 0 \end{bmatrix}}_{[\boldsymbol{b}]} \text{ , on } C . \qquad (4.4.24)$$

Solving the above linear system for the components of $\tilde{\boldsymbol{F}}$ gives

$$\tilde{\boldsymbol{F}} \rightarrow \begin{cases} \tilde{F}_{11} = 1 \\ \tilde{F}_{12} = \dfrac{1}{2s^2 + s + 1} \\ \tilde{F}_{21} = 2s + 1 \\ \tilde{F}_{22} = \dfrac{2s^2 + 3s + 2}{2s^2 + s + 1} \end{cases}, \text{ on } C. \tag{4.4.25}$$

To make sure our linear system agrees with our calculation in (4.4.23), we take the determinant of our matrix $[\boldsymbol{A}]$ in (4.4.24),

$$Det\{[\boldsymbol{A}]\} = \frac{\left(2s^2 + s + 1\right)}{\sqrt{1 + s^2}}, \tag{4.4.26}$$

which is in fact the same as (4.4.23) and therefore positive for our range of s.

To achieve the first partial derivatives of $\boldsymbol{F}$ on C, we substitute (4.4.25) into the linear system in (4.4.16) along with the prescribed values for θ, $\tilde{\boldsymbol{x}}$, and $\tilde{\boldsymbol{y}}$ to get the following matrix representation of the system:

$$\underbrace{\begin{bmatrix} \frac{2s^2+3s+2}{2s^2+s+1} & -(2s+1) & 0 & -\frac{1}{2s^2+s+1} & 1 & 0 \\ 0 & \frac{2s^2+3s+2}{2s^2+s+1} & -(2s+1) & 0 & -\frac{1}{2s^2+s+1} & 1 \\ \frac{s}{\sqrt{1+s^2}} & \frac{1}{\sqrt{1+s^2}} & 0 & \frac{-1}{\sqrt{1+s^2}} & \frac{s}{\sqrt{1+s^2}} & 0 \\ 0 & \frac{s}{\sqrt{1+s^2}} & \frac{1}{\sqrt{1+s^2}} & 0 & \frac{-1}{\sqrt{1+s^2}} & \frac{s}{\sqrt{1+s^2}} \\ 1 & 0 & 0 & 0 & 0 & 0 \\ 0 & 0 & 0 & 1 & 0 & 0 \end{bmatrix}}_{[\boldsymbol{A}_2]} \underbrace{\begin{bmatrix} \tilde{F}_{11,1} \\ \tilde{F}_{11,2} \\ \tilde{F}_{12,2} \\ \tilde{F}_{21,1} \\ \tilde{F}_{21,2} \\ \tilde{F}_{22,2} \end{bmatrix}}_{[\boldsymbol{f}_2]}$$

$$= \underbrace{\begin{bmatrix} 0 \\ 0 \\ \frac{4s^2+4s+3}{\sqrt{1+s^2}\left(2s^2+s+1\right)} \\ 0 \\ 0 \\ -2 \end{bmatrix}}_{[\boldsymbol{b}_2]}, \text{ on } C. \qquad (4.4.27)$$

From (4.4.27), we compute the following first partial derivatives of $\boldsymbol{F}$ on C

$$
\nabla \tilde{\boldsymbol{F}} \rightarrow \begin{cases} \tilde{F}_{11,1} = 0 \\ \tilde{F}_{11,2} = \dfrac{4s+1}{4s^4+4s^3+5s^2+2s+1} \\ \tilde{F}_{12,2} = \dfrac{4s^2+6s-1}{(2s^2+s+1)(4s^4+4s^3+5s^2+2s+1)} \\ \tilde{F}_{21,1} = 0 \\ \tilde{F}_{21,2} = \dfrac{4s^2+4s-1}{4s^4+4s^3+5s^2+2s+1} \\ \tilde{F}_{22,2} = \dfrac{6s^2-3s-4}{(2s^2+s+1)(4s^4+4s^3+5s^2+2s+1)} \end{cases} . \tag{4.4.28}
$$

For this example we will omit the matrix representation of the second partial derivative of $\boldsymbol{F}$ on C ($m = 3$ in (4.4.18)) due to its complexity, but below are the components of $\nabla\nabla\tilde{\boldsymbol{F}}$ solved for in that linear system:

$$
\nabla\nabla \boldsymbol{F} \rightarrow \begin{cases} \tilde{F}_{11,11} = 0 \\ \tilde{F}_{11,12} = \dfrac{2(16s^5+28s^4+26s^3+19s^2+4s+1)}{(1+s^2)(2s^2+s+1)(4s^4+4s^3+5s^2+2s+1)} \\ \tilde{F}_{11,22} = \dfrac{64s^6+112s^5+152s^4+76s^3+45s^2-8s+1}{(1+s^2)(2s^2+s+1)^2(4s^4+4s^3+5s^2+2s+1)} \\ \tilde{F}_{12,22} = \dfrac{64s^7+160s^6+208s^5+136s^4-12s^3-35s^2-52s-3}{(1+s^2)(2s^2+s+1)^3(4s^4+4s^3+5s^2+2s+1)} \\ \tilde{F}_{21,11} = 0 \\ \tilde{F}_{21,12} = \dfrac{2(32s^6+56s^5+68s^4+38s^3+13s^2-4s-1)}{(1+s^2)(2s^2+s+1)(4s^4+4s^3+5s^2+2s+1)} \\ \tilde{F}_{21,22} = \dfrac{64s^7+128s^6+160s^5+64s^4-34s^3-63s^2-46s-3}{(1+s^2)(2s^2+s+1)^2(4s^4+4s^3+5s^2+2s+1)} \\ \tilde{F}_{22,22} = \dfrac{32s^7-32s^6-160s^5-370s^4-337s^3-216s^2-73s+2}{(1+s^2)(2s^2+s+1)^3(4s^4+4s^3+5s^2+2s+1)} \end{cases} , \text{ on } C. \tag{4.4.29}
$$

Using the components of $\boldsymbol{F}$ and it higher order derivatives from (4.4.25), (4.4.28), and (4.4.29) all defined on C, along with θ, $\tilde{\boldsymbol{x}}$, and $\tilde{\boldsymbol{y}}$ prescribed in (4.4.20) - (4.4.22), we now can construct the deformation $\boldsymbol{y}(\boldsymbol{x})$ in the form of a Taylor series using (4.4.8).

For simplicity, we will only use the terms we have computed in this example to construct our deformation, thus omitting the higher order terms of the Taylor Series. However, in order to ensure accuracy of our deformation, we will compare the Jacobian calculated using the Cauchy-Kovalevskaya procedure with that of the actual value of the Jacobian for an area preserving deformation, $J = 1$. To determine the neighborhood in which we will construct our deformation, we will arbitrarily say that for a given point, if the calculated Jacobian is within 90% of the actual value of $J = 1$, then our construction should be a good approximation of the actual deformation. Note though that the method performed here is more accurate then we are showing is this example, and the need for approximation of solutions is only due to our simplifying of the problem.

Due to its complexity, the deformation $\boldsymbol{y}(\boldsymbol{x})$ as expressed in the form of a Taylor series will not be shown, but it can be seen illustrated in Figure 4.2 with a unit square deformed by the generated deformation.

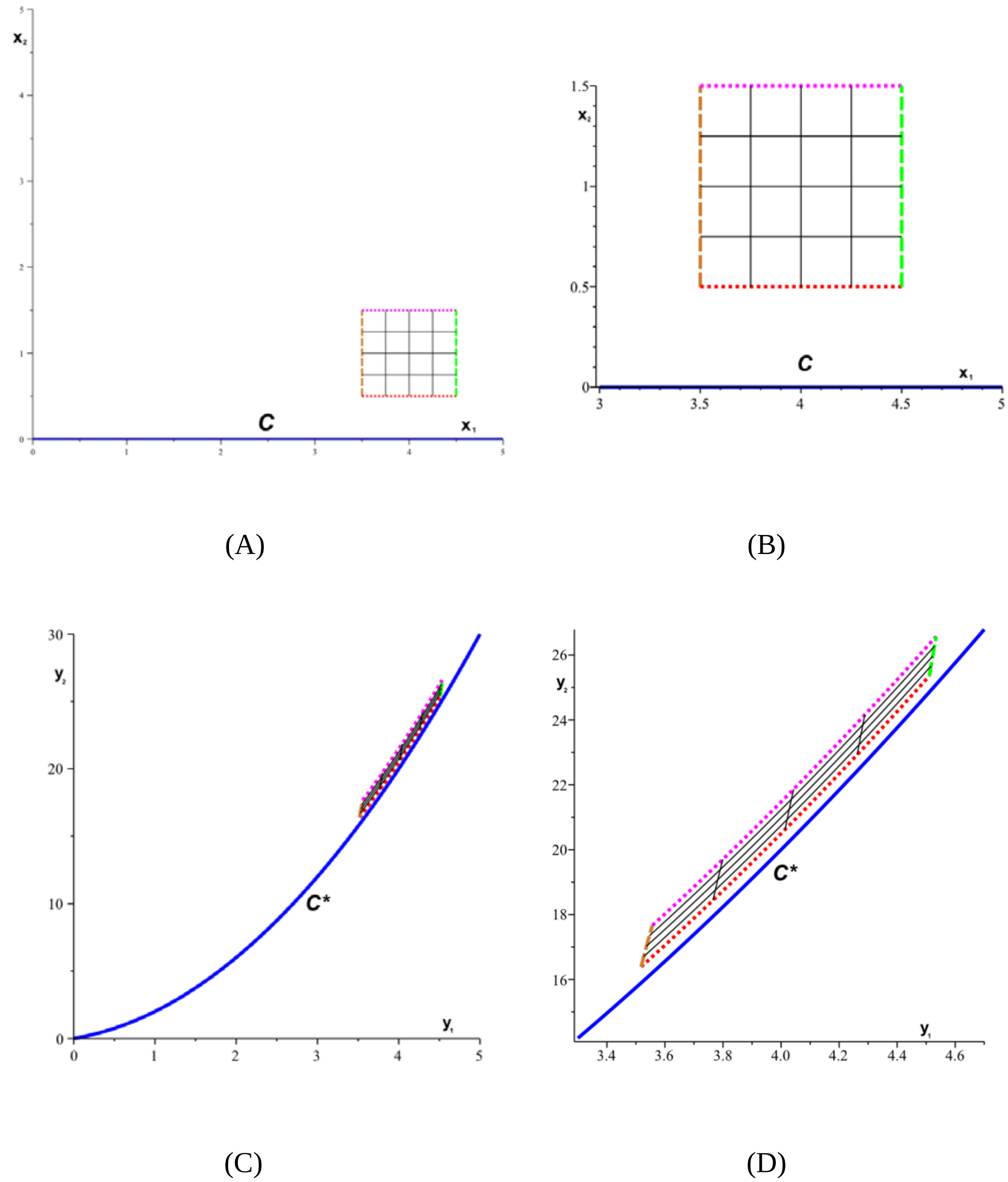

(A) (B)

(C) (D)

Figure 4.2: (A) An undeformed unit square located in the first quadrant of the x_1, x_2 axes, and the curve C defined as a horizontal line along the x_1-axis. (B) A close up view of the undeformed unit square. (C) Square after deformation which corresponds to the prescribed θ in (4.4.20), and the curve C mapped to a parabola, $C*$. (D) A close up view of the deformed unit square.

4.5 Constructing a finite deformation for a prescribed Jacobian

The procedure in **Section 4.4** can be used to construct a plane finite deformation $\boldsymbol{y}(\boldsymbol{x})$, that maps a prescribed curve to another, given a rotation field θ in a region B, in which the Jacobian for the generated deformation field $\boldsymbol{y}(\boldsymbol{x})$ is defined to be a positive scalar function $J(x_1, x_2)$. With the Jacobian defined as $J(x_1, x_2)$, the region B is no longer uniformly area preserving, thus the determinant of the deformation gradient $\boldsymbol{F} = \nabla \boldsymbol{y}$ takes the form

$$J(x_1, x_2) = F_{11}F_{22} - F_{12}F_{21} = y_{1,1}y_{2,2} - y_{1,2}y_{2,1}\,. \tag{4.5.1}$$

As done in the previous section, this equation can be rewritten into a linear format in the same arrangement shown in equations (4.4.13) for an area preserving deformation

$$J(x_1, x_2) = \dot{\tilde{y}}_1(\dot{\tilde{x}}_1\tilde{F}_{22} - \dot{\tilde{x}}_2\tilde{F}_{21}) - \dot{\tilde{y}}_2(\dot{\tilde{x}}_1\tilde{F}_{12} - \dot{\tilde{x}}_2\tilde{F}_{11})\text{, on } C\,. \tag{4.5.2}$$

With (4.5.2), the system in (4.4.14) becomes

$$\underbrace{\begin{bmatrix} \sin(\theta) & \cos(\theta) & -\cos(\theta) & \sin(\theta) \\ \dot{\tilde{x}}_1 & \dot{\tilde{x}}_2 & 0 & 0 \\ 0 & 0 & \dot{\tilde{x}}_1 & \dot{\tilde{x}}_2 \\ \dot{\tilde{x}}_2\dot{\tilde{y}}_2 & -\dot{\tilde{x}}_1\dot{\tilde{y}}_2 & -\dot{\tilde{x}}_2\dot{\tilde{y}}_1 & \dot{\tilde{x}}_1\dot{\tilde{y}}_1 \end{bmatrix}}_{[\boldsymbol{A}]} \underbrace{\begin{bmatrix} \tilde{F}_{11} \\ \tilde{F}_{12} \\ \tilde{F}_{21} \\ \tilde{F}_{22} \end{bmatrix}}_{[\boldsymbol{f}]} = \underbrace{\begin{bmatrix} 0 \\ \dot{\tilde{y}}_1 \\ \dot{\tilde{y}}_2 \\ J(x_1, x_2) \end{bmatrix}}_{[\boldsymbol{b}]}, \tag{4.5.3}$$

with the determinant of matrix $[\boldsymbol{A}]$ still being expressed by (4.4.15). From (4.5.3), it is seen that the equations for higher order derivatives are modified only on the right-hand sides, and so may be solved in the same fashion as in **Section 4.4** for the derivatives of $\boldsymbol{F}$ on C. Therefore, as in the previous section, there appears to exist unique solutions to all higher order terms along the curve C, such that it is possible to construct a plane deformation $\boldsymbol{y}(\boldsymbol{x})$ given a prescribed curve C and it image C^*, and a rotation field fully determined by a scalar function $\theta(x_1, x_2)$ defined on a region B where the Jacobian of the deformation gradient is a positive scalar function $J(x_1, x_2)$ using the Cauchy-Kovalevskaya procedure. This is shown in the example below.

Example 4.3: Finite deformation for a prescribed Jacobian

For this example with will prescribe θ, $\tilde{\boldsymbol{x}}$, and $\tilde{\boldsymbol{y}}$, in the same way we did in Example 4.2, the only difference now being that the deformation is no longer locally area preserving. Let the Jacobian determinant be defined as

$$J(x_1, x_2) = x_1 + x_2. \tag{4.5.4}$$

For this example, we will define our region B to be located such that x_1 and x_2 are always positive. Therefore the $J(x_1, x_2)$ is always positive.

Defining the Jacobian this way only has an effect on the right side of (4.4.18), as expressed previously and shown in (4.5.3). Therefore the matrices $[\boldsymbol{A}_m]$ will be the same as in Example 4.2 (as well as the matrices $[\boldsymbol{f}_m]$, but this is intuitive). The only difference between the problems is from the values in matrices $[\boldsymbol{b}_m]$. Thus we will construct a deformation $\boldsymbol{y}(\boldsymbol{x})$ in the form of a Taylor series using the same Cauchy-Kovalevskaya procedure as shown in (4.4.8). Substituting the prescribed θ, $\tilde{\boldsymbol{x}}$, and $\tilde{\boldsymbol{y}}$, along with the Jacobian as defined in (4.5.4) into (4.5.3) gives the linear system

$$\underbrace{\begin{bmatrix} 0 & -(2s+1) & 0 & 1 \\ 1 & 0 & 0 & 0 \\ 0 & 0 & 1 & 0 \\ \frac{s}{\sqrt{1+s^2}} & \frac{1}{\sqrt{1+s^2}} & \frac{-1}{\sqrt{1+s^2}} & \frac{s}{\sqrt{1+s^2}} \end{bmatrix}}_{[\boldsymbol{A}]} \underbrace{\begin{bmatrix} \tilde{F}_{11} \\ \tilde{F}_{12} \\ \tilde{F}_{21} \\ \tilde{F}_{22} \end{bmatrix}}_{[\boldsymbol{f}]} = \underbrace{\begin{bmatrix} s+x_2 \\ 1 \\ 2s+1 \\ 0 \end{bmatrix}}_{[\boldsymbol{b}]}, \text{ on } C. \tag{4.5.5}$$

Solving the above linear system for the components of $\tilde{\boldsymbol{F}}$ gives

$$\tilde{\boldsymbol{F}} \to \begin{cases} \tilde{F}_{11} = 1 \\ \tilde{F}_{12} = -\dfrac{s^2 + sx_2 - s - 1}{2s^2 + s + 1} \\ \tilde{F}_{21} = 2s+1 \\ \tilde{F}_{22} = \dfrac{2s^2 + 4s + x_2 + 1}{2s^2 + s + 1} \end{cases}, \text{ on } C. \tag{4.5.6}$$

We will omit the calculation of the rest of the components of the deformation gradient $\boldsymbol{F}$ and its higher order derivatives on C since the procedure is so similar to that in Example 4.2. Also, we will use the same approximation as before in determining the neighborhood in which we will construct our deformation, such that the calculated Jacobian must be within 90% of the actual value of $J = x_1 + x_2$, as the condition for a good approximation of the actual deformation.

Due to its complexity, the deformation $\boldsymbol{y}(\boldsymbol{x})$ will not be shown, but it can be seen illustrated in Figure 4.3 with a square of side length 0.4 deformed by the generated deformation.

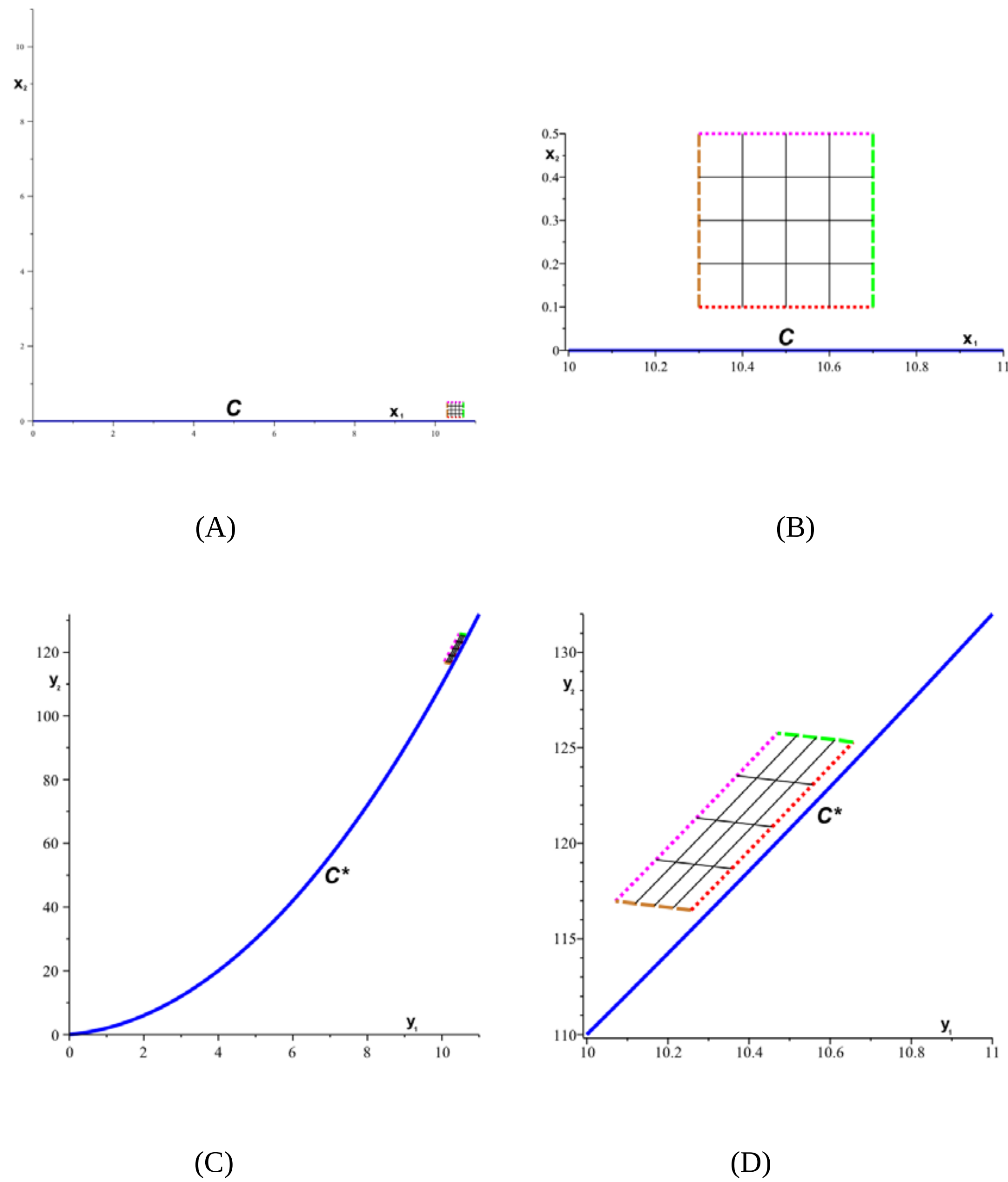

Figure 4.3: (A) An undeformed square of side length 0.4 located in the first quadrant of the x_1, x_2 axes, and the curve C defined as a horizontal line along the x_1-axis. (B) A close up view of the undeformed square. (C) Square after deformation which corresponds to the prescribed θ in (4.4.20), and the curve C mapped to a parabola, $C*$. (D) A close up view of the deformed unit square.

APPENDIX

In the following analysis, we show that in a region B a suitably smooth curve C: $\left\{x_1 = \tilde{x}_1(s),\ x_2 = \tilde{x}_2(s) \quad \left(0 \le s \le s_0\right)\right\}$ can be represented by a function $\tilde{z}(\overline{z})$ that is analytic in $\overline{z}$, with $z = \tilde{z}(\overline{z})$ defining C. Let p and q be the real and imaginary parts of $\tilde{z}$,

$$\tilde{z}(\overline{z}) = p(x_1, x_2) + iq(x_1, x_2) \ \ , \ \overline{z} = x_1 - ix_2 , \tag{A.1}$$

where p and q are harmonic functions that satisfy the Cauchy-Riemann equations for a function analytic in $\overline{z}$

$$\frac{\partial p}{\partial x_1} = -\frac{\partial q}{\partial x_2} \ \ , \ \ \frac{\partial p}{\partial x_2} = \frac{\partial q}{\partial x_1} . \tag{A.2}$$

On the curve C defined in a region B, we require that

$$z = \tilde{z}(\overline{z}) , \tag{A.3}$$

so that,

$$p(\tilde{x}_1(s), \tilde{x}_2(s)) = \tilde{x}_1(s) \ \ , \ q(\tilde{x}_1(s), \tilde{x}_2(s)) = \tilde{x}_2(s) \ \ , \quad (0 < s < s_0) , \tag{A.4}$$

where $\tilde{x}_1(s)$ and $\tilde{x}_2(s)$ define the curve C with s standing for the arc-length along C, and s_0 is a constant defining the upper bound of the arc-length. Further, (A.2) and (A.4) give,

$$\begin{aligned}\frac{d}{ds}\tilde{x}_2(s) &= \frac{\partial q}{\partial x_1}\dot{x}_1 + \frac{\partial q}{\partial x_2}\dot{x}_2 \\ &= \frac{\partial p}{\partial x_2}\dot{x}_1 - \frac{\partial p}{\partial x_1}\dot{x}_2 \\ &= -\boldsymbol{n}\cdot\nabla p \ ,\end{aligned} \tag{A.5}$$

where

$$n_1 = \dot{x}_2 \ , \ n_2 = -\dot{x}_1 , \tag{A.6}$$

are the components of a unit vector normal to C. Thus p, the real part of function $\tilde{z}$, satisfies the following boundary value problem, for a given curve $C:\left\{x_1 = \tilde{x}_1(s),\ x_2 = \tilde{x}_2(s) \quad \left(0 \le s \le s_0\right)\right\}$

$$p(\tilde{x}_1(s),\tilde{x}_2(s)) = \tilde{x}_1(s) \ , \ \boldsymbol{n}\cdot\nabla p = -\frac{d}{ds}\tilde{x}_2(s) \ , \quad (0 < s < s_0) , \tag{A.7}$$

$$\nabla^2 p = 0 . \tag{A.8}$$

According to Holmgren’s theorem, there exists a solution p to the boundary value problem listed above, provided $\tilde{x}_1$ and $\tilde{x}_2$ are real-analytic functions (Courant and Hilbert 1962) (originally named for E. Holmgren, 1901). Once p is determined, its complex conjugate q can be found by integrating the Cauchy-Riemann equations in (A.2).

To determine the function $\tilde{y}(\overline{z})$, which is analytic in $\overline{z}$, with $y = \tilde{y}(\overline{z})$ on the curve C^*, a similar boundary value problem must be solved for the real part r of $\tilde{y}$ where

$$\tilde{y} = r(x_1, x_2) + is(x_1, x_2)\,. \tag{A.9}$$

As before, the real part r of the function $\tilde{y}$ satisfies the following boundary value problem

$$r(\tilde{x}_1(s), \tilde{x}_2(s)) = \tilde{y}_1(s) \ \ , \ \ \boldsymbol{n}\cdot\nabla r = -\frac{d}{ds}\,\tilde{y}_2(s) \ \ , \quad (0 < s < s_0)\,, \tag{A.10}$$

$$\nabla^2 r = 0\,. \tag{A.11}$$

Holmgren's theorem again applies for the existence of a solution r to the boundary value problem above, provided $\tilde{y}_1$ and $\tilde{y}_2$ are real-analytic functions (Courant and Hilbert 1962).

BIBLIOGRAPHY

Ball, J. M., James, R. D. (1987): Fine phase mixtures as minimizers of energy. *Arch. Rational Mech. and Anal.* **100**, 13-52.

Buck, R.C (1978): *Advanced Calculus*. McGraw-Hill, New York.

Courant, R. and Hilbert, D. (1962): *Methods of Mathematical Physics, Volume II*. Interscience, New York.

Ericksen, J. L. (1954): Deformations possible in every isotropic, incompressible, perfectly elastic body. *ZAMP*. **5,** 466-489.

Ericksen, J. L. (1985): Some surface defects in unstressed thermoelastic solids. *Arch. Rational Mech. and Anal.* **88**, 337-345.

Evans, L. C. (2010): *Partial Differential Equations (Graduate Studies in Mathematics), Volume 19, 2nd Edition*. American Mathematical Society.

Fosdick, R. L. and Schuler, K. W. (1969): On Ericksen's problem for plane deformations with uniform transverse stretch. *Int. J. Engng Sci.* **7,** 217-233.

Fosdick, R. L. (1971): Statically possible radially symmetric deformations in isotropic, incompressible elastic solids. *ZAMP*. **22,** 590-607.

Gurtin, M. (1983): Two-phase deformations of elastic solids. *Arch. Rational Mech. and Anal.* **84**, 1-29 (1983).

Hoger, A. and Carlson, D.E. (1984): Determination of the stretch and rotation in the polar decomposition of the deformation gradient. *Quart. Appl. Math*. **42,** 113–117.

Holmgren, E. (1901): Uber Systeme von linearen partiellen Differentialalgleichungen. *Ofversigt af Kongl. Vetenskaps-Academien Forhandlinger*. **58,** 91-103.

James, R. D. (1981): Finite deformation by mechanical twinning. *Arch. Rational Mech. and Anal.* **77**, 143-175.

Parry, G. P. (1986): On shear bands in unloaded crystals. *J. Mech. Phys. Solids.* **35**(3), 367-382.

Pitteri, M. (1985): On the kinematics of mechanical twinning. *Arch. Rational Mech. and Anal.* **88**, 25-57.

Poisson, S. D. (1813): Remarques sur une equation qui se presente dans la theorie des attractions des spheroids. *Nouveau Bull. Soc. Philomathique de Paris*. **3**, 388-392.